Coherence effects in neutron diffraction and gravity experiments

Daniel M. Greenberger*

Department of Physics, City College of the City University of New York, New York, New York 10031

A.W. Overhauser†

Department of Physics, Purdue University, West Lafayette, Indiana 47907

The authors discuss the coherence properties of neutron scattering from perfect crystals and apply them to the splitting and coherent recombination of a neutron beam in a Laue-type interferometer. They also point out the difference between neutron and x-ray scattering in such devices and discuss the effect of a relative displacement of the various interferometer slabs on the fringe pattern. All this can be done without using the detailed dynamical theory of x-ray scattering. Various experiments are discussed, especially the neutron-gravity experiment of Colella, Overhauser, and Werner, which is analyzed both in the laboratory frame and in a frame freely falling with the neutron beam. The older electron diffraction experiment of Marton *et al.*, and its relevance to the Aharonov – Bohm effect, is also discussed and reinterpreted, because the standard interpretation is not consistent with the results of the neutron experiment. An Appendix presents a general discussion of the transformation to a uniformly accelerated reference frame, as a guide to help analyze future such experiments.

CONTENTS

I. INTRODUCTION

The practical availability of nearly perfect single silicon crystals, up to 15 cm in length, has provided a new tool for the performance of neutron and x-ray diffraction experiments. It is now possible to build diffraction devices of both the transmission and the reflection type which can divide a beam into two spatially separated beams, by Bragg or Laue scattering, and subsequently to coherently recombine them.

The first successful such experiments with x rays were performed by Bonse and Hart in 1965. (The Laue-type interferometer is described in Bonse and Hart, 1965a, and analyzed in Bonse and Hart, 1965b, where the role of the Borrmann effect is emphasized; some experiments giving insight into the workings of the interferometer are described in Bonse and Hart, 1966a; the Bragg-type interferometer is described in Bonse and Hart, 1966b.) The first successful use of such techniques with neutrons was by Rauch, Treimer, and Bonse in 1974 (Rauch *et al.*, 1974). Subsequently, the technique was used by Colella, Overhauser, and Werner (COW) (Overhauser and Colella, 1974; Colella *et al.*, 1975) to actually measure the phase shift due to the gravitational potential difference between two neutron beams at different heights (of about 1 cm) in the earth's gravitational field.[1] They also used the technique to show that the wave function of the neutron changes sign upon a rotation of 360° (Werner *et al.*, 1975; essentially the same experiment was done simultaneously by Rauch *et al.*, 1975). Further experiments are being planned by them and others (Werner *et al.*, 1976, whose paper also contains a theoretical analysis of the neutron interferometer).

In the present paper we provide a simplified guide for analyzing the coherence properties of such experiments. We shall develop a consistent technique for following the propagation of a wave by analyzing the phase at a fixed point, whether at a screen or in a crystal. Then if the wave is subject to a minor perturbation it is a

*Research supported in part by a grant from the PSC-BHE Research Award Program of the City University of New York.
†Supported in part by the Materials Research Laboratory Program at the National Science Foundation.

[1]This experiment shall subsequently be referred to as COW.

simple matter to calculate the change in phase at that point. This avoids altogether the very tricky analysis necessary to try to follow the semiclassical trajectories along rays, an especially confusing process when these rays are subject to perturbations. We shall also show that, without using the highly developed dynamical theory of x-ray scattering,[2] one can still gain a quantitative understanding of coherence phenomena, and be able to interpret the various experiments that have been carried out with neutrons, as well as to appreciate the difference between neutron and x-ray scattering. We will specifically discuss the COW experiment in some detail. Our simplified analysis of these phenomena is the analog of the type of phase argument one uses in elementary optics, which successfully treats many diffraction problems, but which for complicated geometries and complex physical situations must be replaced by the much more elaborate rigorous theory.

We also discuss some aspects of the Aharonov–Bohm effect,[3] as well as the electron diffraction experiment of Marton (Marton, 1952; Marton *et al.*, 1953, 1954; the theory of the interferometer is discussed by Simpson, 1954), because the accepted interpretation of this experiment, provided by Werner and Brill, 1960, is not consistent with the experimental results of COW. We shall show that the Werner–Brill result is essentially incomplete[4] and reinterpret Marton's experiment in a manner consistent with both the other Aharonov–Bohm experiments, and the COW experiment.

In order to establish the consistency of our interpretation of the COW gravity experiment, we also analyze the experiment in a uniformly accelerated reference frame, chosen to eliminate the gravitational field. We also provide a guide to the general use of such a transformation, since it may prove useful in further gravity experiments, even for rapidly moving particles. To this end we consider, in an appendix, uniform acceleration in both special and general relativity and apply it to both the nonrelativistic and relativistic Schrödinger equation, and to the Dirac equation.

In Sec. II we discuss the scattering of neutrons from crystals, emphasizing the effect of a small perturbing force, such as that due to gravity, on the outcome. In our discussion we strongly endorse the calculation of changes in phase at a given point, rather than the tracing of individual rays. For a beam that has been coherently split and recombined we show that the ultimate effect of the perturbation is to shift the fringe pattern and the beam envelope in such a way that they keep step with each other. In Sec. III we discuss the effect of transmission through a thick, perfect crystal and describe the Borrmann effect. We describe the neutron interferometer and show how the scattering is affected when the various planes of the crystal are displaced, and also show how the different absorption characteristics of neutrons and x rays yield different behavior for the two types of particles, even under identical conditions. In Sec. IV we discuss the COW experiment, in both the laboratory and free-fall reference frames. Both analyses yield the same fringe shift, as measured by COW. In Sec. V we discuss the Marton experiment, in the light of the Aharonov–Bohm effect, and point out the flaw in the Werner-Brill analysis. We then reinterpret the experiment in a manner consistent with our previous discussion. In Sec. VI we give a short summary of the paper, and finally, in an appendix, we present a discussion of the general problem of uniform acceleration.

II. CRYSTAL EFFECTS ON NEUTRON SCATTERING

A. Propagation in the presence of a weak perturbation

It has often been pointed out that the basic phenomena involved in the scattering of waves off crystals are similar, regardless of the particular type of wave involved. We are not going to discuss the scattering problem in great detail, partly because this has been done previously and partly because we shall need only a limited number of results. Our main interest will be in the coherence and phase properties of the wave function, rather than in cross sections or scattering amplitudes, and so we shall emphasize certain aspects of the subject which are usually passed over briefly.

First, if one has a free particle propagating along, subject to a very weak time-independent perturbing potential, this potential will tend to distort the wave function of the particle, and to deflect its path along a new trajectory, which will be the classically displaced trajectory. Examples are a neutron subject to the earth's gravitational field, or to an inhomogeneous magnetic field, or an electron subject to a static electromagnetic field.

If the Schrödinger equation is

$$(H_0 + U)\phi = E\phi \,, \tag{2.1}$$

where H_0 is the free-particle Hamiltonian and U is the perturbing potential, such that in the absence of the

[2] A thorough review article on the dynamical theory is James, 1963. This paper contains references to the pioneering work of Bragg, von Laue, Darwin, Ewald, etc. A good introductory discussion is contained in Peierls, 1955, though there are now a number of recent textbooks available on the subject (for example, Azaroff *et al.*, 1974). We have also found very useful the ariticle by Batterman and Cole, 1964, which has an extensive discussion of the Borrmann effect (which we describe in Sec. III), and by Slater, 1958, which emphasizes the underlying unity of all problems concerning interacting waves in crystals. Slater's article contains a detailed bibliography. The dynamical theory was extended to neutrons by Goldberger and Seitz, 1947, who gathered and greatly extended earlier unsystematic results. Theoretical discussion of the Laue-type interferometer is contained in Rauch and Suda, 1974, and Werner *et al.*, 1976. Two very recent and much needed review articles on neutron interferometry are Rauch and Petrascheck (1979), and Bonse and Graeff (1977). The most up-to-date reference on the topic will be the Proceedings of the First International Workshop on Neutron Interferometry, Institut v. Laue-Langevin, Grenoble, June, 1978 (Bonse and Rauch, to be published).

[3] Aharonov and Bohm 1959. The effect had been mentioned previously by Ehrenberg and Siday, 1949. While there seems to be universal agreement as to the existence of this effect, there has been considerable debate as to its implications. This debate has been summarized by Ehrlichson, 1970. See also the references cited in Sec. V.

[4] Professors Werner and Brill concur in this conclusion, and a reworked version of their analysis is being published. Brill *et al.*, to be published).

perturbation

$$H_0\phi_0 = E_0\phi\,, \quad \phi_0 = e^{i\mathbf{k}_0\cdot\mathbf{r}}\,, \tag{2.2}$$

then we can find a solution in the form given by Landau and Lifschitz [1958, Sec. 45. If the perturbation is due to a strictly uniform force everywhere in space, the problem can be solved exactly by Airy functions *ibid.*, Sec. 22, and Appendix (b)]:

$$\phi = \phi_0\chi\,, \quad E = E_0\,. \tag{2.3}$$

Since

$$H_0\phi = -(\hbar^2/2m)(-k_0^2\chi + 2i\mathbf{k}_0\cdot\nabla\chi + \nabla^2\chi)\phi_0\,, \tag{2.4}$$

then Eq. (2.1) becomes

$$2i\mathbf{k}_0\cdot\nabla\chi + \nabla^2\chi = (2m/\hbar^2)U\chi\,. \tag{2.5}$$

If we are interested in a semiclassical solution, such that

$$\nabla\chi \ll k_0\chi\,, \tag{2.6}$$

then we can drop the $\nabla^2\chi$ term and solve for χ.

$$\frac{1}{\chi}\frac{\partial\chi}{\partial s} = -\frac{im}{\hbar^2 k_0}U\,, \quad \chi = \exp\left(-\frac{im}{\hbar^2 k_0}\int U\,ds\right), \tag{2.7}$$

where s measures distance in the direction along k_0. Because we have $\hbar k_0/m = p_0/m = v_0$ and $ds/v_0 = dt$, we can write

$$\chi = \exp\left(-\frac{i}{\hbar}\int U\,dt\right). \tag{2.8}$$

The proper interpretation of this solution comes from integrating along the unperturbed trajectory, but it may be extended to include nearby trajectories. As an example, if the particle is propagating in the x direction and subject to a potential

$$U = \alpha z\,, \tag{2.9}$$

which yields a force perpendicular to the beam, then

$$\phi_0 = e^{ik_0x}\,, \quad \phi = \exp(ik_0x - im\alpha xz/k_0\hbar^2) \equiv e^{i\eta}\,. \tag{2.10}$$

The semiclassical momentum is given, to lowest order, by the gradient of the phase

$$\mathbf{k} \approx \nabla\eta = \mathbf{u}_x(k_0 - m\alpha z/k_0\hbar^2) - \mathbf{u}_z(m\alpha x/k_0\hbar^2)\,. \tag{2.11}$$

If one starts at some point, say $x_0 = z_0 = 0$, then along the classical trajectory, $x = v_0t$, $z = \alpha t^2/2m$, $p_0 = mv_0 = \hbar k_0$,

$$\mathbf{p} = \hbar\mathbf{k} = \mathbf{u}_x p_0 - \mathbf{u}_z\alpha t \tag{2.12}$$

to lowest order in α. (The $\mathbf{u}_i$ are unit vectors.)

An equivalent semiclassical wave-packet solution for expressing the propagation along a path from a point r_0 to the point r is

$$\phi = Ap^{-1/2}\exp\left[\frac{i}{\hbar}\left(\int_{r_0}^{r} p\cdot dr - Et\right)\right]u\left(r - \int^t v\,dt\right), \tag{2.13}$$

where the momentum is considered as a function of the classical path at constant energy, between r_0 and r, and both the momentum $p(r)$ and the wave packet u are slowly varying ($\lambda|\partial u/\partial r| \ll |u|$, $\lambda|\partial p/\partial r| \ll |p|$). The exponential controls the phase of the function (and this part of the solution, including the denominator, is the WKB wave function), while the wave packet describes the envelope, which is centered about the classical solution. This solution satisfies the Schrödinger equation under the approximations stated.

This solution is actually equivalent in its effects to that of Eq. (2.8). Consider the following situation, which will be of use later. Imagine an initially horizontal beam of free particles which is split into two parts by some device at point A (see Fig. 1). If the two separate beams are elastically scattered or diffracted through various assortments of crystals, such that the magnitude of the momentum remains p, and the total time taken over the upper and lower paths are the same, then there will be no phase difference between the unperturbed beams when they are recombined at point B (which may be at different height than A).

If now there is a very weak force in the z direction, the difference in phase between the two beams will be, from Eq. (2.8),

$$\psi_1^{(i)} = \psi_{0,1}^{(i)}\exp\left(\frac{-i}{\hbar}\int_{C_i}^{C_{i+1}} U\,dt\right),$$
$$\psi_2 = \psi_{0,2}^{(i)}\exp\left(\frac{-i}{\hbar}\int_{C_i'}^{C_{i+1}'} U\,dt\right), \tag{2.14}$$

where $\psi_{0,1}^{(i)}$ and $\psi_{0,2}^{(i)}$ are the unperturbed wave functions along the ith segment, and $\psi_1^{(i)}$ and $\psi_2^{(i)}$ are the perturbed ones. Then, if T is the total time between A and B,

$$\psi_0(T) = \Pi\psi_{0,1}^{(i)} = \Pi\psi_{0,2}^{(i)} \tag{2.15}$$

and

$$\psi_1(T) = \Pi\psi_1^{(i)} = \psi_0(T)\exp\left(\frac{-i}{\hbar}\int_{ACB} U\,dt\right),$$
$$\psi_2(T) = \Pi\psi_2^{(i)} = \psi_0(T)\exp\left(\frac{-i}{\hbar}\int_{AC'B} U\,dt\right), \tag{2.16}$$

so that

$$\psi_1(T) = \psi_2(T)\exp\left(\frac{-i}{\hbar}\int \Delta U\,dt\right), \tag{2.17}$$

where ΔU is the difference in potential between corres-

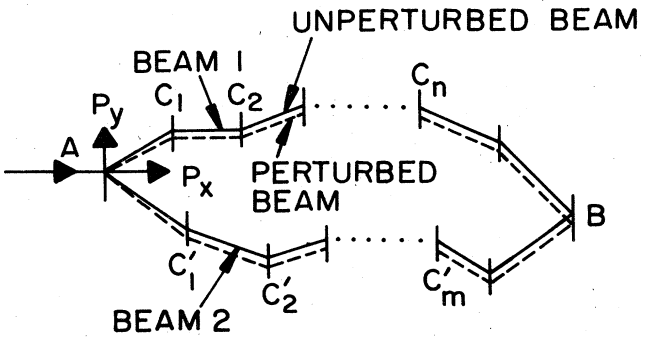

FIG. 1. Effect of very weak force on phase of recombined beam. A beam of particles is split at A into two beams, each of which may be further elastically scattered, such that the time of flight is the same for both unperturbed beams when they are coherently recombined at B. Then $\Psi_1(T) = \Psi_2(T)\exp(-i\int \Delta U\,dt/\hbar)$, where ΔU is the potential difference between corresponding points on paths 1 and 2.

ponding points on paths 1 and 2, i.e., between points reached at equal times along the respective unperturbed classical trajectories. This is an important formula, which we shall use frequently. If the two unperturbed beams reach point B at the same time (which will always be the case for the problems we shall analyze), then even if the perturbed beams reach B at slightly different times, this time difference will produce a second-order effect in the phase integral of Eq. (2.17) and thus can be ignored.

If we look at the same experiment from the point of view of Eq. (2.13), we shall have to integrate along the actual path, which is slightly perturbed from the straight-line paths. For ψ_1, we have

$$\psi_1(z) = \psi_{1,0} \exp\left(\frac{i}{\hbar} \int_A^{z_1} \delta p_z \, dz\right) . \tag{2.18}$$

Now, we have

$$\delta p_z = \int F_z \, dt = - \int \left(\frac{\partial U}{\partial z}\right) dt , \tag{2.19}$$

so that

$$\psi_1(z) = \psi_{1,0} \exp\left\{\frac{-i}{\hbar} \int^t \left[\int_A^{z_1} \left(\frac{\partial U}{\partial z}\right) dz\right] dt\right\}$$

$$= \psi_{1,0} \exp\left(\frac{-i}{\hbar} \int^t (U(z_1) - U(A)) dt\right) ; \tag{2.20}$$

when one carries this over the entire path ACB, and compares it with that over $AC'B$, the total effect will clearly be that given by Eq. (2.17).

Another simple but very important property we shall frequently use concerns the question of how the phase of the wave function at a point is affected by adding a small perturbation U. Assume a free-particle wave is propagating between points A and B. The classical trajectory is shown by AB in Fig. 2. Now let a small perturbation change the trajectory to AB'. We ask what the phase of the distorted wave is as it hits the same point B.

The elapsed phase between A and B is

$$\phi = 2\pi \int \frac{ds}{\lambda} = \int \frac{p \cdot ds}{\hbar} . \tag{2.21}$$

Therefore, the phase will not change unless p changes. However, p will change only if the force has a component along the motion. In other words, if the force is perpendicular to the beam, the beam will bend, but to lowest order the path length will not change.

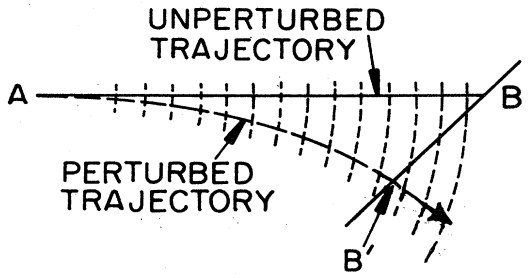

FIG. 2. Insensitivity of phase to the bending of the beam. The bending of the envelope of the beam due to a weak perturbing force (and therefore the shifting of the classical trajectory from AB to AB') has no effect on the phase striking a particular point, B, on a screen. (Of course, if the wavelength changes, it will alter the phase at B.) The phase at B' may be different from that at B, but it too is unaffected by the bending.

If there is a screen in the path of the beam, as in Fig. 2, the center of the envelope of the beam (the classical path) will move from B to B'. And the phase striking B' will be different from that at B if the screen is not normal to the motion, but nonetheless the phase at point B will be the same as before.

Thus there will be no phase change at a fixed point (to lowest order in the external force parameter) due purely to the bending of the beam. However, the phase can still change at a fixed point because of a change in λ, and therefore p; this will happen if the force has a component parallel to the motion. The phase shift due to this will be given by $[(i/\hbar) \int \delta p \, dr]$ or, equivalently, by $[(-i/\hbar) \int U \, dt]$, as given by Eq. (2.8).

Because of the insensitivity of the phase to the bending between neighboring paths, it does not matter whether one integrates along the original path, as in Eq. (2.8), or along the altered path, as in Eq. (2.13), in calculating the phase. In the case of the force parallel to the motion, if one writes $p = p_0 + \delta p$ and $E = p_0^2/2m$, then

$$(p + \delta p)^2/2m + U = E , \quad |\delta p| = -mU/p \tag{2.22}$$

at constant E, and

$$\int |\delta p| dr = \int \delta p \, dr = - \int U \, dr/v = - \int U \, dt , \tag{2.23}$$

showing the equivalence between Eqs. (2.8) and (2.13) in this case also.

B. Scattering from an individual force center

If V represents a short-range potential surrounding a target particle, the Schrödinger equation

$$(H_0 + V)\psi = E\psi , \quad E = E_0 \tag{2.24}$$

can be written as an integral equation

$$|\psi\rangle = |k_0\rangle + (E - H_0)^{-1} V |\psi\rangle , \tag{2.25}$$

where $|k_0\rangle$ represents a free-particle incoming wave, and the second term represents the scattered wave (Baym, 1969, Chap. 9; or any modern quantum mechanics text). In configuration space, the Green's function becomes

$$\langle r | \frac{1}{E - H_0} | r' \rangle = - \frac{2m}{\hbar^2} \left(\frac{1}{2\pi}\right)^3 \int d^3k \, \frac{e^{i\mathbf{k}\cdot(\mathbf{r}-\mathbf{r}')}}{k_0^2 - k^2}$$

$$= - \frac{m}{2\pi\hbar^2} \frac{e^{ik_0|r - r_0|}}{|r - r'|} . \tag{2.26}$$

The asymptotic form of the equation is

$$\psi_{k_f}(r) = e^{i\mathbf{k}_0 \cdot \mathbf{r}} + a_{k_f} e^{ikr}/r , \tag{2.27}$$

where $\mathbf{k}_f = k_0 \mathbf{u}_r$, and

$$a_{k_f} = - \left(\frac{m}{2\pi\hbar^2}\right) \int d^3r' \, V(r') e^{-i\mathbf{k}_f \cdot \mathbf{r}'} \psi_{k_f}(r') \tag{2.28}$$

is the scattering amplitude. In the Born approximation, ψ under the integral becomes $\exp(i\mathbf{k}_0 \cdot \mathbf{r})$ and

$$a_{k_f} = a(\Delta k) = - \left(\frac{m}{2\pi\hbar^2}\right) \int d^3r' \, e^{-i\Delta\mathbf{k} \cdot \mathbf{r}'} V(r') , \tag{2.29}$$

where $\Delta\mathbf{k}=\mathbf{k}_f-\mathbf{k}_0$. For low-energy neutrons, a is a constant independent of direction, the scattering length. In a crystal like silicon, where there is no nuclear spin, a is also independent of the polarization.

If the scattering now takes place in the presence of a weak background field with potential U, the Schrödinger equation can be written

$$(H_0+V+U)\psi=E\psi\,,\quad E=E_0\,. \tag{2.30}$$

If the equation with U alone can be solved, as in Sec. II. A

$$(H_0+U)\phi\equiv H_1\phi=E\phi\,, \tag{2.31}$$

then the scattering equation can be written

$$|\psi\rangle=|\phi_0\rangle+(E-H_1)^{-1}V|\psi\rangle\,. \tag{2.32}$$

This is similar to Eq. (2.25), except that now the solutions of U, the $|\phi\rangle$'s, play the role that the free particles $|k\rangle$ played previously.

The Green's function takes the form

$$\begin{aligned}\langle r|(E-H_1)^{-1}|r'\rangle &= \int d^3k\langle r|\phi_k\rangle\langle\phi_k|(E-H_1)^{-1}|\phi_k\rangle\langle\phi_k|r'\rangle\\ &=-\frac{2m}{\hbar^2}\frac{1}{(2\pi)^3}\\ &\times\int d^3k\,\frac{\exp(i\int\mathbf{k}\cdot\mathbf{dr})\exp(-i\int\mathbf{k}\cdot\mathbf{dr}')}{k_0^2-k^2}\,.\end{aligned} \tag{2.33}$$

In this equation, since H_1 is diagonal in the $|\phi\rangle$, the only difference from Eq. (2.26) is the use of the functions $\langle r|\phi\rangle$ for the plane waves. There are a number of simplifications to be made in Eq. (2.33). First, the equation has poles at $k=\pm k_0$ so only the corrections in this region are important. We write the corrections to the phase factor in the form

$$\exp\left(i\int\mathbf{k}\cdot\mathbf{dr}\right)=\exp[i\mathbf{k}\cdot\mathbf{r}+i\delta\alpha(k,r)]\,. \tag{2.34}$$

Since we shall be integrating later over r' only in the region of the scattering center, and U has a negligible effect over such a small region, we need not bother at all with the $\delta\alpha$ term for the exponential in r'. Finally, as we integrate over d^3k, we note that in the direction of k parallel to r, we are along the classical trajectory, while as we vary the direction, we have seen that for small variations, the phase is independent of the trajectory. In other directions, the phase will vary rapidly and tend to cancel out.

This statement is equivalent to saying that, off the classical direction, the phase varies as the second order in the coupling constant of U. So we can pull the term $\delta\alpha(k,r)$ out of the integral, since only the value of k, in the direction of r, of magnitude k_0, is important to us. We can finally write Eq. (2.32) asymptotically as

$$|\psi_{k_f}\rangle=\exp\left(i\int\mathbf{k}_0\cdot\mathbf{dr}\right)+a_{k_f}\exp\left(i\int\mathbf{k}\cdot\mathbf{dr}\right)/r\,, \tag{2.35}$$

where in the last expression $\mathbf{k}$ is parallel to $\mathbf{r}$. Thus the only changes from the free-particle result are that one must use the phase as modulated by the potential U, in Eq. (2.35), rather than plane waves.

C. Scattering from a crystal

If one has a three-dimensional periodic crystal of scatterers, then the potential $V(r)$ will have the same periodicity as the crystal. If the origin of the nth unit cell is located at

$$\mathbf{r}_n=n_1\mathbf{a}_1+n_2\mathbf{a}_2+n_3\mathbf{a}_3\,,\quad n=(n_1,n_2,n_3)\,, \tag{2.36}$$

where the $\mathbf{a}_i$ are independent vectors defining the periodicity of the crystal (assuming for simplicity one scatterer per unit cell), and the n_i are integers, then within the crystal,

$$V(\mathbf{r}+\mathbf{r}_n)=V(\mathbf{r})\,. \tag{2.37}$$

For distances $\mathbf{r}$ far from that part of the crystal in contact with the incident beam, as well as far from the individual scatterers, we have

$$\psi(r)=e^{i\mathbf{k}_0\cdot\mathbf{r}}+\frac{-m}{2\pi\hbar^2}\left(\int d^3r'\,e^{-i\Delta\mathbf{k}\cdot\mathbf{r}'}V(r')\right)\frac{e^{ikr}}{r} \tag{2.38}$$

where r is measured from an arbitrary point within the crystal. Because of its periodicity, the integral can be broken into a sum over each unit cell $\mathbf{r}'=\mathbf{r}_n+\rho_n$,

$$\begin{aligned}\int d^3r'\,e^{-i\Delta\mathbf{k}\cdot\mathbf{r}'}V(r') &= \sum_n\int d^3\rho_n\\ &\times e^{-i\Delta\mathbf{k}\cdot(\mathbf{r}_n+\rho_n)}V(r_n+\rho_n)\\ &=\sum_n e^{-i\Delta\mathbf{k}\cdot\mathbf{r}_n}\int d^3\rho_n e^{-i\Delta\mathbf{k}\cdot\rho_n}V(\rho_n)\\ &=a(\Delta k)\sum_n e^{-i\Delta\mathbf{k}\cdot\mathbf{r}_n}\,,\end{aligned} \tag{2.39}$$

so that

$$\psi(r)=e^{i\mathbf{k}_0\cdot\mathbf{r}}+\left(a\sum_n e^{i\Delta\mathbf{k}\cdot\mathbf{r}_n}\right)\frac{e^{ikr}}{r}\,. \tag{2.40}$$

An alternate derivation of this result that does not assume the smallness of the crystal is to write separately the scattering amplitudes for each scattering center,

$$\begin{aligned}\psi_n &= e^{i\mathbf{k}_0\cdot\mathbf{x}_n}\\ &+\left(\frac{-m}{2\pi\hbar^2}\int dr'\,V_n(r')e^{-i\Delta\mathbf{k}\cdot\mathbf{r}'}\right)\frac{e^{i\mathbf{k}_0\mathbf{x}_n}}{\mathbf{x}_n}\,,\end{aligned} \tag{2.41}$$

where $\mathbf{x}_n$ is the vector from the atom to the field point and $\mathbf{r}$ is the vector from the arbitrary origin to the field point (Fig. 3). Thus,

$$\mathbf{r}=\mathbf{x}_n+\mathbf{r}_n \tag{2.42}$$

and V_n is the potential centered about the atom at r_n. Since all the scatterers are identical, so are all these integrals. However, we have for $\mathbf{x}_n$,

$$\begin{aligned}\mathbf{x}_n &= |\mathbf{r}-\mathbf{r}_n|=(r^2-2\mathbf{r}\cdot\mathbf{r}_n+r_n^2)^{1/2}\\ &\approx r(1-\mathbf{r}_n\cdot\mathbf{r}/r^2)\approx r-\mathbf{u}_r\cdot\mathbf{r}_n\,,\end{aligned} \tag{2.43}$$

so that

$$k\mathbf{x}_n\approx kr-k\mathbf{u}_r\cdot\mathbf{r}_n=kr-\mathbf{k}\cdot\mathbf{r}_n\,, \tag{2.44}$$

and therefore, since the $\mathbf{x}_n$ in the denominator differs from r only in higher order,

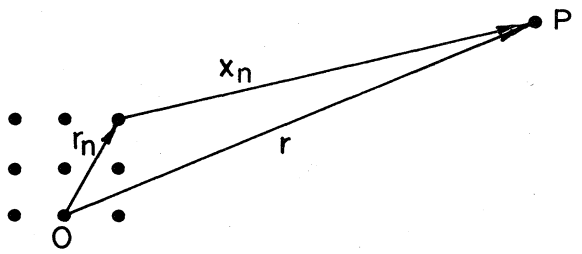

FIG. 3. Geometry of scattering from a crystal. The vector $\mathbf{r}$ is the vector from the origin 0 to the field point P; $\mathbf{r}_n$ is the vector from the origin to atom n of the crystal, and $\mathbf{x}_n$ is the vector from the atom to the field point.

$$\psi_n = e^{i\mathbf{k}_0\cdot(\mathbf{r}-\mathbf{r}_n)} + ae^{ikr}e^{-i\mathbf{k}\cdot\mathbf{r}_n}/r\,. \tag{2.45}$$

We now add up all the amplitudes. However, they all receive the same incident wave $e^{i\mathbf{k}_0\cdot\mathbf{r}}$, so we must multiply ψ_n by a phase factor to reflect this fact,

$$\psi_n' = e^{i\mathbf{k}_0\cdot\mathbf{r}_n}\psi_n = e^{i\mathbf{k}_0\cdot\mathbf{r}} + ae^{ikr}e^{-i(\mathbf{k}-\mathbf{k}_0)\cdot\mathbf{r}_n}/r$$
$$= e^{i\mathbf{k}_0\cdot\mathbf{r}} + (ae^{-i\Delta\mathbf{k}\cdot\mathbf{r}_n})e^{ikr}/r\,. \tag{2.46}$$

The total scattered wave will be the contribution from all of the scattering parts of the ψ_n', so finally,

$$\psi = e^{i\mathbf{k}_0\cdot\mathbf{r}} + \sum_n \psi_{n,\text{scat}}'$$
$$= e^{i\mathbf{k}_0\cdot\mathbf{r}} + \left(a\sum e^{-i\Delta\mathbf{k}\cdot\mathbf{r}_n}\right)\frac{e^{ikr}}{r}\,. \tag{2.47}$$

The sum $\sum \exp(-i\Delta\mathbf{k}\cdot\mathbf{r}_n)$ will add to zero, unless all the contributions are in phase, which will happen when $\Delta\mathbf{k}$ is an integral sum of reciprocal-lattice vectors $\mathbf{K}_i$ defined by

$$\mathbf{K}_i\cdot\mathbf{a}_j = 2\pi\,\delta_{ij}\,. \tag{2.48}$$

This relation, together with energy conservation

$$k^2 = (\mathbf{k}_0+\Delta\mathbf{k})^2 = k_0^2\,, \tag{2.49}$$

gives the Bragg condition as a necessary prerequisite to getting a scattered wave (Peierls, 1955; or Slater, 1958). Along such directions, which satisfy the Bragg conditions (see Fig. 4)

$$(n\mathbf{K})^2 + 2\mathbf{k}_0\cdot n\mathbf{K} = 0\,,$$
$$\tfrac{1}{2}nK = k_0\sin\theta\,,\quad K = 2\pi/d\,,\quad k_0 = 2\pi/\lambda\,, \tag{2.50}$$
$$n\lambda = 2d\sin\theta\,,$$

(where d is the atomic spacing), we have

$$e^{-i\Delta\mathbf{k}\cdot\mathbf{r}_n} = \begin{cases} N, & \text{along Bragg directions}\,, \\ 0, & \text{elsewhere}\,, \end{cases} \tag{2.51}$$

where N is the number of scatterers in the crystal. If the Bragg conditions are met, then the wave function will be

$$\psi = e^{i\mathbf{k}_0\cdot\mathbf{r}} + Nae^{ikr}/r\,. \tag{2.52}$$

Now if there is a small background perturbing potential U, of the type described previously, the wave function of Eq. (2.52) will be altered in the manner of Eq. (2.35), namely the factors $\mathbf{k}\cdot\mathbf{r}$ and kr will become integrals along the classical path of the displaced beam.

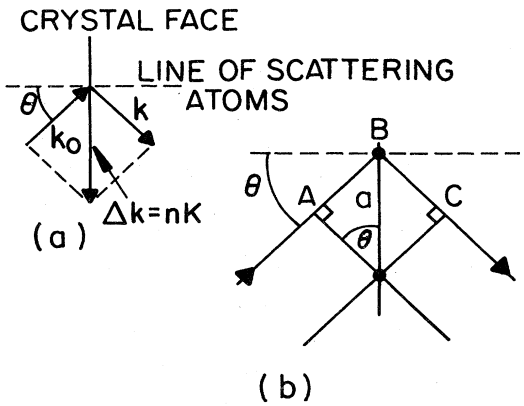

FIG. 4. Bragg condition for Laue scattering. (a) The scattered and incident wave vectors are connected by $|\Delta k| = 2n|k| = 2|k_0|\sin\epsilon$. (b) The path difference ABC is given by $ABC = n\lambda = 2a\sin\theta$.

If the incident wave is Bragg scattered (or Laue scattered, with transmission) by a crystal, the scattered waves will have to be rescattered by a second crystal if they are to be coherently recombined again (Fig. 5), as was done by COW, as well as by Bonse and Hart. But if the beam has been displaced by a perturbing force, it will hit the second crystal at a slightly different angle, and so will no longer satisfy the Bragg condition.

This statement is true even though the phase at a given point, where it strikes the crystal, will be unchanged by the bending of the beam, as we have shown. But the envelope determining the intensity of the beam will follow its classical trajectory, and so will arrive slightly out of line.

How then can the beam be rescattered? One way is to accomplish the scattering by a thin film or grating, rather than a thick crystal. In this case the scattering is only two dimensional, and there is no restriction on the normal direction. Thus, one can always solve the equations to find a scattered direction, where both the diffraction conditions and energy conservation hold. This was the case in the Marton experiment we shall

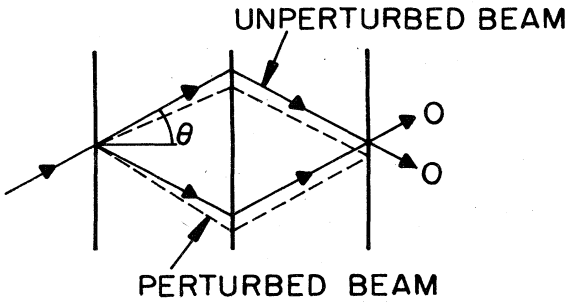

FIG. 5. Effect of a perturbation on the Bragg condition. For a coherent recombination of the beam, it must be scattered off successive crystal faces. In the presence of a perturbing force, the bending of the beam can misalign the beam, so that the Bragg condition is no longer satisfied, and reflection will no longer take place.

describe later.

However, in the case of a thick crystal, one has three Bragg conditions, and the momentum is completely specified. Only at the Bragg angles is energy conserved as well. Thus, the only way one can Bragg scatter such a wave is if the Bragg condition does not hold perfectly.

There are two important reasons why it will not. The first is the finite size of the crystal, and of the beam being scattered. This leads to diffraction phenomena, so that the beam is spread out. The second reason depends on the nature of the crystal itself. Because of the interaction with the scatterers within the crystal, the beam as it propagates through the crystal is not a perfectly free-particle beam. Thus the dispersion relation defining the energy $\omega(k)$ will be different inside and outside the crystal. For a small range of k values around the Bragg angle, it will not be possible to match them perfectly, and one will have perfect reflection in the Bragg case, and a high degree of reflection in the Laue case. This phenomenon is intimately connected with the existence of forbidden regions in the theory of energy bands within the crystal. This effect for the COW experiment is discussed in Sec. III (and plotted in Fig. 15) and the width of the region of reflection about the Bragg angle in that case turns out to be about 1 sec or arc, or 5×10^{-6} rad.

We can also estimate the opening for Bragg scattering due to the finite size of the crystal. Either from simple optical considerations, such as from Eq. (2.71), or directly from the uncertainty principle, one can say

$$\delta\theta \sim \sin\theta_0/N_1 , \tag{2.53}$$

where N_1 is the number of scatterers in a linear array. For the COW experiment, the beam width was 3×6 mm, so that $N_1 \sim 1.8\times10^7$, and

$$\delta\theta \sim 0.38/1.8\times10^7 \sim 2\times10^{-8} \text{ rad}. \tag{2.54}$$

The crystal interaction effect is much larger, and therefore represents the actual spread about the Bragg angle. The bending of the beam due to gravity is determined by

$$y \sim \tfrac{1}{2}gt^2 \sim gL^2/2v^2\cos^2\theta \sim 3.8\times10^{-7} \text{ cm}. \tag{2.55}$$

(The experimental parameters for the COW experiment are quoted in Sec. III. A.) This corresponds to an angular deflection of approximately

$$\delta\theta_{\text{grav}} \sim 2y/L \sim 1.1\times10^{-7} \text{ rad}. \tag{2.56}$$

This assumes that gravity was 100% effective in bending the beam (a rotation of 90° for the crystal). Actually coherence was lost when the beam was rotated by about $\phi \sim 20°$. Therefore, for the effective gravitational field,

$$g_{\text{eff}} \sim g\sin\phi \sim 0.34g , \tag{2.57}$$

so that

$$(\delta\theta_{\text{grav}})_{\text{eff}} \sim 0.34\delta\theta_{\text{grav}} \sim 3.8\times10^{-8} \text{ rad}. \tag{2.58}$$

This is two orders of magnitude smaller than the region available for reflection, and would indicate that gravity was too weak to bend the beam sufficiently to destroy the reflection condition. (It is also one order of magnitude smaller than the innermost pendellösung fringe in Fig. 15.)

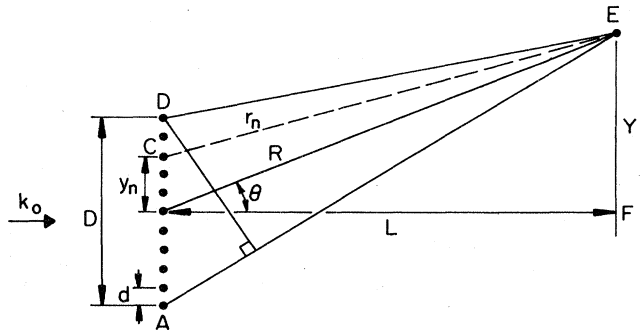

FIG. 6. Geometry of scattering of a two-dimensional crystal. The width of the beam is D, and the atomic spacing is d. The distance from the center of the beam B to the field point E is R, and the angle is θ. The nth atom is located at C, at a height y_n above the center of the beam, and its distance to E is r_n. The field point itself is at a height Y above B, and at a perpendicular distance L from the scattering plane.

D. Behavior of the beam envelope

Another effect which is very important in understanding crystal diffraction experiments concerns the behavior of the envelope of the scattered wave. For simplicity, we shall analyze a two-dimensional crystal, since the same result will hold in three dimensions. Imagine a finite beam of width D impinging on the crystal, and scattering into the angle θ, as in Fig. 6. Because of the finite width, we must consider the incident beam as having a spread in y momentum,

$$\psi_{\text{inc}} = e^{ik_0x}(2\pi)^{-1/2}\int dk_y \tilde{f}(k_y)e^{ik_yy} = e^{ik_0x}f(y) , \tag{2.59}$$

where $\tilde{f}$ is the Fourier transform of f. Since the width of the beam is D, which will determine the spread in angle, then $\delta\theta \sim \sin\theta/N$, where N is the number of atoms included within the beam, $N=D/d$; this will also determine the spread Δk_y which we must consider.

In order to examine this spread, we shall have to consider our scattering amplitude in more detail. Equation (2.27) determines the amplitudes as a function of the incident momentum k_0, and the scattering angle θ is measured from this direction. If we take the incident beam to have a y component of momentum, as in Eq. (2.59), then it will be traveling at some angle from the direction k_0, and will therefore scatter at a different angle (see Fig. 7).

We are interested in one component of Eq. (2.59),

$$e^{i(k_0x+k_yy)} = e^{i\mathbf{k}\cdot\mathbf{r}} , \tag{2.60}$$

where $k_y \ll k_0$. If we write $\mathbf{k}=R(\varphi)\mathbf{k}_0$, where R is the appropriate rotation operator, then

$$\psi_{\mathbf{k}}(R\mathbf{r}) = \psi_{R\mathbf{k}_0}(R\mathbf{r}) = \exp(iR\mathbf{k}_0\cdot R\mathbf{r}) - \frac{e^{ik_0r}}{r}\frac{m}{2\pi\hbar^2}\int d^3(R\mathbf{r}')V(r')\exp[(-i)(k_0R\mathbf{u}_r\cdot R\mathbf{r}' - R\mathbf{k}_0\cdot R\mathbf{r}')] = \psi_{\mathbf{k}_0}(\mathbf{r}) , \tag{2.61}$$

where we label the wave function by its incident direction, and have assumed that the potential is a function of $|\mathbf{r}'|$.

Therefore the scattering of $\mathbf{k}$ into angle $(\theta+\varphi)$ will be the same as that of $\mathbf{k}_0$ into angle θ. This proof also shows that

$$\psi_{\mathbf{k}}(\mathbf{r}) = \psi_{R\mathbf{k}_0}(\mathbf{r}) = \psi_{\mathbf{k}_0}(R^{-1}\mathbf{r}) . \tag{2.62}$$

The integral in the scattered wave of Eq. (2.61) is

$$\begin{aligned}\int d^3r'\, V(r') \exp[(-i)(k_0 R^{-1}\mathbf{u}_r \cdot \mathbf{r}' - \mathbf{k}_0 \cdot \mathbf{r}')] &= \int d^3r'\, V(r') \exp[(-i)(k_0 \mathbf{u}_r \cdot R\mathbf{r}' - R\mathbf{k}_0 \cdot R\mathbf{r}')] \\ &= \int d^3r'\, V(r') \exp[(-i)(k_0 \mathbf{u}_r \cdot \mathbf{r}' - R\mathbf{k}_0 \cdot \mathbf{r}')] \\ &= \int d^3r'\, V(r') \exp[(-i)(k_0 \mathbf{u}_r \cdot \mathbf{r}' - k_0 x' - k_y y')] ,\end{aligned} \tag{2.63}$$

while the incident wave is $\exp[i(k_0 x + k_y y)]$. Multiplying by $\tilde{f}(k_y)$ and integrating over k_y gives

$$\psi = f(y) e^{ik_0 x} - \frac{e^{ik_0 r}}{r} \frac{m}{2\pi\hbar^2} \times \int d^3r'\, V(r') f(y') e^{-i\Delta\mathbf{k}\cdot\mathbf{r}'} . \tag{2.64}$$

Thus the scattered wave is weighted by $f(y')$. For the nuclear case, where $V(r')$ is concentrated over a very small region around the nucleus y_n, Eq. (2.64) leads to

$$\psi_{sc,n} = a_n(\Delta k) f(y_n) e^{ikr_n}/r_n , \tag{2.65}$$

as might have been anticipated (and where r has been replaced by the r_n of the specific nucleus, from Fig. 6).

The distance from the nucleus to the field point E in Fig. 6 is

$$r_n = (R^2 - 2y_n R \sin\theta + y_n^2)^{1/2} \approx R - y_n \sin\theta , \tag{2.66}$$

so that Eq. (2.65) becomes, assuming all the a_n are equal,

$$\begin{aligned}\psi_{sc} = \Sigma\psi_{sc,n} &= [a\Sigma f(y_n) e^{-iky_n \sin\theta}] e^{ikR}/R \\ &= [a\Sigma f(nd) e^{-iknd \sin\theta}] e^{ikR}/R ,\end{aligned} \tag{2.67}$$

and therefore

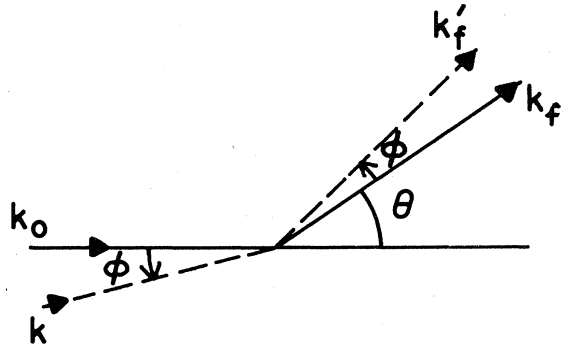

FIG. 7. Spread of incident beam. If the incident beam is spread about the incident direction $\mathbf{k}_0$, we need the following theorem to analyze the scattering, which follows from rotational invariance. The scattering amplitude for scattering from direction $\mathbf{k}_0$ into direction $\mathbf{k}_f$, at an angle of θ, is the same as the scattering amplitude for scattering from direction $\mathbf{k}$ into direction $\mathbf{k}_f'$, at an angle θ, where $\mathbf{k}$ differs from $\mathbf{k}_0$ by having been rotated through an angle φ, and $\mathbf{k}_f'$ differs from $\mathbf{k}_f$ by the same rotation.

$$\psi_{sc} = (a\tilde{f}(kd \sin\theta)) e^{ikR}/R , \tag{2.68}$$

where we have used the fact that the y_n are equally spaced,

$$y_n = nd , \quad -\infty < n < +\infty . \tag{2.69}$$

In Eq. (2.68), $\tilde{f}$ represents the Fourier *series* amplitude, since $f(y)$ is now a periodic function. The function $\tilde{f}$ is also periodic, and has the period of the reciprocal lattice, and peaks very sharply at the various diffraction maxima.

We see that the scattering amplitude is weighted by the transform of the shape of the incident beam. If the beam were infinitely wide, the $\tilde{f}$'s would be δ functions. For a finite beam of width $D = Nd$,

$$f(y_n) = \begin{cases} 1, & -\tfrac{1}{2}N \le n \le \tfrac{1}{2}N , \\ 0, & \text{otherwise} , \end{cases} \tag{2.70}$$

the envelope will be determined by

$$\begin{aligned}\tilde{f} = \Sigma f(y_n) e^{-iky_n \sin\theta} &= \sum_{-N/2}^{N/2} e^{-(ikd \sin\theta)n} \\ &= \frac{\sin(\frac{1}{2}Nkd \sin\theta)}{\sin(\frac{1}{2}kd \sin\theta)} ,\end{aligned} \tag{2.71}$$

which is strongly peaked in the directions θ_j given by the diffraction condition $\frac{1}{2}kd \sin\theta_j = j\pi$, $j\lambda = d \sin\theta_j$. About each order there is an envelope of width

$$\delta(\sin\theta) \sim \lambda/Nd . \tag{2.72}$$

For the function of Eq. (2.71) we can use the approximation

$$\begin{aligned}\tilde{f}_0 &= \sin(\tfrac{1}{2}Nkd \sin\theta)/\sin(\tfrac{1}{2}kd \sin\theta) \\ &\sim N \exp[-\tfrac{1}{24}(N^2k^2d^2 \sin^2\theta)] .\end{aligned} \tag{2.73}$$

In higher orders we can write, in general, since $\tilde{f}$ is periodic,

$$\tilde{f} = \Sigma\tilde{f}_j = \Sigma\tilde{f}_0(kd(\sin\theta - \sin\theta_j)) , \tag{2.74}$$

and consider only the central maximum in each order. Finally, we can write the scattered wave as a sum of each diffraction order

$$\psi_{sc} = \sum_j \psi_{sc}^{(j)} = \left(a \sum_j \tilde{f}_0(kd(\sin\theta - \sin\theta_j))\right) \frac{e^{ikR}}{R} , \tag{2.75}$$

where the phase $\exp(ikR)$ radiates out uniformly in all

directions, but the amplitude is sharply attenuated in almost all directions, namely, those not close to a diffraction peak, by the envelope factor $\tilde{f}_0$.

We can now inquire as to how this is affected by the presence of a perturbing background potential U. We have already seen that at a fixed point there is no change in phase due to the bending of the beam. Nonetheless there is a definite effect, due to the phase factor of Eq. (2.8), which takes into account the changing wavelength. For simplicity we shall assume that there is a field in the $-y$ direction, with potential αy. To calculate the integrated phase factor $\int U\,dt$ along path r_n (see Fig. 6), we note that along the path from C to E, the average height is $\frac{1}{2}(y_n+Y)$, and so

$$\int_0^T U\,dt = \alpha\bar{y}T = \tfrac{1}{2}\alpha(y_n+Y)T\,, \tag{2.76}$$

where

$$T = R/v_0 = L/v_0\cos\theta\,, \quad Y = L\tan\theta\,. \tag{2.77}$$

Thus, the scattered wave function becomes, in Eq. (2.67), using the modification of Eq. (2.35),

$$\begin{aligned}\psi_{sc} &= [a\Sigma f(y_n)\exp(-iky_n\sin\theta)\\ &\quad\times\exp(-i\alpha(y_n+Y)T/2\bar{n}]e^{ikR}/R\\ &= [a\tilde{f}(kd\sin\theta+\alpha dT/2\bar{n})]\\ &\quad\times\exp(i(kR-\alpha YT/2\bar{n}))/R\,.\end{aligned} \tag{2.78}$$

Therefore we see that although there is no extra effect to be accounted for directly by the bending of the beam, the phase shift accomplishes two separate tasks. First, by shifting the argument of $\tilde{f}$, it lowers the envelope. To calculate this lowering at one of the maxima, we write

$$\theta_j \to \theta_j' = \theta_j + \delta\theta_j\,, \tag{2.79}$$

where

$$kd\sin\theta_j' + \alpha dT/2\bar{n} = kd\sin\theta_j\,, \tag{2.80}$$

so that

$$\delta(\sin\theta_j) = \cos\theta_j\delta\theta_j = -\alpha T/2\bar{n}k\,. \tag{2.81}$$

This gives the change in angle. To see how far the shift is in Y, the height at the screen, we use

$$Y = L\tan\theta_j\,, \quad \delta Y = L\sec^2\theta_j\delta\theta_j\,, \tag{2.82}$$

which gives, with Eq. (2.81),

$$\delta Y = L\sec^2\theta_j\left(\frac{-\alpha T}{2\bar{n}k\cos\theta_j}\right) = -\frac{L\alpha T}{2mv_0\cos^3\theta_j}\,. \tag{2.83}$$

Then, using $L/v_0 = R\cos\theta_j/v_0 = T\cos\theta_j$, we get

$$\delta Y = -(1/\cos^2\theta_j)\tfrac{1}{2}(\alpha/m)T^2 = -(1/\cos^2\theta_j)\delta y_\alpha\,, \tag{2.84}$$

where δy_α is the displacement due to the force α, since the acceleration is $-\alpha/m$. Thus, for small angles θ_j,

$$\delta Y_j \approx \delta y_\alpha \tag{2.85}$$

and

$$\psi_{sc} = [a\tilde{f}(kd(\sin\theta-\sin\theta_j'))]e^{i(kR-\alpha YT/2\bar{n})}/R\,, \tag{2.86}$$

where θ_j' is the displaced value of θ_j.

Therefore, we see that for small angles of scattering, the envelope shifts down to keep step exactly with the classical falling of the wave packet. But the second effect we alluded to is that there is also a shift in phase of the wave packet, in Eq. (2.86). In order to interpret this phase shift, imagine that the beam is allowed to interfere with another coherent beam, scattered off another plane with angle ϕ_j, not necessarily parallel to the first plane, and the resultant pattern is viewed on a vertical screen at some point (Fig. 8).

The angle between the beams is $\beta = \theta_j - \phi_j$. The diagonal distance between wave fronts is $l = \lambda/\sin\beta$. The lines of maxima (AA', BB', and CC') propagate at angle γ from the horizontal, where $\gamma = \phi_j + \frac{1}{2}\beta = \frac{1}{2}(\theta_j+\phi_j)$. The distance between parallel lines of maxima (AA' to BB')

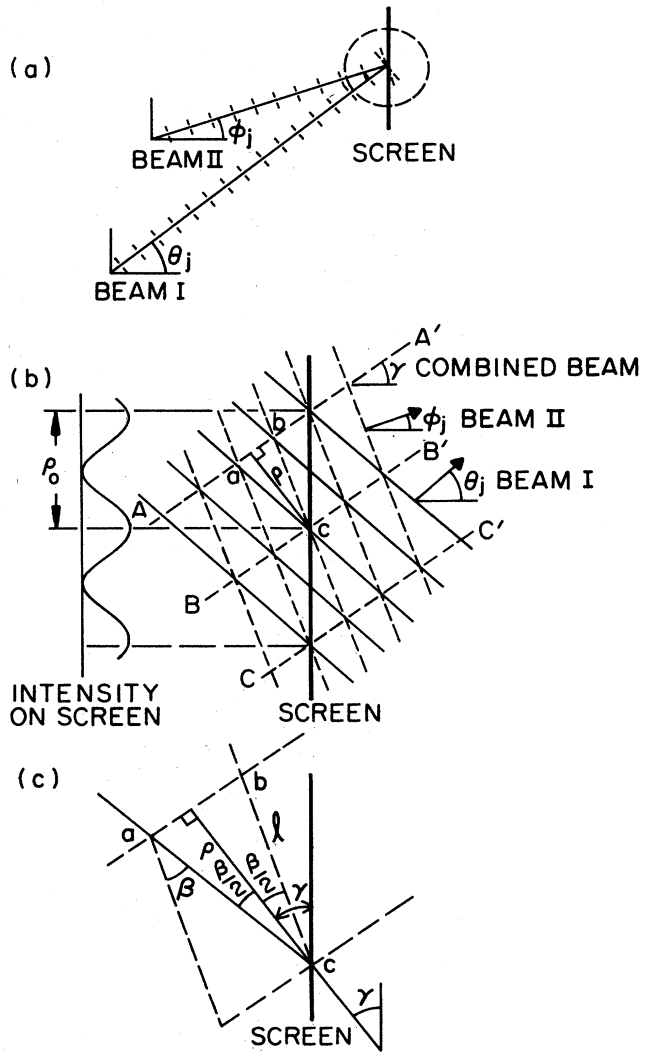

FIG. 8. Interference pattern of two beams on a screen. (a) Beam I, at angle θ_j to the horizontal, and Beam II, at angle ϕ_j, produce an interference pattern at a screen. The circled region is blown up in (b). (b) Successive maxima lie along lines AA', BB', and CC'; they produce a pattern on the screen with maxima separated by distance ρ_0. The lines AA', etc., are at an angle $\gamma = \frac{1}{2}(\theta_j+\phi_j)$ with the horizontal. (c) A blowup of the triangle abc, showing the angular relationships.

is

$$l\cos(\tfrac{1}{2}\beta) = [\lambda\cos(\tfrac{1}{2}\beta)]/\sin\beta = \lambda/2\sin(\tfrac{1}{2}\beta) \equiv \rho\,. \qquad (2.87)$$

Therefore, on the vertical screen, the distance between maxima is $\rho/\cos\gamma = \lambda/2\sin(\frac{1}{2}\beta)\cos\gamma \equiv \rho_0$, so that

$$\lambda = 2\rho_0 \sin\tfrac{1}{2}(\theta_j - \phi_j)\cos\tfrac{1}{2}(\theta_j + \phi_j)$$
$$= \rho_0(\sin\theta_j - \sin\phi_j)\,. \qquad (2.88)$$

Now the phase angle $k(R - \alpha YT/2\hbar k)$ of Eq. (2.86) has the interpretation of changing R by the amount

$$\alpha YT/2\hbar k = \alpha L\tan\theta_j T/2mv_0$$
$$= (\alpha/2m)(T\cos\theta_j)T\tan\theta_j$$
$$= (\alpha T^2/2m)\sin\theta_j = \delta y_\alpha \sin\theta_j\,. \qquad (2.89)$$

If we assume (without loss of generality, since it merely removes an overall constant) that the two beams have traveled the same time before recombining, then their difference in phase will be, from Eq. (2.89),

$$k\delta y_\alpha(\sin\theta_j - \sin\phi_j) = k\delta y_\alpha\lambda/\rho_0 = 2\pi\,\delta y_\alpha/\rho_0\,; \qquad (2.90)$$

but this means that every time the beam drops by $\delta y_\alpha = \rho_0$, the pattern shifts by one fringe. So the phase shift exactly keeps up with the falling of the beam!

We have therefore derived the following result. If two beams are allowed to interfere, then in the presence of a perturbing force, the envelopes of the beams will drop according to the classical trajectories. But the phase of the interference fringes will also change in such a way that these fringes will shift at exactly the same rate. Thus the interference pattern will remain identical, except that it will be shifted by the amount of the classical motion (Fig. 9). Thus this effect, which has been beautifully confirmed experimentally[5] for the propagation of perturbed free-particle beams, is also true for the interference of particles diffracted off crystals.

In this and subsequent analyses we shall make constant use of the fact that the effect of the perturbation consists of a change in phase of the beam, as given by Eq. (2.8), which is caused by the change in wavelength. This effect produces all the shifts in fringes and in the envelope that occur, as we have seen. There is no extra effect due to the bending of the classical center of the beam (it has been taken into account by the phase shift). Alternatively, one could directly take account of the change in wavelength, as a way of calculating the phase factor. But in no case is there any extra correction to the phase at a particular point due to the bending of the beam.

III. PROPAGATION OF NEUTRONS THROUGH A THICK CRYSTAL

A. Transmission through a perfect crystal

When a beam of neutrons strikes a crystal, to a first approximation the beam will be totally transmitted. It is only when a line of atomic planes is so situated as to produce coherent constructive interference that reflection can take place at a specific angle, the Bragg angle. In that case there are two very different physical situations that can occur. If the reflecting planes are parallel to the face of the crystal, one has the classic Bragg case, and the incident beam will be reflected back out of the crystal. There will be a small but finite range of angles in the neighborhood of the Bragg angle, the Bragg "mirror" region, where this reflection will be total. Outside of this region the reflectivity drops rapidly to zero.

[5]See the discussion of the Aharonov-Bohm effect, Sec. V.

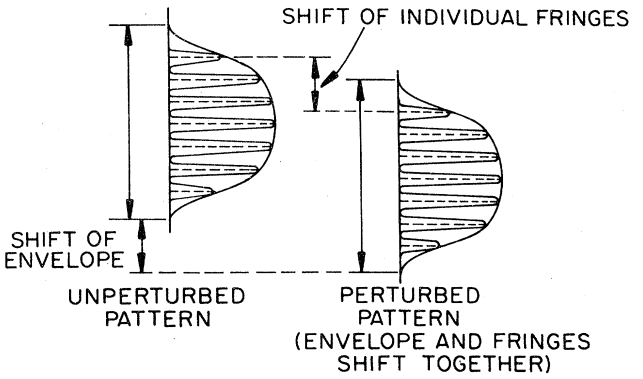

FIG. 9. Effect of perturbing force on interference pattern. In the presence of the perturbation, the individual fringes and the overall envelope, representing the classical trajectories, shift together, so that the interference pattern remains identical, but displaced. (An exception occurs in the pure Aharonov–Bohm effect, Sec. V, where there is no force on the two beams, so that the fringes shift within the envelope, but the envelope itself remains undisplaced.)

But if the scattering planes are so situated that the reflected beam is inside the crystal (for example in a cubic crystal, for scattering off a plane perpendicular to the face of the crystal—see Fig. 10) then one has the case of Laue scattering. In this case the reflection is not complete at the Bragg angle, and its falloff is more gradual as one moves further away from the Bragg angle. In the Laue case, there are also additional phenomena that occur, one of which will be very important for us, the Borrmann effect.[6]

To understand this effect, assume that the incident wave is $e^{ik\cdot r}$, where the y direction is the direction parallel to the crystal, in the plane defined by the di-

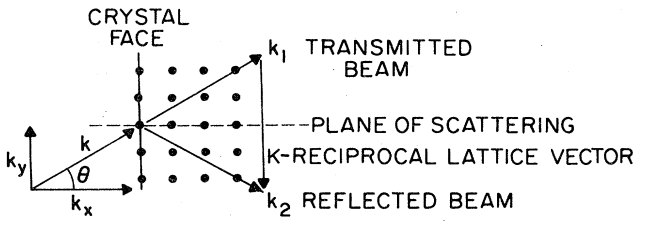

FIG. 10. Geometry of Laue scattering. The incident beam k has the same wave vector as the transmitted beam k_1, and differs from the reflected beam k_2 by a lattice vector K for perfect Bragg reflection.

[6]This effect was first systematically studied by Borrmann, 1950, although it was first noticed in Borrmann, 1941. It was independently described by Campbell, 1951a, b. The Borrmann effect was first explained theoretically by von Laue, 1949. It is treated in detail by Battermann and Cole, 1964. It is also discussed from a field-theoretic point of view by Ashkin and Kuriyama, 1966.

rection of propagation and the normal to the crystal—the plane of the paper in Fig. 10—and the x direction is perpendicular to the crystal face. The direction of propagation k is close to that producing Bragg reflection off the atoms in the x-z plane (the z axis is out of the paper in Fig. 10. As the wave strikes the crystal it will continue to propagate in the x direction. But if the crystal is perfect and sufficiently thick, then the crystal itself will play the role of a waveguide, so that the behavior of the beam is best understood by considering the appropriate standing waves in the y direction, which propagate along the x axis, rather than the two plane waves represented by k_1 and k_2 in Fig. 10. These standing waves are then guided in the x direction along the line of atoms, and will emerge at the far end of the crystal where they will form the two traveling waves propagating in the directions k_1 and k_2.

We shall carry our discussion through in only enough detail to give a qualitative picture of the transmission process, because this is sufficient to yield an understanding of the various experiments which have been done to date that relate to the coherence properties of separated and recombined beams of neutrons and x rays. For this, one does not need to know the details of the dynamical theory of wave propagation. For a discussion that offers a much more comprehensive treatment of the phenomena involved, see Rauch and Petrascheck (1979).

For both the Bragg and the Laue cases, one must examine the Schrödinger equation inside the crystal, and match the wave function of the free particle outside the crystal with that of the particle propagating inside the crystal. The interesting case, when reflection occurs, happens when these two functions behave very differently, namely, in the neighborhood of a zone boundary.

Because for low-energy neutrons the potential is nonzero only at the locations of the atomic nuclei in the crystal, which results only in s-wave scattering, we can consider the potential to be a sum of δ functions located at each of the atomic nuclei,

$$V(\mathbf{r}) = \frac{L^3}{N}\sum_n V_0\delta(\mathbf{r}-\mathbf{a}_n) = V_0\sum_s e^{i\mathbf{k}_s\cdot\mathbf{r}}\,, \tag{3.1}$$

where we have expanded the δ function in a Fourier series, over the size of the unit cell, so that every reciprocal-lattice constant $\mathbf{K}_s$ appears with equal amplitude. The expansion will automatically have the correct periodicity. The atomic locations themselves are $\mathbf{a}_n = (n_1a_x, n_2a_y, n_3a_z)$. Here L is the size of the crystal, which contains N atoms, and V_0 must be interpreted as the average nuclear potential over the unit cell. One can express V_0 in terms of the measurable parameter, the scattering length b, a constant which plays the role of the scattering amplitude a of the last section. If d is the atomic spacing, then $d = L/N^{1/3}$ (for a cube) and (Blatt and Weisskopf, 1952)

$$V_0 \sim 2\pi\hbar^2 b/md^3\,, \tag{3.2}$$

which in this form depends on the parameter b [the a of Eqs. (2.29) and (2.52)] and not on the shape of the potential well. (The quantity d^{-3} is also the nuclear density.) With a simple multiplicative factor, one can also correct this for the reduced mass of the neutron-crystal nucleus, and also for the finite temperature of the crystal. In general, the various nuclei in the unit cell must be weighted differently, via the nuclear structure factor, which need not concern us here.

With this potential, Eq. (3.1), we can set up the Schrödinger equation for the propagation of neutrons inside the crystal. If we write the solution in the form of a Bloch function

$$\psi = e^{i\mathbf{k}_0\cdot\mathbf{r}}\Sigma A_n e^{i\mathbf{K}_n\cdot\mathbf{r}}\,, \tag{3.3}$$

then the Schrödinger equation becomes (Slater, 1958)

$$\begin{aligned} &-(\hbar^2/2m)\nabla^2\psi + V\psi = E\psi\,,\\ &(\hbar^2/2m)\Sigma(\mathbf{k}_0+\mathbf{K}_n)^2A_n e^{i\mathbf{K}_n\cdot\mathbf{r}} \\ &+ V_0\Sigma A_n e^{i(\mathbf{K}_s+\mathbf{K}_n)\cdot\mathbf{r}} = E\Sigma A_n e^{i\mathbf{K}_n\cdot\mathbf{r}}\,. \end{aligned} \tag{3.4}$$

If we change the labeling $(\mathbf{K}_n+\mathbf{K}_s-\mathbf{K}_n)$ in the second term and equate coefficients of each $\exp(i\mathbf{K}_n\cdot\mathbf{r})$ term, then

$$(\mathbf{k}_0+\mathbf{K}_n)^2A_n + \sum_s V_0A_{n-s} = EA_n\,. \tag{3.5}$$

[In this equation we have swallowed the $(\hbar^2/2m)$ factor into the definition of k.]

Since we are near the Bragg angle, only the two waves k_1 and k_2 of Fig. 11 (which are different for the Bragg and Laue cases) will be strongly interacting, and if we call their difference K,

$$\mathbf{k}_2 = \mathbf{k}_1 + \mathbf{K}\,, \tag{3.6}$$

and let $k_2^2 = k_1^2$, then, since in this case the incident wave $\mathbf{k}_0$ is just $\mathbf{k}_1$, we have from Eq. (3.5),

$$\begin{aligned} &k_1^2A_1 + V_0A_1 + V_0A_2 = EA_1\,,\\ &(\mathbf{k}_1+\mathbf{K})^2A_1 + V_0A_2 + V_0A_1 = EA_2\,. \end{aligned} \tag{3.7}$$

Since $(\mathbf{k}_1+\mathbf{K})^2 = k_2^2 = k_1^2$, the secular equation becomes

$$(k_1^2 + V_0 - E)^2 - V_0^2 = 0\,, \tag{3.8}$$

with solutions

$$E = k_1^2 + \begin{cases} 2V_0\,, \\ 0\,. \end{cases} \tag{3.9}$$

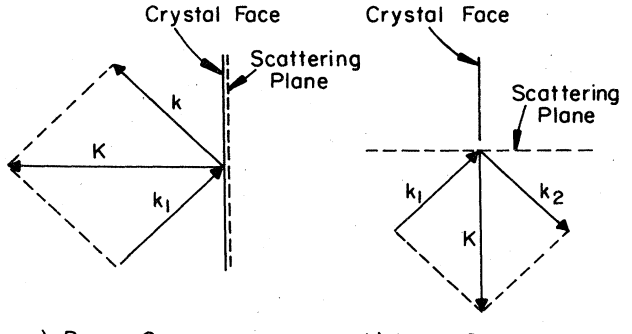

a) Bragg Case b) Laue Case

FIG. 11. Relation between the strongly interacting waves in the crystal. (a) In the Bragg case the appropriate lattice vector, $\mathbf{K} = \mathbf{k}_2 - \mathbf{k}_1$, is perpendicular to the crystal face. (b) In the Laue case the lattice vector is parallel to the crystal face (for a cubic crystal).

The solutions (A_1, A_2) mix the two waves with equal amplitudes. The solutions are

$$(A_1, A_2) = 2^{-1/2}(1, 1);\ 2^{-1/2}(1, -1). \tag{3.10}$$

In the Bragg case, the interacting waves are $A_1 = (k_x, k_y)$ and $A_2 = (-k_x, k_y)$, while in the Laue case the two waves are $A_1 = (k_x, k_y)$ and $A_2 = (k_x, -k_y)$. In the Bragg case, in the mirror region close to the Bragg angle, there will be no real solutions for the energy because the solutions to the secular equation produce an energy gap. At the edge of the region, the energy outside the crystal is of the form $E_{\text{out}} = \hbar^2 k_0^2/2m$, while inside, E_{in} is given by Eq. (3.8). In order to have a solution that is continuous everywhere along the crystal face, which also possesses a continuous first derivative, we must have $(k_y)_{\text{in}} = (k_y)_{\text{out}}$. Then, since the frequency will be the same inside and out, only k_x can differ between the two cases (see Fig. 12).

It then becomes impossible to match these solutions because inside the Bragg region any solution to the wave equation will damp in the y direction. One can see this by trying to solve Eq. (3.8) for k_1 as a function of the energy. Now we cannot satisfy the Bragg condition, so we cannot say $k_2^2 = k_1^2$. If we write

$$\mathbf{k}_1 = k_x \mathbf{u}_x + (-\tfrac{1}{2}K + \eta)\mathbf{u}_y, \tag{3.11}$$

where η is a small perturbation about the Bragg condition and the $\mathbf{u}_i$ are unit vectors, then the secular equation (3.8) becomes

$$(k_x^2 + (\tfrac{1}{2}K - \eta)^2 + V_0 - E)(k_x^2 + (\tfrac{1}{2}K + \eta)^2 + V_0 - E) - V_0^2 = 0. \tag{3.12}$$

If we write

$$\sigma \equiv k_x^2 + V_0 - E, \tag{3.13}$$

this becomes

$$\sigma^2 + 2(\tfrac{1}{4}K^2 + \eta^2)\sigma + (\tfrac{1}{4}K^2 - \eta^2)^2 - V_0 = 0. \tag{3.14}$$

We can solve this for η^2 (dropping the η^4 term), getting

$$\eta^2 = [(\tfrac{1}{4}K^2 + \sigma)^2 - V_0^2]/2(\tfrac{1}{4}K^2 - \sigma). \tag{3.15}$$

If we assume that the energy is in the neighborhood of the correct Bragg condition energy,

$$E = k_x^2 + \tfrac{1}{4}K^2 + \varepsilon, \tag{3.16}$$

then Eq. (3.15) reduces to

$$\eta^2 = [(V_0 - \varepsilon)^2 - V_0^2]/2(\tfrac{1}{2}K^2 + \varepsilon - V_0) \approx \varepsilon(\varepsilon - 2V_0)/K^2. \tag{3.17}$$

Equation (3.17) explicitly shows that when $0 \leq \varepsilon \leq 2V_0$, which is the Bragg region, then $\eta^2 < 0$. Thus there must be damping in this region. Equation (3.17) also shows explicitly that the Bragg mirror region is not symmetrical about the Bragg angle, for neutrons.

Our main interest, however, is in the Laue case, as depicted in Fig. 10. In this case the physical situation differs considerably from that of the Bragg case. Here the incident beam

$$e^{ik_x x} e^{ik_y y} = e^{ik_x x}(\cos k_y y + i \sin k_y y)$$

splits into two standing waves in the y direction inside the crystal, and propagates along the atomic planes in the x direction, as shown in Fig. 13. One of these standing waves $e^{ik_x x} \cos k_y y \equiv \psi_2$ is centered at the atomic sites, and as it moves through the crystal it interacts strongly with the crystal atoms. The other wave $e^{ik_x x} \sin k_y y \equiv \psi_1$ is centered between the atoms, and it moves through the crystal relatively undisturbed. When the beam reaches the far end of the crystal, it splits into its components $e^{\pm ik_y y}$ and continues on in free space as these two traveling waves. This surprising result constitutes the Borrmann effect.

In the standing-wave solutions, from Figs. 10 and 11, we see that

$$|k_y| = \tfrac{1}{2}K = \pi/a_y, \tag{3.18}$$

so that the waves ψ_1 and ψ_2 have amplitudes

$$|\psi_2|^2 = \cos^2 \pi y/a_y, \quad |\psi_1|^2 = \sin^2 \pi y/a_y. \tag{3.19}$$

We have implicitly assumed that there is an atom located at $y = 0$, where the phase of $\exp(ik_y y)$ is zero; however, one cannot be sure that the incident wave will see an atom located exactly at the origin, so that in general

$$|\psi_1|^2 = \sin^2(k_y y - \alpha), \quad |\psi_2|^2 = \cos^2(k_y y - \alpha), \tag{3.20}$$

where α is chosen so that ψ_1 is centered between the atoms and ψ_2 is centered at the atomic sites. If one is interested in keeping track of the traveling-wave parts of

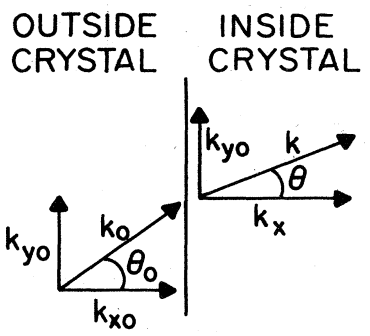

FIG. 12. Continuity at crystal surface. The tangential component of the beam k_{y0} must be continuous at the interface, so that only the normal component k_x can change.

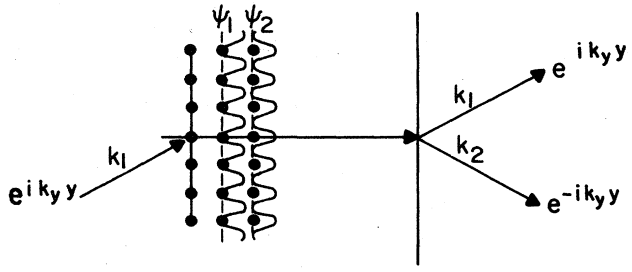

FIG. 13. The Borrmann effect. The incident traveling wave, whose transverse spatial dependence is $\exp(ik_y y)$, sees the crystal as a waveguide. It splits into two standing waves: $\psi_1 = \sin k_y y$, which is centered between the atomic sites, and $\psi_2 = \cos k_y y$, which is centered at the atomic sites. These two waves propagate normally to the crystal surface, along the lattice planes, and ψ_2 interacts much more strongly with the crystal atoms. At the far end of the crystal they recombine into the traveling wave $\psi = a \exp(ik_y y) + b \exp(-ik_y y)$ which propagates as the transmitted $[a \exp(ik_y y)]$ and reflected $[b \exp(-ik_y y)]$ waves.

the solution, one can use the fact that

$$\left|\tfrac{1}{2}(e^{ik_y y}+e^{i\eta}e^{-ik_y y})\right|^2=\cos^2(k_y y-\tfrac{1}{2}\eta)=\sin^2[k_y y-(\tfrac{1}{2}\eta+\tfrac{1}{2}\pi)],$$
$$\left|\tfrac{1}{2}(e^{ik_y y}-e^{i\eta}e^{-ik_y y})\right|^2=\sin^2(k_y y-\tfrac{1}{2}\eta), \tag{3.21}$$

for some arbitrary phase η.
Because of this, we shall write (calling $k_y=k$ and suppressing k_x)

$$\psi_y=e^{iky}=\tfrac{1}{2}(e^{iky}+e^{i\eta}e^{-iky})+\tfrac{1}{2}(e^{iky}-e^{i\eta}e^{-iky})\equiv\psi_1+\psi_2. \tag{3.22}$$

We shall assume that the η phase has been chosen so that ψ_1 represents a wave centered between the atomic sites, and ψ_2 represents a wave centered on the atomic sites.

Thus, as the wave propagates through the crystal, the wave ψ_2 undergoes a much stronger interaction with the crystal. By the time the wave reaches the far end of the crystal, ψ_y has the form

$$\psi_y\sim\psi_1+a\,e^{i\alpha}\psi_2. \tag{3.23}$$

Here a is real and $0\leq a\leq 1$. We shall generally be concerned only with the relative strength and relative phase of ψ_1 and ψ_2, so even though ψ_1 itself may be attenuated and phase shifted, we will usually normalize its amplitude to 1 (or $\frac{1}{2}$). For any substance a and α can be calculated. They depend not only on the scattering amplitude and crystal structure, but also on the thickness of the crystal. For the crystals that have been used so far, which are silicon of several millimeters thickness, there is minimal absorption for neutrons, so that we can approximately take $a=1$, while there is total absorption for x rays, for which $a=0$.

While inside the crystal the standing waves are appropriate, beyond the far end of the crystal there will be a transmitted and reflected wave, so the proper representation will be in terms of the two traveling waves, the transmitted wave e^{iky}, and the reflected wave e^{-iky}. For x rays, where $a=0$, one has

$$\psi\sim e^{ik_x x}\psi_1\sim\tfrac{1}{2}(e^{ik_y y}+e^{i\eta}e^{-ik_y y})e^{ik_x x}$$
$$\sim\tfrac{1}{2}e^{i(k_x x+k_y y)}+\tfrac{1}{2}e^{i\eta}e^{i(k_x x-k_y y)}, \tag{3.24}$$

so that the transmitted and reflected waves have different phases, but both have the same magnitude.

For neutrons, where $a=1$, we have (again suppressing k_x)

$$\psi\sim\psi_1+e^{i\alpha}\psi_2=\tfrac{1}{2}(1+e^{i\alpha})e^{iky}+\tfrac{1}{2}(1-e^{i\alpha})e^{i\eta}e^{-iky}, \tag{3.25}$$

so that in this case, the ratio of reflected to transmitted wave is

$$|\psi_r|^2/|\psi_t|^2=\left|(1-e^{i\alpha})/(1+e^{i\alpha})\right|^2=\tan^2(\tfrac{1}{2}\alpha), \tag{3.26}$$

but because there is no absorption, the total amplitude is

$$|\psi|^2\sim\tfrac{1}{4}\left|(1+e^{i\alpha})\right|^2+\tfrac{1}{4}\left|(1-e^{i\alpha})\right|^2=1, \tag{3.27}$$

a constant, independent of α. Thus the total amplitude remains constant, although it is apportioned differently between the transmitted and reflected parts.

We might point out that inside the crystal the neutron wave packet, propagating normal to the surface of the crystal, has a group velocity $v\cos\theta$, rather than v. This is because

$$v_x=\frac{\partial\omega}{\partial k_x}=\frac{\partial}{\partial k_x}(k_x^2+k_y^2)^{1/2}=\frac{k\cos\theta}{\omega}=v\cos\theta, \tag{3.28}$$

which is true for both the $\exp(\pm iky)$ components of the beam separately, and therefore for both ψ_1 and ψ_2. In this, the neutron behaves similarly to a propagating electromagnetic wave in a waveguide. Curiously, this has been the subject of some dispute, but it has been experimentally verified by Shull and co-workers (Horne, *et al.*, to be published). Theoretically it was convincingly demonstrated by Squires (Squires, 1978).

This is really all that one needs to know in order to understand the coherence experiments that have been done to date, some of which seem quite incomprehensible at first sight. In reality though, the picture we have presented is a gross oversimplification of all that actually happens within the crystal, although it is sufficient for our purposes. Before we proceed we shall merely mention some of the complications that the full dynamical theory must confront in the Laue case.

For a given energy E within a narrow region about the Bragg angle, if one asks what values of k_x are compatible, one must solve the secular equation (3.8) and one gets Eq. (3.12) with $\eta=0$. This yields

$$k_x^2=E^2-\tfrac{1}{4}K^2-V_0\pm V_0, \tag{3.29}$$

with two real solutions k_{x1} and k_{x2}, that differ by a very small amount. Since this equation always possesses real solutions, there is no sharp cutoff of solutions as in the Bragg case; the region of Laue reflection forms a wider band about the Bragg angle than in the Bragg case, and only gradually diminishes to zero.

Thus one has four waves inside the crystal, whose boundary conditions must be matched to the original incident wave at the crystal face. (A further complication, which we ignore here, is internal reflection at the back face of the crystal.) Thus, within the crystal one has a wave function,

$$\psi=(a_1e^{ik_{x1}x}+a_2e^{ik_{x2}x})+e^{ik_y y}$$
$$+(b_1e^{ik_{x1}x}+b_2e^{ik_{x2}x})e^{-ik_y y}. \tag{3.30}$$

If one calculates the currents, one finds

$$J_y=(\hbar k_y/2m)(\alpha-\beta),$$
$$J_x=(\hbar k_x/2m)[\alpha+\beta+O(\Delta/k_x)], \tag{3.31}$$

where

$$\alpha=|a_1|^2+|a_2|^2+2\,\mathrm{Re}(a_1a_2^*e^{2i\Delta x}),$$
$$\beta=|b_1|^2+|b_2|^2+2\,\mathrm{Re}(b_1b_2^*e^{2i\Delta x}) \tag{3.32}$$

and

$$k_x=\tfrac{1}{2}(k_{x1}+k_{x2}),\quad \Delta=\tfrac{1}{2}(k_{x1}-k_{x2}), \tag{3.33}$$

so that there is a y component of the current present and the wave propagates through the crystal at some angle normal to the surface.

It is actually possible to see the effects of the interference between these two wave fields. If the angle of incidence θ is exactly on the Bragg angle θ_B, the energy flow within the crystal will be normal to the crystal surface and along the atomic planes, giving the Borrmann effect as we have described it. But if the angle of

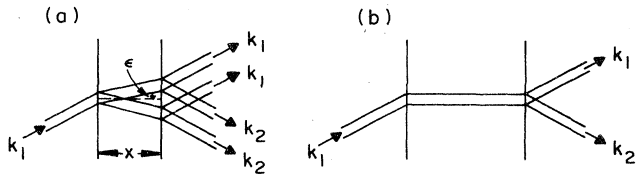

FIG. 14. Pendellösung. (a) If the incident beam is restricted by a very narrow slit, then waves within the Bragg region, but which are not exactly in the Bragg direction, propagate at some angle ϵ to the normal direction, varying between 0 and θ_B. The energy distribution oscillates between the upper and lower beam as a function of $\theta - \theta_B$. This effect (pendellösung) has actually been observed in neutron beams (see text for references). (b) For a wide incident beam and thick crystal, the energy will propagate normal to the crystal face, along the atomic planes, producing the Borrmann effect.

incidence is slightly off the Bragg angle, the energy flow will separate into two beams propagating at some angle $\pm\epsilon$ to the normal (see Fig 14). This angle ϵ depends critically on $(\theta - \theta_B)$, and as θ varies from θ_B to a value typically a few seconds away, ϵ will vary over the whole range θ to θ_B. As ϵ varies, the fraction of the total energy going into the reflected, rather than transmitted, beam is a rapidly oscillating function of ϵ.

Under the appropriate conditions, for example, if one uses a very narrow entrance slit and the incident beam is a spherically expanding wave covering a range of angles, this oscillation of the energy distribution, which Ewald called "pendellösung," leads to observable fringes in the transmitted and reflected waves; the phenomenon is well known for x rays (James, 1963; Batterman and Cole, 1964) and has also been seen for neutrons in germanium and silicon crystals by Shull, in a lovely series of experiments [Shull, 1968; Oberteuffer and Shull, 1972; Shull and Shaw, 1973; theoretical considerations for the neutron case have been discussed by Werner *et al.*, 1976; Rauch and Suda, 1974; and Rauch and Petrascheck, (1979)]. The oscillation frequency Δ depends on V_0, from Eq. (3.29), and therefore on the scattering amplitude b, and its measurement yields a precise determination of the scattering amplitude, orders of magnitude more accurate than that obtainable by any other method.

For a reasonably perfect crystal which is sufficiently thick and for which the incident beam is a relatively wide plane wave, such as in the COW experiment, these phenomena will average out and the straight Borrmann effect will predominate, so that our simplified analysis is sufficient. In the situation we shall be considering, the interferometer will be used to produce coherent, spatially separated beams, and what will be important to us is the relative phase at the point where the beams recombine, which can be affected by small perturbing fields along the paths of the separated beams, or by displacement of one of the crystal slabs used in producing or refocussing the separated beams, or by the insertion of a strip or wedge of aluminum, etc., into the path of one of the beams to shift its phase. Our technique will be very useful in analyzing all these situations.

In a sense, our simplified analysis is equivalent to the type of phase analysis one does in elementary optics, which for simple geometries gives a good qualitative picture (with many quantitative aspects) of a large number of diffraction phenomena. While it provides a good intuitive picture of many physical situations, it does not pretend to replace detailed calculations using vector diffraction theory, in the general case. Similarly, our analysis provides a useful model for experiments such as the COW experiment, where the relative phases of the separated beams are important. However the method cannot describe in detail the complex pendellösung effects taking place inside the crystal, in which the beam spreads into an angular region from $-\theta_B$ to $+\theta_B$ (which region is sometimes called the Borrmann "fan"), and which lead to complicated intensity profiles across each of the separated beams.

Where these effects are important, one must use the full dynamical theory. Also, our analysis does not provide criteria for its own limits of applicability, and such limits will have to be provided by the dynamical theory. Unfortunately, the detailed effects of finite slit sizes and finite crystal thickness, which limit our analysis, have barely been explored, although they are now coming under increased theoretical and experimental scrutiny. (A long series of papers on this topic has been presented by Indenbom and co-workers. See Indenbom and Chukhovskii, 1972, for a review article, and Indenbom *et al.*, 1976, for a full set of references to their work.)

It is interesting to note the size of the pendellösung effects in Laue reflection for a wide plane-wave incident beam, such as was used in the COW experiment (where the beam cross section was 3×6 mm). In Fig. 15 we have plotted the intensity of the reflected wave leaving a crystal slab relative to the incident wave intensity (the beam marked k_2 in Fig. 13, relative to the incident beam) as a function of the angle $\Delta\theta$, the angle by which the beam differs from the perfect Bragg angle θ_B, for the case of the parameters used in the COW experiment. These parameters were (Colella *et al.*, 1975): neutron wavelength, $\lambda_n = 1.445 \times 10^{-8}$ cm; energy, $E = 0.039$ eV; velocity, $v \sim 2.7 \times 10^5$ cm/sec; crystal slab thickness, $a \sim 0.2$ cm (the distance AA' in Fig. 16); overall length of crystal, $2L \sim 7$ cm; spacing of slabs ~ 3.5 cm; Bragg angle, $\theta_B = 22.1°$; length of the fcc cube in a silicon crystal, $d = 5.42$ Å; and since the silicon crystal consists of two displaced fcc cubes, there are eight atoms in the unit cell; the scattering length of silicon (Oberteuffer and Shull, 1972) is $b_{Si} = 0.415 \times 10^{-12}$ cm. We have used the theoretical formulas for the Laue case kindly provided us by Werner (private communication; see also Werner *et al.*, 1976) to plot the intensity of the reflected wave in this experiment. The plot in Fig. 15 shows the envelope of the Laue region, whose width is about 1 sec of arc, as well as the width of the pendellösung fringes. The calculation assumes no absorption of the neutron beam, which is not a bad approximation to the actual case.

B. The Laue-type interferometer

If one single perfect crystal is grown large enough so that three slabs, all parallel, relatively thick, and equally spaced, can be cut from it with enough of the

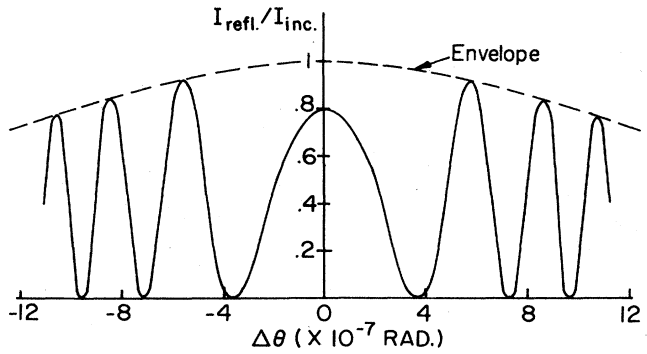

a) Reflected Intensity as a Function of $\Delta\theta$

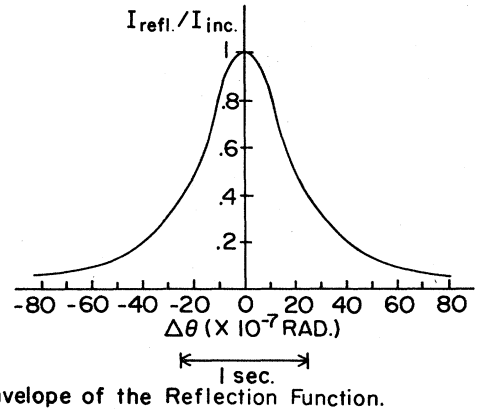

b) Envelope of the Reflection Function.

FIG. 15. Variation of reflection with deviation from the Bragg angle, for the Laue case. (a) The fraction of the incident beam going into the reflected beam is shown as a function of the deviation from the Bragg angle. The oscillation of the energy between the reflected and transmitted beam as the angle is varied is called pendellösung. This curve was calculated for the parameters of the COW experiment. (b) The envelope of the reflection function shown in (a). The overall width is about 1 sec of arc and falls gradually to zero, rather than sharply, as in the Bragg case.

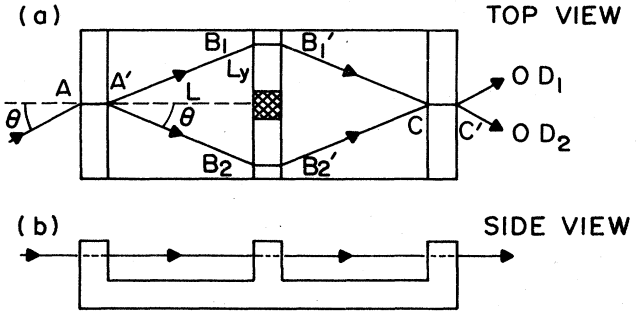

FIG. 16. Construction of Laue-type interferometer for x rays or neutrons. (a) Top view. Three slabs are cut from a single perfect crystal so that the atoms in all three slabs are aligned. The beam is split at A, and recombined at C, after which the amplitudes of the two components are monitored at D_1 and D_2. For some experiments, slab B is split in two parts (crosshatching) so that the slabs passing beams B_1 and B_2 may be displaced independently. Note that the beams inside the slabs travel normal to the face of the slab (Borrmann effect). (b) Side view.

crystal left to maintain structural stability, then the atoms in each of the three slabs will be fairly perfectly aligned. This device can then be used to coherently split and recombine the incident beam, as in Fig. 16. This is the Laue-type interferometer.

We shall analyze the following situation for an x-ray beam because it is simpler, rather than for a neutron beam, although a completely analogous discussion holds in that case. For an incident x-ray beam hitting the first slab at point A, we shall assume that each slab is thick enough so that the wave ψ_2 is completely absorbed. As the beam hits at A, it will be split into two waves, ψ_1 and ψ_2 in Eq. (3.22), where ψ_1 is centered between the atoms and ψ_2 is centered on the atoms. Thus

$$\psi_A = \tfrac{1}{2}(e^{iky} + e^{i\eta} e^{-iky}) + \psi_2 . \tag{3.34}$$

(Again we ignore the x dependence.)

When the beam leaves the slab at A', the wave ψ_2 will have been absorbed. Thus the e^{iky} part of ψ_1 continues on to point B_1, while the $e^{i\eta}e^{-iky}$ part continues on to B_2. The wave striking the second slab at B_1 has been translated by L_y, so

$$\psi_{B1} = e^{ik(y-L_y)} = \tfrac{1}{2}(e^{ik(y-L_y)} + e^{i\eta}\, e^{-ik(y-L_y)}) + \psi_2 . \tag{3.35}$$

When the beam exits at B_1', the ψ_2 part will have been absorbed. Because we are assuming that the crystal is perfect, the correctness of the Bragg condition at A also guarantees that the atoms are properly aligned at B, so the Bragg condition will also hold there. In order to write Eq. (3.35) as we did without an extra phase factor, we had to assume that L_y was an exact multiple of the atomic spacing a_y. We shall show in Sec. III.C that this assumption is not necessary, but for now, we shall accept it.

When the e^{-iky} part of the beam hits point B_2 it will have been translated by $-L_y$ so that

$$\begin{aligned}\psi_{B2} &= e^{i\eta} e^{-ik(y+L_y)} \\ &= (\tfrac{1}{2} e^{i\eta})[(e^{-ik(y+L_y)} + e^{-i\eta} e^{ik(y+L_y)}) \\ &\qquad + (e^{-ik(y+L_y)} - e^{-i\eta} e^{ik(y+L_y)})] \\ &= \psi_1' + \psi_2' .\end{aligned} \tag{3.36}$$

Once again, in Eq. (3.36), the wave ψ_1' is the transmitted wave, since the combination

$$\begin{aligned}e^{-iky} + e^{-i\eta} e^{iky} &= e^{-i\eta}(e^{iky} + e^{i\eta} e^{-iky}) \\ &= e^{-i\eta}\psi_1(y)\end{aligned} \tag{3.37}$$

is just a multiple of ψ_1, but expressed in the proper fashion for a wave moving in the $(-y)$ direction. Also, the wave ψ_2' is the absorbed one. So the wave reaching the far end of the slab is just

$$\psi_{B'2} = (e^{ik(y+L_y)} + e^{i\eta} e^{-ik(y+L_y)}) . \tag{3.38}$$

At both points B_1' and B_2' the beam splits into two traveling waves again, and one part of each recombines at C. The wave reaching C from point B_1' is the e^{-iky} part, $\psi^{(-)}$ (which has been translated by $-L_y$). Thus from Eq. (3.35),

$$\psi^{(-)}_{B'1} = \tfrac{1}{2} e^{i\eta} e^{-ik(y-L_y)} , \tag{3.39}$$

and this beam, when it reaches C, is

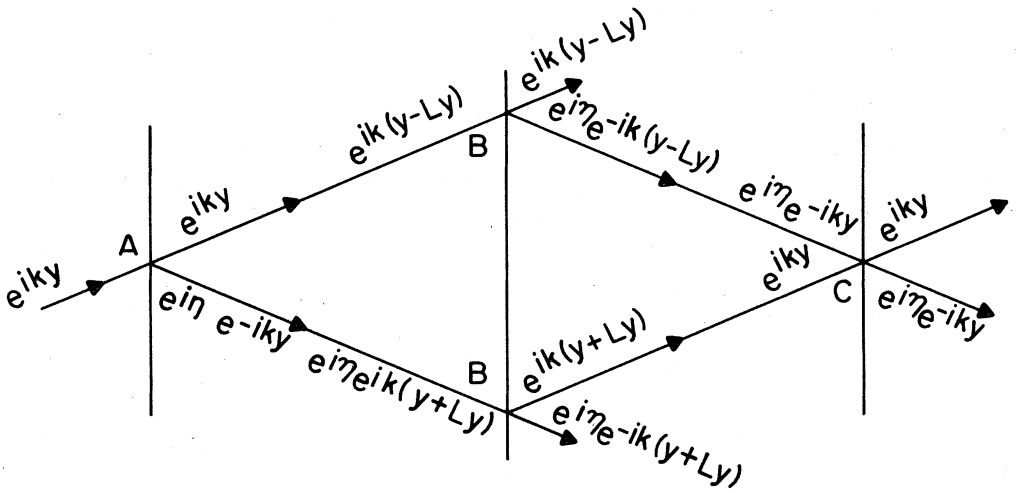

FIG. 17. Representation of traveling waves passing through a perfect crystal interferometer. At each slab (A, B_1, B_2, C) the incident wave becomes a combination of standing waves ψ_1 and ψ_2. For x rays, only the wave ψ_1 emerges from the far end of the slab, ψ_2 being absorbed, and the wave once again breaks into its component traveling waves, as described in the text. The phases on entering and leaving each slab are shown.

$$\psi_C^{(-)}(y) = \psi_{B'_1}^{(-)}(y + L_y) = \tfrac{1}{2} e^{i\eta} e^{-iky} . \tag{3.40}$$

On the other hand, the beam leaving B'_2 also splits, and in this case it is the e^{iky} part that reaches C, so that from Eq. (3.38),

$$\psi_{B'_2}^{(+)} = \tfrac{1}{2} e^{ik(y+L_y)} , \tag{3.41}$$

and

$$\psi_C^{(+)}(y) = \psi_{B'_2}^{(+)}(y + L_y) = \tfrac{1}{2} e^{iky} . \tag{3.42}$$

Therefore

$$\psi_C = \psi_C^{(+)} + \psi_C^{(-)} = (e^{iky} + e^{i\eta} e^{-iky}) . \tag{3.43}$$

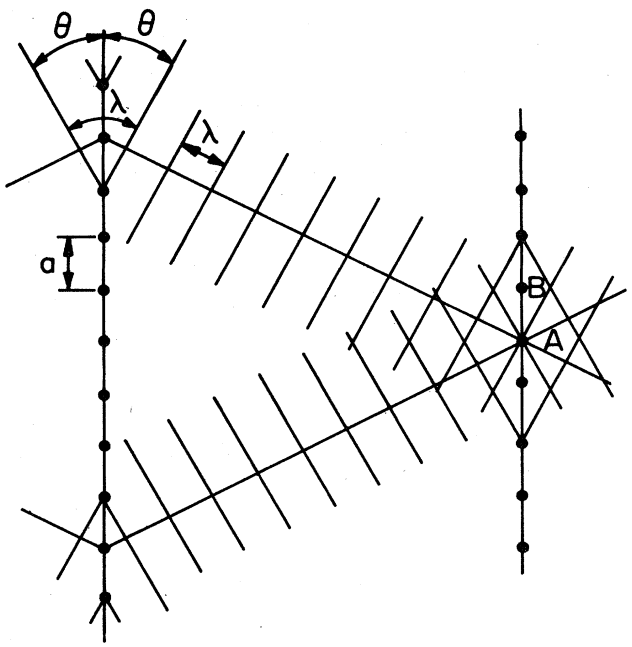

FIG. 18. Interference pattern due to Bragg scattering. Because of the Bragg condition $n\lambda = 2a \sin\theta$, the phase lag of either beam separately, between two successive atoms (say A and B), is only π. However, there will be a maximum (or minimum) at every atom because the phase difference between the two beams, between two successive atoms, is 2π.

But this is precisely the combination that produces ψ_1, the standing wave that is transmitted. The situation is graphically depicted in Fig. 17. Note also that the displacement L_y has completely canceled from the calculation.

It might be noted that in the ensuing interference pattern, because of the Bragg condition $n\lambda = 2a \sin\theta$, where a is the lattice spacing, each beam separately takes two atomic spacings to achieve a phase lag of 2π, but the superposition has a maximum or minimum at every atomic site, as the difference in phase between the two interfering beams varies by 2π over one atomic spacing (see Fig. 18).

C. Effect of relative displacement of the interferometer slabs

In the above analysis we showed that for a perfect crystal the third slab will fully transmit the wave impinging on it. However this slab actually acts as an analyzer, in the sense that if one could shift the slab sideways by $\frac{1}{2}$ the atomic spacing then the maxima would fall directly on the atoms, rather than between them. Thus the beam would be completely absorbed and there would be no transmission.

We can ask what the effect would be if we shifted any of the slabs sideways by a distance l_i. We shall assume that the middle slab, B, has been split by a saw (the thatched region in Fig. 16, so that the sections containing B_1 and B_2 can be shifted independently. Consider that the incident beam is the same as before, but that at each location where the beam encounters the crystal, the slab, and therefore the atoms within it, have been shifted in the $+y$ direction, at A by l_1, at B_1 by l_2, at B_2 by l'_2, and at C by l_3.

The incident wave striking point A will still be e^{iky}, but now we must relate it to the position of the atoms at A, which have been shifted by l_1. Thus,

$$\begin{aligned}\psi_A = e^{iky} &= e^{ikl_1} e^{ik(y-l_1)} \\ &= (\tfrac{1}{2} e^{ikl_1})[(e^{ik(y-l_1)} + e^{i\eta} e^{-ik(y-l_1)}) \\ &\qquad + (e^{ik(y-l_1)} - e^{i\eta} e^{-ik(y-l_1)})] \\ &= \psi_1 + \psi_2 .\end{aligned} \tag{3.44}$$

Once again the wave ψ_2 will be absorbed in the slab, so that wave leaving the slab $\psi_{A'}$ will be ψ_1. Furthermore, the wave $\psi_{A'}$ will split into two traveling waves, as represented by the $e^{\pm iky}$ parts of ψ_1. Thus

$$\psi_{A'}^{(+)} = e^{iky}, \qquad \psi_{A'}^{(-)} = e^{ikl_1} e^{i\eta} e^{-ik(y-l_1)} = e^{2ikl_1} e^{i\eta} e^{-iky}. \tag{3.45}$$

When these beams reach slab B, we will have

$$\psi_{B1} = e^{ik(y-L_y)}, \quad \psi_{B2} = e^{2ikl_1} e^{i\eta} e^{-ik(y+L_y)}. \tag{3.46}$$

Now the slab at B_1 is shifted by l_2, and that at B_2 by l_2', and we must relate ψ_{B1} and ψ_{B2} to the relevant atomic positions, so

$$\begin{aligned}\psi_{B1} &= e^{ikl_2} e^{ik(y-l_2-L_y)} \\ &= (\tfrac{1}{2} e^{ikl_2})(e^{ik(y-l_2-L_y)} \\ &\quad + e^{i\eta} e^{-ik(y-l_2-L_y)}) + \psi_2,\end{aligned} \tag{3.47}$$

where ψ_2 stands for that part of the wave which will be absorbed. The transmitted wave $\psi_{B'1}$ is just this wave without ψ_2.

Similarly, the wave striking at B_2 is

$$\begin{aligned}\psi_{B2} &= e^{2ikl_1} e^{i\eta} e^{-ikl_2'} e^{-ik(y-l_2'+L_y)} \\ &= (\tfrac{1}{2} e^{2ikl_1} e^{i\eta} e^{-ikl_2'}) \\ &\quad \times (e^{-ik(y-l_2'+L_y)} + e^{-i\eta} e^{ik(y-l_2'+L_y)}) + \psi_2,\end{aligned} \tag{3.48}$$

where we have made the same decomposition as for ψ_{B2} in the unshifted case. Finally the wave striking at C will be $\psi_{B'1}^{(-)}$ and $\psi_{B'2}^{(+)}$ as before, where $\pm$ refer to the $e^{\pm iky}$ part of the wave, so that

$$\begin{aligned}\psi_C^{(-)}(y) &= \psi_{B'1}^{(-)}(y+L_y) = \tfrac{1}{2} e^{2ikl_2} e^{i\eta} e^{-iky}, \\ \psi_C^{(+)}(y) &= \psi_{B'2}^{(+)}(y-L_y) = \tfrac{1}{2} e^{2ikl_1} e^{-2ikl_2'} e^{iky},\end{aligned} \tag{3.49}$$

and

$$\begin{aligned}\psi_C &= \psi_C^{(+)} + \psi_C^{(-)} = \tfrac{1}{2}(e^{2ikl_1} e^{-2ikl_2'} e^{iky} \\ &\quad + e^{2ikl_2} e^{i\eta} e^{-iky}).\end{aligned} \tag{3.50}$$

This situation is depicted in Fig. 19.

In Eq. (3.50) we have the beam which impinges on the point C. In order to tell how much of it is transmitted if the crystal at C has been shifted, we must first relate this function to the atomic sites. Thus in Eq. (3.49) we first write e^{iky} as $e^{ikl_3} e^{ik(y-l_3)}$ and e^{-iky} as $e^{-ikl_3} e^{-ik(y-l_3)}$. Then we write $e^{ik(y-l_3)}$ and $e^{i\eta} e^{-ik(y-l_3)}$ as linear combinations of ψ_1 and ψ_2. This gives

$$\begin{aligned}\psi_C &= [\tfrac{1}{2}(e^{2ik(l_1-l_2')} e^{ikl_3} + e^{2ikl_2} e^{-ikl_3}) \\ &\quad \times (e^{ik(y-l_3)} + e^{i\eta} e^{-ik(y-l_3)})] \\ &\quad + [\tfrac{1}{2}(e^{2ik(l_1-l_2')} e^{ikl_3} - e^{2ikl_2} e^{-ikl_3}) \\ &\quad \times (e^{ik(y-l_3)} - e^{i\eta} e^{-ik(y-l_3)})] = \psi_1 + \psi_2.\end{aligned} \tag{3.51}$$

Again, only the ψ_1 wave will be transmitted, thus the amplitude of the transmitted wave is proportional to $\exp[2ik(l_1 + l_2' + \frac{1}{2} l_3)] + \exp[2ik(l_2 - \frac{1}{2} l_3)]$ and therefore the intensity becomes

$$\begin{aligned}I &\sim I_0 \cos^2\{k[(l_1 + l_3) - (l_2 + l_2')]\} \\ &\equiv I_0 \cos^2 \phi_D.\end{aligned} \tag{3.52}$$

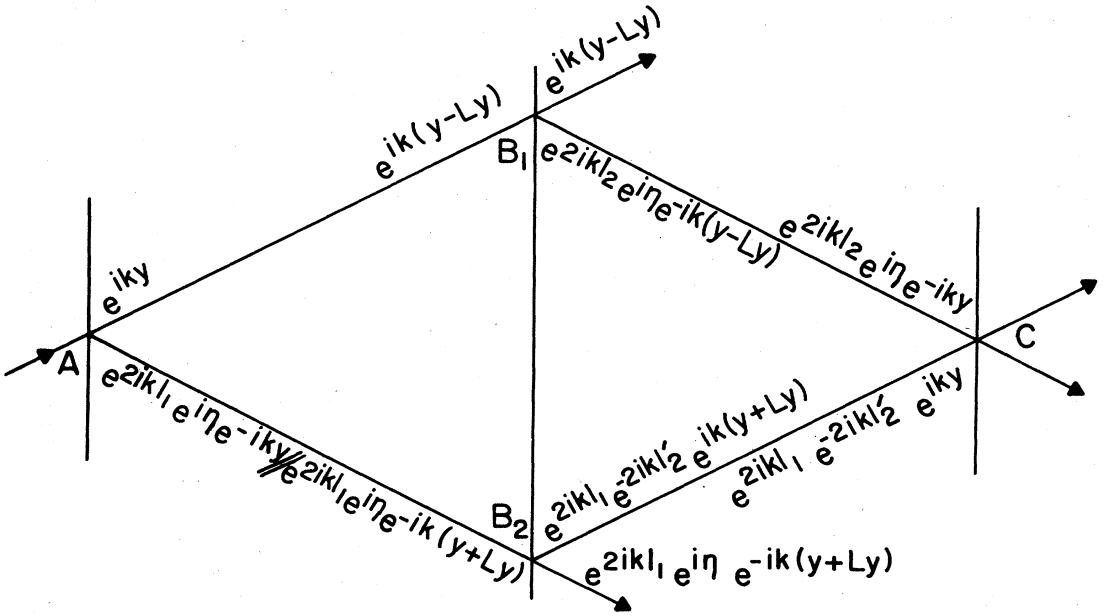

FIG. 19. Representation of traveling waves passing through a distorted crystal interferometer. Slab A has been displaced upward by l_1, slab B_1 by l_2, slab B_2 by l_2', and slab C by l_3. The shifting of the phase of the wave from that at the equivalent point in the perfect undisturbed crystal (Fig. 17) is shown. The slab at C acts as an analyzer, and the emerging phase is described in the text.

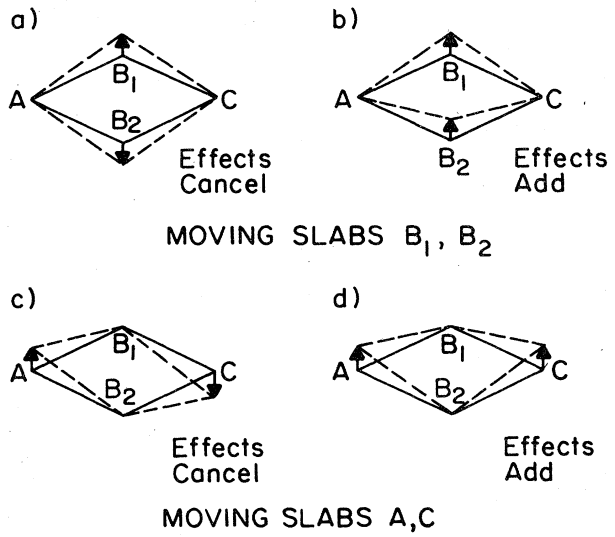

FIG. 20. Intuitive picture of effect of distorting the crystal. (a) If slabs B_1 and B_2 are displaced in opposite directions, the effects on the two beams are symmetrical and cancel out. (b) If slabs B_1 and B_2 are displaced in the same directions, the effects are asymmetrical and add. (c) If slabs A and C are displaced in opposite directions, the effects are symmetrical and cancel out. (d) If slabs A and C are displaced in the same directions, the effects are asymmetrical and add.

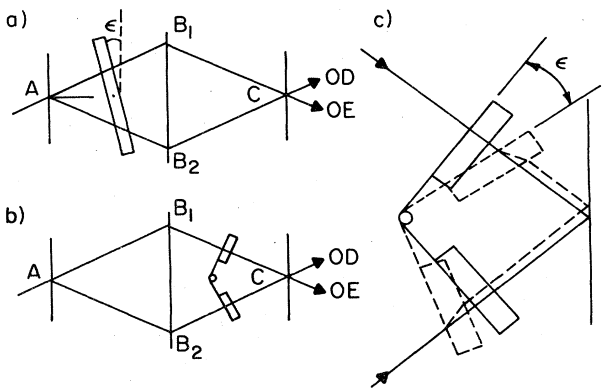

FIG. 21. Effect on the interference patterns of altering the beams. (a) If a sheet of aluminum is placed in the path of both beams and rotated, it will alter the optical path of each beam differently, and thus affect the interference pattern (Rauch *et al.*, 1974). Because of absorption, the effect on x rays will be different from that on neutrons (see Fig. 22). (b) When two sheets of aluminum are arranged perpendicular to the beam, both beams will be equally shifted as the device is rotated (C. G. Shull, private communication). Yet there is *no* effect on the interference fringes, as the bending of the beam does not affect the phase striking a point on the screen, as per the text. Only the envelopes of the beams are shifted. (c) Close-up illustrating the bending of the classical trajectories (and therefore the envelope of the beam).

This result agrees with one's intuitive feeling of how these effects ought to behave, from simple symmetry considerations. For example, if B_1 and B_2 are moved in opposite directions ($l_2 = -l_2'$) the effects cancel, while if they are moved in the same direction the effects add (see Fig. 20). Similarly, if slabs A and C are moved in opposite directions the effects cancel, while if they are moved in the same direction the effects add. Also, if any of the slabs are shifted by $\frac{1}{2}a$ ($k_y = \pi/a$), the pattern will shift from a maximum to a minimum. This was experimentally verified by Bonse and Hart (1966a), who also gave a simple explanation by plotting wave fronts.

This intuitive argument also shows that the results calculated for neutrons must be similar to those calculated for x rays. And in fact had we calculated the transmitted intensity for neutrons, using the incident wave function, Eq. (3.34), and taking into account the phase shift $\exp(i\alpha)$ for ψ_2, at every crystal slab (assuming no absorption) we would have obtained for the transmitted and reflected waves

$$I_T = I_0 \sin^2\alpha, \quad I_R = I_0 \cos^2\alpha \tag{3.53}$$

for the perfect crystal. For a crystal with the various planes displaced as above, Eq. (3.52) would read

$$\begin{aligned} I_T' &= I_0 \sin^2\alpha \cos^2\phi_D = I_T \cos^2\phi_D \leq I_T, \\ I_R' &= I_0 (1 - \sin^2\alpha \cos^2\phi_D) = I_0 - I_T'. \end{aligned} \tag{3.54}$$

Thus the transmitted beam intensity I_T, as determined by the nuclear scattering, is modulated by the same displacement phase factor, governed by the same ϕ_D, as in the x-ray case.

In Sec. III. B we assumed that L_y was a multiple of the atomic spacing. If it is not, it is still formally equivalent to the above treatment, as moving the beam with respect to the crystal is equivalent to moving the crystal with respect to the beam. A change in L is equivalent to shifting B_1 and B_2 in opposite directions, which we have seen cancels out.

There are two further experiments we should like to mention briefly since they illustrate the principles we have been discussing. Rauch *et al.* (1974) put a sheet of aluminum between slabs A and B (see Fig. 21a). When it was parallel to the slabs, it produced no effect. But when it was tilted at an angle, it caused a difference in optical path between the beams, which shifted the pattern recorded. When the experiment was performed with x rays, the transmitted intensity varied with the angle of the aluminum sheet, but the intensities of the beams at points D and E were equal (see Fig. 22a). When the experiment was repeated with neutrons, the maxima of intensity shifted back and forth between D and E while the total intensity for the sum of the beams remained constant (Fig. 22b).

The explanation for this surprising result is given by Eqs. (3.24) and (3.27), namely, that, for x rays, altering the relative optical paths will shift the positions of the maxima, so the transmitted intensity varies. However, since $\psi_1 \sim e^{iky} + e^{in} e^{-iky}$, the two beams e^{iky} and e^{-iky} always appear with equal amplitude, and they will both have equal intensity, although the total intensity varies. On the other hand, for neutrons, the total intensity remains constant, since there is almost no absorption, but the relative intensities will vary with the optical path difference.

The second experiment was performed by Shull and Callerame (1977, private communication). They welded two sheets of aluminum to a bar, so that both were normal to the beam, as in Fig. 21b. Then they rotated the

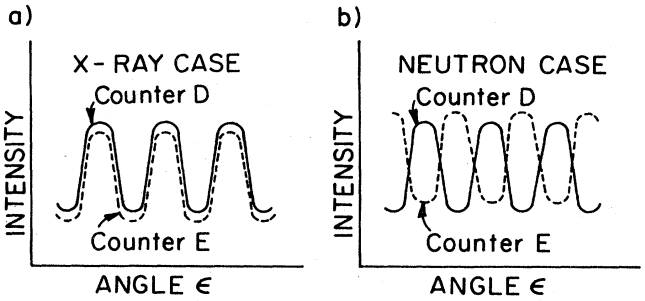

FIG. 22. Different behavior of x ray and neutron beams. (a) When the experiment pictured in Fig. 21(a) is performed with x rays, the intensity at each counter varies with the angle ϵ, but both counters, D and E, record equal intensities. This is because the wave striking C consists of a combination of ψ_1 and ψ_2. At C, ψ_2 is absorbed, but $\psi_1 \sim \sin ky \sim (e^{iky} - e^{-iky})$ contains equal amplitudes of both traveling waves, $e^{\pm iky}$. (b) When the experiment is performed with neutrons, the total intensity remains constant, but the distribution of intensity between counters D and E alternates between them. This is because there is little absorption of the neutron beam, and therefore no loss of intensity. However, the relative phase between ψ_1 and ψ_2 varies, leaving different relative amplitudes for the e^{iky} and e^{-iky} parts propagating to D and E.

assembly about a pivot point. Since the beams were both bent in the same direction by this process, one might expect that the fringe pattern would move (Fig. 21c). In fact, they found that the fringe pattern was unaffected.

The explanation for this is that for small angles of deflection from the normal, even though the beam is shifted, there is no difference in optical path to a given point on the screen, as we have repeatedly emphasized. In other words the deflection of the beam from the normal does not affect the phase arriving at a given point in the neighborhood of C. The apparent shift that takes place in Fig. 21c is actually in the envelope of the beam, representing the classical trajectory, and not in the relative phase.

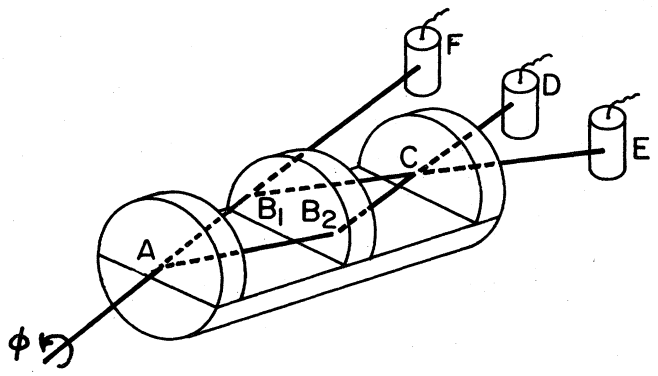

FIG. 23. The COW experiment. Three slabs were cut from a single silicon crystal such that a neutron beam incident on the first slab at A would be coherently recombined at the third slab, at C. Specifically, the relative intensities of the reflected and transmitted wave at C were monitored by counters D and E. The original incident beam was monitored at F. The entire apparatus was then rotated around the incident beam AB_1, in order to induce a gravitational potential difference between the two beams at B_1 and B_2, and the relative intensities at D and E were measured as functions of ϕ, the angle of rotation.

IV. THE COW EXPERIMENT

A. The experiment in the laboratory frame

In the COW experiment (Colella *et al.*, 1975), three slabs were cut from a single cylindrical silicon crystal having a diameter of about 2 in. and a length of about 3 in. The beam was then split by the first slab and coherently recombined in the last slab (Fig. 23). Neutron counters at D and E monitored the beam and recorded the relative intensities of the transmitted and reflected beam. Originally the split beams were in the horizontal plane. But by rotating the apparatus through an angle ϕ about the incident beam, they created a gravitational gradient

$$g = g_0 \sin\phi \,, \tag{4.1}$$

where g_0 is the earth's gravitational acceleration.

This gravitational field acts as a small perturbation on the beam, and thereby affects the experiment in three ways. First, it alters the stress on the crystal assembly, thus producing distortions in the crystal. This effect was measured by passing an x-ray beam through the crystal, the x-ray beam not being affected by gravity to this order. Since this effect was measured and compensated for by the experimenters, we shall not worry about it further. Second, the beam itself was bent into a parabolic path. We have seen that this effect has no influence on the phase of the wave function as it strikes the third slab. And since the intensity at the counters is a direct measure of the relative phase of the two beams, this effect has no bearing on the result.

The only important influence of gravity on the experiment is the third, which is the addition of the phase factor $-\int \Delta U\, dt/\hbar$, of Eq. (2.17), to the beam. We have seen that, for a single beam, the change in phase keeps pace with the shifting of the envelope of the beam. In this case, the phase shift is produced by the difference in potential between the two beams.

In Fig. 24 one can see that the path ab is at a height $(2L + a)\sin\theta$, while fd is at height 0, and ae is at an average height $(L + a)\sin\theta$, while cd is at average height $L\sin\theta$. Also, the times $t_{ab} = t_{cd} = t_{ae} = t_{fd} = L/v\cos\theta$, and

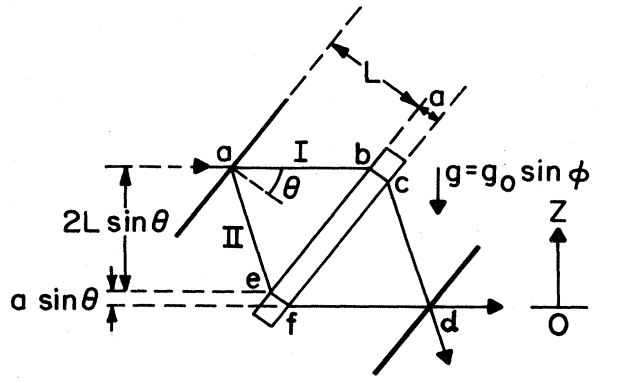

FIG. 24. Schematic representation of the COW experiment. The rotation of the apparatus about the incident beam by an angle ϕ creates a gravitational field with component $g\sin\phi$ in the plane of the beams. The upper beam, *abcd*, is called beam I, and the lower beam, *aefd*, is beam II.

$t_{bc}=t_{ef}=a/v\cos\theta$, since inside the crystal[7] $v_i=v\cos\theta$. Therefore,

$$
\begin{aligned}
-\int\frac{\Delta V\,dt}{\hbar} &= -\left(\overline{V}_I\int_I dt-\overline{V}_{II}\int_{II}dt\right)\Big/\hbar \\
&= -\Big((\overline{V}_{ab}-\overline{V}_{fd})\int dt_{ab}+(\overline{V}_{bc}-\overline{V}_{ef})\int dt_{bc} \\
&\quad +(\overline{V}_{cd}-\overline{V}_{ae})\int dt_{ae}\Big)\Big/\hbar \\
&= -\frac{mg}{\hbar}\left[(2L+a)\sin\theta\left(\frac{L}{v\cos\theta}\right)+2L\sin\theta\left(\frac{a}{v\cos\theta}\right)\right. \\
&\quad \left.-a\sin\theta\left(\frac{L}{v\cos\theta}\right)\right] \\
&= -\left(\frac{2mgL^2}{\hbar v}\right)\tan\theta\left(1+\frac{a}{L}\right), \qquad (4.2)
\end{aligned}
$$

where $\overline{V}$ is the average potential for a given path, a is the thickness through a slab, and L is the distance between neighboring slabs. This phase shift, with $g=g_0\sin\phi$, determines the relative phase of the two beams as a function of ϕ, and was experimentally confirmed by COW.

B. The accelerated frame

Although the previous analysis seems straightforward and has been confirmed experimentally, we shall see that it contradicts the accepted explanation of the results of a coherent-beam electron diffraction experiment done by Marton in 1953. We believe the explanation of that experiment to be incorrect, but we should like to rederive our result in a totally different manner, as a check on the answer. We shall do this by analyzing the experiment in an accelerating coordinate system, falling with the acceleration of gravity. According to the principle of equivalence, such a system would be equivalent to one at rest in a static gravitational field.

In a coordinate system falling with acceleration g, the neutron beam is no longer accelerating but classically moves in a straight line. However, the real complicating factor is that in the accelerating frame, falling with gravity, the crystal slabs are accelerating upward, imparting a time-dependent Doppler shift to the falling beam. This situation is rather tricky to analyze, but it turns out that there is a particular coordinate system that eliminates most of the difficulties. This is a coordinate system that is not only accelerating, but at some particular time (call it $t=0$) has a velocity exactly equal to that of the crystal slabs.

We shall imagine that a snapshot has been taken in this particular coordinate system, at time $t=0$. At this moment, the slabs are at rest, but they have an acceleration g upward. The time chosen for $t=0$ can have no effect on the derivation, as the situation will look the same to any other accelerating observer, whose velocity at some given moment is exactly that of the slabs.

[7] The velocity inside the crystal has been experimentally verified by C. Shull and co-workers (to be published). At the time of the COW experiment it was incorrectly thought that $v_i=v$, and this wrong value was used in their analysis. It leads to an error of less than 1%, well within their experimental error.

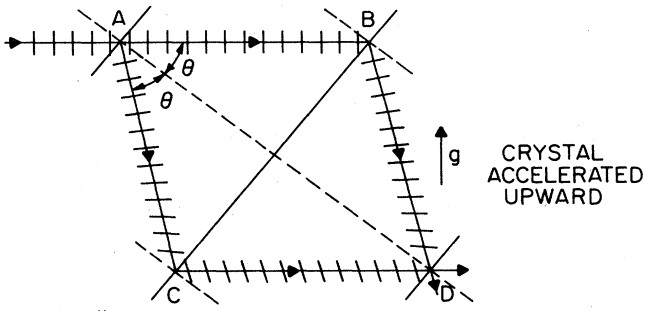

FIG. 25. "Wave fronts" in the accelerated system. In a system in free fall with the neutron beam, the crystal is instantaneously at rest, but is accelerating upward. In this system, as explained in the text, the "wave fronts" do not evolve into each other, as the neutrons have constant velocity, but were scattered at different times by the accelerating crystal. Rather, they represent that value of k which would be the center of a neutron wave packet at that point. Along AC and BD they start as perpendicular but gradually bend away, since the waves closer to C,D were scattered earlier, when the crystal was moving downward, with a speed proportional to the distance from A or B. The wave fronts along CD are all parallel, but inclined to the line CD.

Since we are dealing with a steady-state situation in the accelerated system, where there is no gravity, we will examine lines of constant phase, the plane waves, in this system. In the original system, the laboratory system with a static gravitational field, the time-independent solutions to the Schrödinger equation are Airy functions. The transformation to an accelerated system is not a static one, but a time-dependent one, and so there is no very simple one-to-one relationship between the time-independent solutions in each reference frame. Rather, we can compose the time-independent solutions in one frame from linear combinations of the solutions in the other frame. We shall discuss this question in more detail in the Appendix on accelerated reference frames.

In the snapshot taken at $t=0$, while all the neutrons moving between, say, A and C (see Fig. 25) are moving with constant velocity, they do not all have the same velocity and direction, as they were scattered from slab A at different previous times, when the slab was not at rest. (For simplicity we shall ignore the thickness of the slabs.) The momentum vector of the center of the wave packet for each neutron is determined by the Doppler shift when that neutron was scattered by slab A.

In Fig. 25 the appropriate central plane wave for each particle packet is drawn as though one had a stationary wave front, where each wave evolves into the next. This is only true in a static reference frame. Here, each neutron moves with constant speed, and so the "snapshot" of Fig. 25 is only true at $t=0$. It should be borne in mind that each plane wave depicted in Fig. 25 represents only the appropriate k_0 about which to construct a neutron wave packet at that point. Because one is used to a static configuration in such problems, we have spelled out the physical description in our reference frame in more detail in Sec. IV.C.

First consider a neutron impinging upon point A. Part of the wave function is transmitted to B, while part is reflected off the dotted crystal plane in Fig. 25, perpendicular to the crystal face, and passes "on to" point C. At

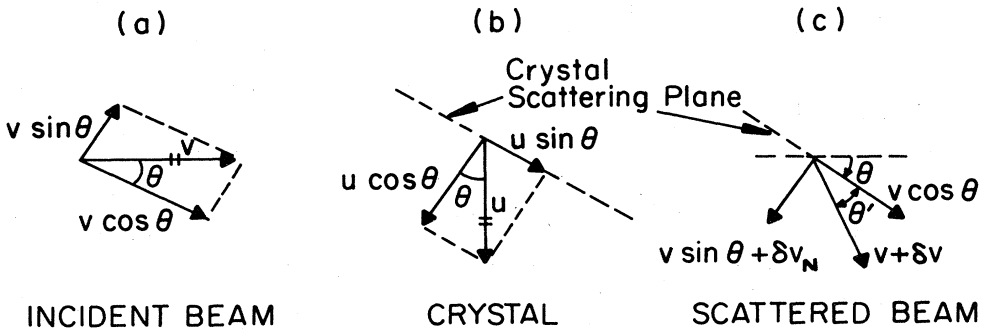

FIG. 26. Scattering at point A of crystal at earlier time. (a) At $t=0$, the crystal is momentarily at rest in the accelerating system. The beam that reaches point C at $t=0$ scattered off point A at a time T previously. The incident beam was moving horizontally. (b) At time $T=-T$, the crystal was moving downward at speed u (since it is accelerating upward). (c) The scattered beam has its component normal to the scattering plane reversed. It also picks up a Doppler shift, $\delta v_N = 2u\cos\theta$, due to the normal motion of the crystal.

point A, since the crystal is at rest at $t=0$, there will be no Doppler shift. The wave transmitted to B also is not affected.

Now consider a neutron arriving at point C. This particle will have been scattered at point A some time ago ($T = L/v\cos\theta$, ignoring acceleration effects, which are of higher order), when the slab at A was traveling downward with velocity u, where

$$u = gT = gL/v\cos\theta\,. \tag{4.3}$$

(Remember that the crystal is accelerating upward.) The situation at point A when the particle scattered is shown in Fig. 26. The particle hit the scattering plane with a normal velocity $v\sin\theta$, and the plane was approaching the particle with a velocity $u\cos\theta$. Upon scattering, the normal velocity was reversed, but it also picked up the Doppler velocity

$$\delta v_N = 2u\cos\theta\,, \tag{4.4}$$

because the scattering plane was moving (the factor of 2 coming from the "moving mirror effect"). The velocity parallel to the scattering plane is unaffected. Thus the velocity of the scattered particle is

$$\begin{aligned} v' &= [(v\sin\theta + 2u\cos\theta)^2 + (v\cos\theta)^2]^{1/2} \\ &\approx v + u\sin 2\theta \equiv v + \delta v\,. \end{aligned} \tag{4.5}$$

The change in angle is given by

$$\begin{aligned} \tan\theta' &= \tan(\theta+\delta\theta) = (v\sin\theta + 2u\cos\theta)/v\cos\theta \\ &= \tan\theta + 2u/v = \tan\theta + \sec^2\theta\,\delta\theta\,, \end{aligned} \tag{4.6}$$

so that

$$\delta\theta = (2u/v)\cos^2\theta\,. \tag{4.7}$$

While a neutron reaching C was scattered at a time T previously, another neutron only halfway between A and C was scattered at time $\frac{1}{2}T$ previously, etc., so that the angle $\delta\theta$ increases linearly from zero at A until its value in Eq. (4.7) at C. (This will be discussed in more detail in Sec. IV.C.) These considerations lead to two possible effects on the waves composing the wave packet at C. First, the bending of the beam through $\delta\theta$ causes no phase shift at a given point on the crystal at C, as we have stressed previously. Second, there will be a change in wave number $\delta k = m\,\delta v/\hbar$ leading to a change in phase $\delta\phi = \int \delta k\, dl$. We shall not calculate this change in phase, though, because the path from B to D has identical geometry to the path from A to C. Therefore the same change in phase occurs along this path, with the ultimate effect that the two cancel out.

So the only remaining effect which can change the phase of the neutron wave packet is that along the path CD. The neutron striking at D at time $t=0$ was scattered off A at time $2T$ in the past, where it picked up a velocity $\delta v = 4u\cos\theta$, twice as great as that of Eq. (4.5), because the plane was then moving at twice the speed $2u$. When this neutron reached C, the plane at C was moving downward, away from the neutron, with velocity $u\cos\theta$. One can analyze this situation exactly as was done for the plane at A. But one can see that if moving toward the beam changes the speed and angle in one direction, then moving away will change it in the opposite direction.

Thus in scattering off C, the angle will change from $2\delta\theta$ back to $\delta\theta$, while the speed will change from $v+2\delta v$ back to $v+\delta v$, with δv given by Eq. (4.3). So after the neutron is scattered from C it will maintain the constant angle $\delta\theta$ from the vertical in Fig. 3, and the constant speed $v+\delta v$. There is another way to see this result, and that is to note that from the point of view of our snapshot, C is momentarily at rest, and so it will induce no extra Doppler shift. Therefore the particle striking it with speed $v+\delta v$ and angle $\theta+\delta\theta$ will be scattered at this same speed and angle.

The effect of this on the phase at D is merely $\delta\phi = \int \delta k\, dl$. Once again the shift in angle causes no change in phase at a given point. And so the final effect is given by

$$\delta\phi = \frac{\delta k \cdot L}{\cos\theta} = \frac{m\delta v}{\hbar}\,\frac{L}{\cos\theta} = \frac{m(u\sin 2\theta)L}{\hbar\cos\theta}$$
$$= \frac{2mL\sin\theta}{\hbar}\,\frac{gL}{v\cos\theta} = \frac{2mgL^2}{\hbar v}\tan\theta\,, \qquad (4.8)$$

using δv from Eq. (4.5) and u from Eq. (4.3). This result agrees both in magnitude and in sign ($\delta\phi$ greater for the lower beam) with the result of Eq. (4.2). (We have ignored the thickness of the crystal.)

Thus our two derivations, in the laboratory frame and in an accelerating frame, both give the same effect, which was experimentally confirmed in the COW experiment.

C. The Doppler shift from an accelerating mirror

In the accelerated system the neutrons propagate as a free-particle beam, while the crystal appears to be accelerating. In this section we shall analyze the Doppler shift from the accelerating crystal, partly to justify some of the statements made in Sec. IV.B, and partly because the situation is in some respects quite different from that in the constant-velocity case, and this ought to be pointed out (although the results confirm the calculation of the last section). The amount of absorption or transmission of the beam does not affect the essential features of the Doppler shift, and so it will suffice for us to analyze a much simpler situation in order to indicate the important properties involved. Therefore we shall examine the case of reflection from a one-dimensional perfectly reflecting mirror.

Consider a narrow wave packet $\psi(x,t)$, with velocity v, for which the group velocity approximation is valid, which is incident upon a mirror whose position is given by $x_m = \xi(t)$, with $\xi(0) = 0$ (see Fig. 27). In order to analyze the motion of the packet, we shall have to consider the component plane waves. The incident and reflected (image) wave both satisfy the free-particle time-dependent Schrödinger equation, and so the appropriate plane-wave solution is

$$\phi(x,t) = \exp(ikx - i\omega t) + A(k')\exp(-ik'x - i\omega' t)\,, \qquad (4.9)$$

where

$$\hbar\omega = (\hbar k)^2/2m, \quad \hbar\omega' = (\hbar k')^2/2m\,. \qquad (4.10)$$

The incident wave is moving in the $+x$ direction, initially approaching the mirror from the left, while the reflected wave is moving in the $-x$ direction, and is initially located to the right of the mirror; as usual the entire solution only has physical meaning to the left of the mirror. We are not assuming that $k = k'$, or $\omega = \omega'$, so that the incident and reflected waves have different energies. Rather, the relation between k and k' is determined by the boundary condition that ψ vanishes at the mirror, where $x = \xi(t)$. Thus

$$\phi(x = \xi(t), t) = 0 = \exp[ik\xi(t) - \omega t] + A\exp[-ik'\xi(t) - i\omega' t]\,. \qquad (4.11)$$

In order for this equation to have solutions for all times, the time dependence in the two exponents must be equal, so

$$k\xi(t) - \omega t = -k'\xi(t) - \omega' t\,. \qquad (4.12)$$

Now in general there is no reflected wave of this form that satisfies this condition. However, we can find an approximate solution that works under the condition that the wave packet is narrow in momentum space. (It works as well as the group velocity approximation itself.) We are also assuming that gravity is a weak perturbation. In this case the velocity of the mirror $\dot{\xi}$ is always much less than the velocity of the packet, $\dot{\xi} \ll v$.

Consider that the packet strikes the mirror at time τ, so that $\psi(x,t)$ will be zero in the vicinity of the mirror except for $t \sim \tau$. Then we shall see that it is necessary for us to consider the velocity of the mirror only when the particle is near it (when $v_{\text{mirror}} \equiv u$), so that we can write

$$\xi(t) \approx \xi(\tau) + \left(\frac{d\xi}{dt}\right)_\tau (t-\tau) = \xi_\tau + u(t-\tau)\,,$$
$$u \equiv \left(\frac{d\xi}{dt}\right)_\tau . \qquad (4.13)$$

Then Eq. (4.11) becomes

$$\exp\{ik[\xi_\tau + u(t-\tau)] - i\omega t\}$$
$$= -A\exp\{-ik'[\xi_\tau + u(t-\tau)] - i\omega' t\}\,. \qquad (4.14)$$

Equating the time-dependent terms in the exponential gives

$$(ku - \omega)t = (-k'u - \omega')t \qquad (4.15)$$

or

$$\hbar k'^2/2m + uk' + uk - \hbar k^2/2m = 0\,, \qquad (4.16)$$

using the explicit form for $\omega(k)$, Eq. (4.10). Therefore,

$$(\hbar/2m)(k'^2 - k^2) + u(k' + k) = 0\,,$$
$$k' - k \equiv \delta k = -2mu/\hbar\,. \qquad (4.17)$$

This equation can also be written

$$\delta v = \hbar\delta k/m = -2u\,. \qquad (4.18)$$

So we have the classical result that we anticipated in Sec IV. B, that the reflected wave will pick up twice the speed of the mirror. (This result is independent of the fact that the phase velocity of the wave is not v.) We also have from this that

$$A = -\exp[i(k + k')(\xi_\tau - u\tau)] = e^{i\alpha}\,. \qquad (4.19)$$

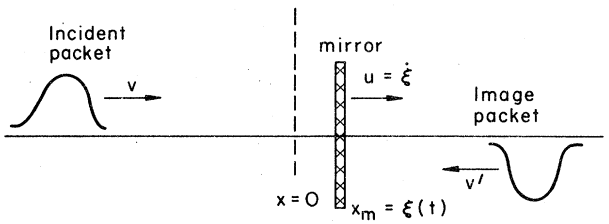

FIG. 27. Scattering from an accelerating mirror. The incident wave packet starts at $x = -x_0$ at time $t = -t_0$, and approaches the mirror from the left with velocity v. The image packet approaches from the right. The mirror is located at $x_m = 0$ at $t = 0$, which is where the waves would cross if it were at rest. But actually, $x_m = \xi(t)$, with $\xi(0) = 0$, $u = \dot{\xi} \ll v$, and the wave strikes the mirror at $t = \tau$.

Now we can write a wave-packet solution in terms of this plane-wave solution. Introduce the wave packet

$$f(x) = \int dk\, a(k-k_0)\, e^{ikx}. \tag{4.20}$$

The wave function then becomes

$$\psi(x,t) = \int dk\, a(k-k_0)\, \phi(x,t)$$

$$= \int dk\, a(k-k_0)[\exp(ikx - i\omega t) - e^{i\alpha}\exp(-ik'x - i\omega' t)]. \tag{4.21}$$

Assume that this narrow wave packet is centered about momentum $k = k_0$, so that the velocity is

$$v = \left(\frac{\partial\omega}{\partial k}\right)_{k_0}. \tag{4.22}$$

Then the first exponential is the incident wave, which we shall assume to be originally centered at some point $x = -x_0$, at time $t = -t_0$. These points, x_0 and t_0, are related by the fact that the particle will strike the mirror at $t = \tau$, or

$$x_0 + \xi(\tau) = v(\tau + t_0). \tag{4.23}$$

The reflected wave will be approximately located at $x = +x_0$ at this same time.

The first exponential becomes

$$e^{ikx - i\omega t} = e^{i(k_0 x - \omega_0 t)}\, e^{i(k-k_0)(x-vt)} \equiv e^{i\beta_1}\, e^{i(k-k_0)(x-vt)}, \tag{4.24}$$

where, from Eq. (4.22), we have written

$$\omega \sim \omega_0 + v(k-k_0). \tag{4.25}$$

The second exponential becomes

$$\exp(-ik'x - i\omega' t) = \exp(-ik_0 x - i\delta k x - i\omega_0 t + 2ik_0 u t) \times \exp\{-i(k-k_0)[x + (v-2u)t]\} \equiv \exp(i\beta_2)\exp\{-i(k-k_0)[x + (v-2u)t]\}, \tag{4.26}$$

where we have used

$$\omega' = (\hbar^2/2m)[k_0 + (k-k_0) + \delta k]^2, \tag{4.27}$$

with δk given by Eq. (4.17), and we have discarded the terms in $(k-k_0)^2$ and $(\delta k)^2$.

If we assume that $f(x)$ is real, so that $a(k-k_0) = a^*(k_0 a^*(k_0 - k)$, then Eqs. (4.21), (4.24), and (4.26), yield

$$\psi(x,t) = e^{i\beta_1} f(x - vt) - e^{i(\alpha_0 + \beta_2)} f(x + (v-2u)t + \delta x). \tag{4.28}$$

This solution, which has physical significance on only one side of the mirror, $x < \xi(t)$, represents the incident beam approaching the mirror followed by the reflected beam bouncing off it with the appropriate corrected velocity. (The small shift δx comes from the $\exp(i\alpha)$ term as a correction to the initial position.) The boundary condition $\psi(x = \xi(t), t) = 0$, is automatically satisfied when the wave packet is not near the mirror, because of the narrowness of the wave packet. It is only when the packet is near the mirror, at time $t \sim \tau$, that one need worry about this condition, but the plane-wave solutions were explicitly constructed to satisfy the condition at this time, which justifies the approximation in Eq. (4.13).

This calculation also justifies the assumption we made in the last section, that the Doppler shift for a particular neutron wave packet is determined by the velocity of the slab at the moment that the wave packet was scattered by the slab. (The individual plane waves themselves are distributed over all space, of course, and so individually they are never aware of the slab. It is the wave packet that is scattered by the slab.)

The final feature we shall mention concerns the nature of the "snapshot" we are using in the accelerated system (Fig. 25). In the laboratory system, the neutrons are falling as they move between the crystal slabs, and so the plane-wave fronts describing them become distorted. But in the accelerated system the gravitational field is not present, and so the neutrons move in straight lines at constant speed between the slabs. Nonetheless, if you follow the beam along the path AC in Fig. 25, you will see that at each point the neutrons have slightly different velocities, because they were scattered by the crystal at different times, and the crystal velocity is varying.

But if you follow the same accelerating system to the next instant of time, the situation would be different, because the neutrons at one point have constant velocity, and are not "evolving" into the neutrons at the next point. It is also true that at this next instant, the crystal would no longer be at rest. In our system, at $t = 0$, the series of wave fronts along line AC, as shown in Fig. 25, really represents the following situation. If at some point along AC you wanted to compose a wave packet for a neutron at that point, you would use plane waves going in the direction shown at that point in the diagram. These are the waves that had been scattered with the appropriate Doppler shift velocity $u(t)$, at the right time.

One might also add parenthetically that if instead one took the next snapshot at a slightly shifted velocity, such as would be needed to keep the crystal at rest, the extra velocity boost required at a time dt later would be just sufficient for the neutrons at one point to evolve into the neutrons at the next point. But of course, one would then have a truly static situation, and in fact one would be back in the laboratory system.

It should be borne in mind that the argument in the accelerated frame depends only on the transformation between the static and accelerated frames, and has nothing to do with how simple or complicated a model one uses for the crystal. In order to demonstrate this point, Horne and Zeilinger have developed a very simple model which needs to consider scattering off of only one atom in the initial interferometer slab, two atoms in the second slab, and four atoms in the third slab (to be published).

V. THE AHARONOV-BOHM EFFECT AND THE MARTON EXPERIMENT

We have pointed out that the basic wave phenomena involved in coherent scattering off of crystals are the same, independently of whether one is using a beam of electrons, neutrons, or x rays. However, the now

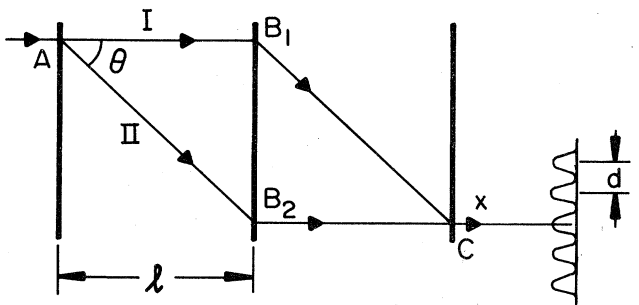

FIG. 28. Schematic diagram of Marton's experiment. An electron beam was successively diffracted through three very thin copper sheets, which acted as diffraction gratings, rather than Bragg scatterers. At the third sheet the beams were realigned. The fringes on the film were caused by imperfect realignment of the beams.

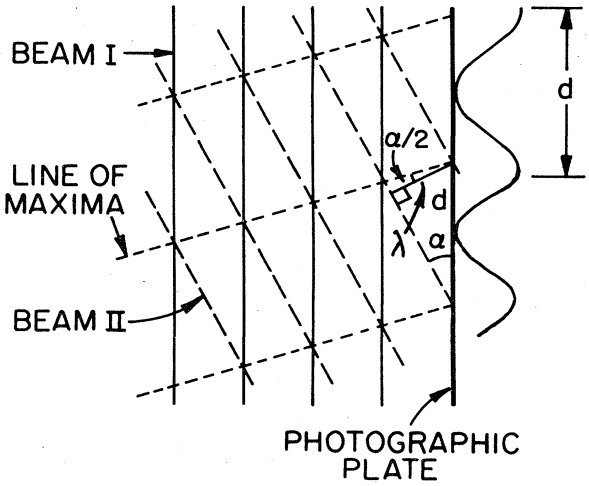

FIG. 29. Interference fringes in Marton's experiment. Due to buckling of the planes and lack of parallelism the two beams were not perfectly aligned after the third diffraction plane. If the two beams were out of parallel by angle α, the line of maxima would travel at angle $\frac{1}{2}\alpha$ to each, and the fringe spacing would be $d=\lambda/\sin\alpha$.

standard interpretation of one of the classic electron diffraction experiments directly contradicts the results of the neutron experiment of COW. This electron experiment, done by Marton (Marton, 1952; Marton *et al.*, 1953, 1954) at NBS was an extremely difficult experiment to perform, and the evolution of its interpretation has had an interesting history. The problem posed by this interpretation was the original motivating force for the present paper, and since we believe it to be incorrect, we shall discuss it in some detail.

A schematic diagram of Marton's experiment is shown in Fig. 28. He modified an electron microscope to serve as an interferometer, and was the first to successfully separate an electron beam into two disjoint parts and then coherently recombine them. The beam was scattered off three successive thin copper films. At the first film, one beam passed straight through while the other underwent first-order diffraction. (The film was sufficiently thin to act as a diffraction grating, rather than a Bragg scatterer, being only about 150 Å thick.) These copper films were themselves difficult to produce and had some slight buckling in them, due to internal strains. At the third film the beams were recombined. Because of the imperfect film coplanarity, plus the fact that they had been aligned by hand, they were not perfectly parallel after the third film, and produced a series of interference fringes on a photographic plate in their path (Fig. 29). (If the beams were out of parallel by angle α, the fringe spacing would be $d=\lambda/\sin\alpha$.)

Each plate was exposed for 6 minutes, and over 1200 exposures were required before the first diffraction pattern was observed. These patterns were all but invisible to the naked eye and had to be measured with a microdensitometer. In spite of the incredible patience and care of Marton and his co-workers, and their systematic optimization of the numerous experimental parameters and elimination of "noise," all carefully reported in their account of the experiment, highly visible fringe patterns were never obtained, a fact we believe to be highly significant. It should also be noted that there was no persistence among the fringe patterns obtained, and they usually disappeared after two or three exposures, and never lasted longer than six exposures.

In 1959, Aharonov and Bohm (1959) wrote their famous paper pointing out that one could observe some effects from an electromagnetic potential even in regions where there are no actual fields present. A simple description of the idea involved is provided by noting that the gauge invariance of electromagnetic theory yields a prescription for introducing electromagnetic fields, via their potentials, into any Hamiltonian theory. One simply replaces the momentum $\mathbf{p}$ by the quantity $\mathbf{p}-(e/c)\mathbf{A}$, wherever it occurs in the Hamiltonian. Then in quantum theory,

$$p_\mu\psi \to [p_\mu - (e/c)A_\mu]\psi\,, \tag{5.1}$$

in the Schrödinger equation.

One way to describe the effect of this transformation is to write

$$\psi(x)=\psi_0(x)\exp\left(\frac{ie}{\hbar c}\int_{x_0}^{x} A_\mu\, dl_\mu\right)$$

$$=\psi_0(x)\exp[i\phi(x)]\,, \tag{5.2}$$

where x_0 is some arbitrary initial reference point, and the integral runs over some path P between x_0 and x. Then

$$(p_\mu - (e/c)A_\mu)\psi_0 e^{i\phi}$$
$$=[(\hbar/i)(\partial_\mu\psi_0 + (ie/\hbar c)A_\mu\psi_0) - (e/c)A_\mu\psi_0]e^{i\phi}$$
$$=(p_\mu\psi_0)e^{i\phi}\,. \tag{5.3}$$

Thus, if ψ_0 obeys the Schrödinger equation without any electromagnetic field present, it would also seem to obey the same equation with the potential present, and the whole electromagnetic effect appears to have been reduced to the single quantity $e^{i\phi(x)}$, which factors out leaving no observable consequences. Wherein, then, does the reality of the electromagnetic field lie?

The answer, of course, is that one has assumed the existence of the function $\phi(x)$ in Eq. (5.2). But in fact, there exists such a function only if the line integral

$\int A_\mu\, dl_\mu$ is independent of the path chosen P, between x_0 and x. Otherwise there is a different ϕ for every path chosen, and

$$\phi = \phi(x, P)\,. \tag{5.4}$$

In this case ϕ is not a single-valued function of x only. And the criterion for the existence of a unique ϕ is just that the curl of A_μ vanishes

$$\partial_\mu A_\nu - \partial_\nu A_\mu = F_{\mu\nu} = 0\,. \tag{5.5}$$

So the criterion for the potential's producing no real effect is just that there be no electromagnetic field present anywhere in the region. If there are real fields present, then the factorization of Eq. (5.2) is path dependent.

This argument shows the inherently nonlocal character[8] of electromagnetic potentials. There must be no electromagnetic fields present anywhere in the region for the argument to work, not merely over the path one happens to be interested in. The specific, remarkable experiment discussed by Aharonov and Bohm concerned the coherent splitting of an electron beam into two paths passing on either side of a solenoid. The magnetic field of the solenoid is confined to the region inside the solenoid itself; if the axis of the solenoid is perpendicular to the paper in Fig. 30, the magnetic field will also be.

If there is no magnetic field in the solenoid, the wave functions for the electron taking paths I and II will be $\psi_0^{(\mathrm{I})}$ and $\psi_0^{(\mathrm{II})}$. If there is a magnetic field present in the solenoid, the wave functions at point b, where the waves recombine, will be

$$\psi_0^{(\mathrm{I})} \exp\left(\frac{ie}{\hbar c}\int_{\mathrm{I}} \mathbf{A}\cdot\mathbf{dl}\right)$$

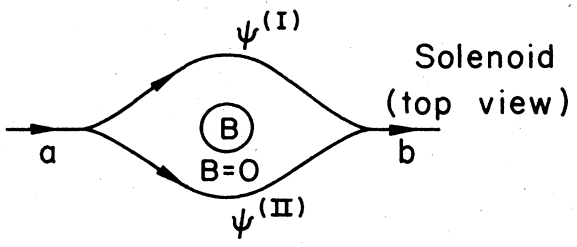

FIG. 30. The Aharonov–Bohm effect. A long solenoid contains a uniform magnetic field B. Outside the solenoid, $B=0$. An electron beam is split at point a, and the separate beams pass on opposite sides of the solenoid and are then coherently recombined at b. The two beams will pick up a measurable gauge-invariant phase difference proportional to $\oint \mathbf{A}\cdot\mathbf{dl} = \int \mathbf{B}\cdot\mathbf{dS}$, the flux through the area contained by the two beams. This is true even though *neither* beam ever enters the region of magnetic field, or feels any magnetic force.

and

$$\psi_0^{(\mathrm{II})} \exp\left(\frac{ie}{\hbar c}\int_{\mathrm{II}} \mathbf{A}\cdot\mathbf{dl}\right).$$

(Even though $B=0$ outside the solenoid, $A\neq 0$ there, and A circulates around the solenoid.) The recombined wave function will be

$$\psi = \psi_0^{(\mathrm{I})} \exp\left(\frac{ie}{\hbar c}\int_{\mathrm{I}} \mathbf{A}\cdot\mathbf{dl}\right) + \psi_0^{(\mathrm{II})} \exp\left(\frac{ie}{\hbar c}\int_{\mathrm{II}} \mathbf{A}\cdot\mathbf{dl}\right)$$

$$= \exp\left(\frac{ie}{\hbar c}\int_{\mathrm{I}} \mathbf{A}\cdot\mathbf{dl}\right)\left(\psi_0^{(\mathrm{I})} + \psi_0^{(\mathrm{II})} e^{i\eta}\right), \tag{5.6}$$

where

$$\eta = \frac{e}{\hbar c}\left(\int_{\mathrm{I}} - \int_{\mathrm{II}}\right)\mathbf{A}\cdot\mathbf{dl} = \frac{e}{\hbar c}\oint \mathbf{A}\cdot\mathbf{dl} = \frac{e}{\hbar c}\int \mathbf{B}\cdot\mathbf{dS}\,. \tag{5.7}$$

This phase difference between the beams η is gauge invariant, depending on the flux of B through the path. The only contribution comes from the flux of B inside the solenoid. Thus turning on the solenoid creates a phase difference between the two beams, which is of course measurable by its interference effects, even though *neither* beam ever enters the magnetic field region.

Since neither beam is ever subject to a magnetic force, the envelope of the combined beam pattern will be unshifted, but within this envelope the fringe pattern of the recombined beams will shift when the magnetic field is turned on. These conclusions have since been beautifully verified experimentally by Chambers, using a magnetic whisker for a solenoid[9] and by Bayh.[10] But at the time the experiment was first proposed, the reality of the Aharonov-Bohm effect was subject to a lively debate.

It was quickly realized that the phase factor in Eq. (5.2) had to be present in order to cause the semiclassical bending of an electron beam moving in a real electromagnetic field, and so the Aharonov-Bohm predictions were a necessary consequence of elementary quantum-mechanical considerations.

The relevance of the Marton experiment to these early discussions is that it was pointed out at that time that during the Marton experiment there were stray 60-cycle magnetic fields present in his laboratory (H. Mendlowitz, 1960). Thus, if there were a flux of magnetic field perpendicular to the plane of the paper in Fig. 28, it would introduce a phase shift

$$\eta = \frac{e}{\hbar c}\int \mathbf{B}\cdot\mathbf{dS} \approx \frac{eBl^2\theta}{\hbar c} \tag{5.8}$$

[8]We agree with Y. Aharonov (private communication) in this interpretation. However it has been subject to debate. The consistency of the Aharonov–Bohm (A–B) effect with the uncertainty principle was discussed by Furry and Ramsey, 1960. The single-valuedness of the wave functions in the A–B effect was discussed by Tassie and Peshkin, 1961, and problems on locality and the meaning of potentials were considered by DeWitt, 1962, and Belinfante, 1962. Further work and answers to their critics, were contained in papers by Aharonov and Bohm, 1961, 1962, 1963. Alternative, controversial interpretations of the A–B effect have been presented by Boyer, 1973, and Liebowitz, 1965.

[9]Chambers, 1960. His beautiful fringe patterns verified the results that the Aharonov-Bohm effect caused a fringe shift, while the bending of the beam shifted the beam envelope. Further whisker experiments were done by Fowler *et al.*, 1961. Magnetic zone boundaries were used to produce the interference by Boersch *et al.*, 1960.

[10]A more versatile tool, the electrostatic analog of an optical biprism, was built by Möllenstedt and Bayh, 1962a, b and used by Bayh, 1962, in conjunction with a tiny solenoid to verify the Aharonov–Bohm effect very strikingly. A summary of experimental work, with some more up to date experiments, can be found in Woodilla and Schwarz, 1971.

for small θ, which by varying between $\pm\eta$, 60 times/sec, would have washed out his interference fringes.

The data quoted by Marton (Marton *et al.*, 1954) for his experiments, when referred to Fig. 28, show that $l \sim 35$ mm, $\theta \sim 0.02$ rad, $d \sim 1650$ Å, and we estimate $x \sim 10$ cm. In addition, the wavelength of his electrons was $\lambda = 0.048$ Å. The amplification factor of his magnetic lens was about 500, so that d_0, the fringe distance at the third copper film, was about 3.3 Å. This gives about 1° for angle α between the beams in Fig. 29, which seems reasonable, considering the buckling of his films. (One can independently verify this magnitude for α, which is about the size of the first-order deflection θ. Marton proved that his diffraction patterns came from the recombination of the separated beams, by successively blocking the individual beams and noting that the fringes disappeared. However, not all fringing effects disappeared. There were residual small fringes of about the same spacing in the individual beams, which would be produced by buckling of the film by this order of magnitude.) One can also check the other effects of the stray fields on his experiments from this data. The most significant factor, however, is that the phase shift η, from Eq. (5.7), is about

$$\eta \sim 6\times 10^5 B \text{ rad} (B \text{ in G}) . \tag{5.9}$$

An *ac* line cord, carrying 1 A current, about 1 m from the apparatus, would produce a stray field of about 10^{-5} G, which is also of the order of various solenoids, transformers, etc. However, the total stray *ac* field in a typical laboratory can reach 10^{-3} G, and so we estimate that a reasonable value for the fringe shift in his laboratory would be

$$N = \eta/2\pi \sim 100 \text{ fringes} . \tag{5.10}$$

Because of this, it was originally suggested that the Aharonov–Bohm effect could not be real, because it predicted that any stray fields in Marton's laboratory would have blurred out his fringes. However, it was soon realized by a number of people, and explicitly calculated by Werner and Brill, that there was a second effect present (Werner and Brill, 1960; they also mention the debate over the reality of the effect at that time). Unlike the case in the original Aharonov–Bohm experiment, in the Marton experiment the stray magnetic field extends over the actual paths of the electron beams, and thus the beams are bent by these fields.

In Fig. 31, the two beams are both bent into the arcs of large circles, and Werner and Brill argued that therefore they no longer have exactly the same path length, which alters their relative phase. The amazing fact is that, to lowest order, this effect is exactly the same as that of the phase shift due to the magnetic flux through the path, and so cancels it out. Thus, according to Werner and Brill, it was the presence of both these effects, the bending and the magnetic phase factor, which made the Marton experiment possible. If there had been no Aharonov–Bohm effect, there would have been no beam stability. And so instead of Marton's experiment proving the inconsistency of the effect, it proved the necessity for it.

This beautiful result has become the standard interpretation of the Marton experiment, and coupled with

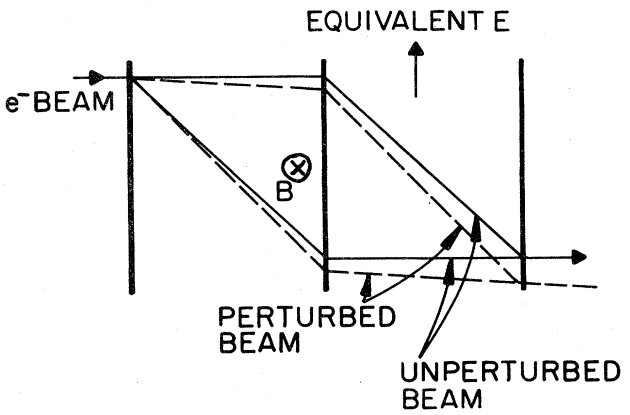

FIG. 31. Effect of an external magnetic field on electron trajectories. In the Marton experiment, the external magnetic field bent the trajectories of the beams into large circles, changing the relative path length of the beams. The magnitude of the effect is exactly that of the Aharonov–Bohm effect, to lowest order. But it is also true that the beams land at different points on the last grating, and that the subsequent shifting of the beams relative to each other cancels the bending effect, leaving only the original phase shift, $\int \mathbf{A}\cdot\mathbf{dl}$. This shift is exactly what is needed to confirm our result that the fringes and beam envelope shift equally.

the successful confirmations of the Aharonov–Bohm effect itself, it has seemed to close the book on the subject. Nonetheless, the Werner and Brill interpretation is essentially incomplete, as originally presented (although of course, the Aharonov–Bohm effect is certainly real). Professor Werner and Prof. Brill agree with this conclusion (see footnote 4). However, one should not underestimate the historical importance of the Werner-Brill paper. It was their paper which convinced many scientists that the Marton experiment did not disprove the Aharonov-Bohm effect in the period before the effect was directly confirmed.

First we would like to point out that if the original Werner and Brill analysis were applied to the COW neutron-gravity experiment, the results would disagree with those of the actual experiment. If instead of a magnetic field there had been a vertical, uniform electric field, as shown in Fig. 31, the analysis would follow almost identically. In this case the phase factor from the line integral $\int A_\mu\, dl_\mu$ would be $-c\int V\, dt$ instead of $\int \mathbf{A}\cdot\mathbf{dl}$. Therefore, the phase difference η between the beams $\psi^{(\mathrm{I})}$ and $\psi^{(\mathrm{II})}$, which appears in Eqs. (5.6) and (5.7), would be

$$\exp\left(\frac{-ie}{\hbar}\int \Delta V\, dt\right), \quad \Delta V = (V_{\mathrm{I}} - V_{\mathrm{II}}) . \tag{5.11}$$

Here the difference in potential between the two beams at any point x replaces the line integral of A. This effect would again be canceled out by the change in path length between the two beams. In this case the beams would be bent into a parabolic, rather than a circular, arc but to lowest order this does not affect the result. Neither does the fact that here it is v_x that is unchanged, rather than the magnitude of v. So, according to the original Werner and Brill analysis, the same cancellation occurs for an electric field as for a magnetic one.

Finally, there is no formal difference, in the nonrelativistic limit, between a static electric field and any other force produced by a potential. Of course for any other force the phase factor is not produced by gauge invariance, but nonetheless it is there as a correction to the energy, and in fact a comparison of Eq. (5.11) for the electric case, and Eq. (2.17) for a conservative force, shows that the phase shift is identical for the two cases. The bending of the beam into a parabola will also be identical, if the force is uniform and vertical.

Thus the original Werner–Brill analysis leads to the conclusion that *any* stray static or slowly varying field, not only a magnetic or even electromagnetic one, will produce no shift in fringes. However, in the COW experiment, the tilting of the apparatus to produce a gravitational potential difference between the two beams had the effect of creating just such a stray field, namely a "stray gravitational field." Therefore, if the Werner–Brill argument were complete, COW would *not* have seen any fringes. But we know that this result differs from those of both the experiment and the theoretical analysis, which we performed in Sec. IV from two separate viewpoints.

In what way, then, is the Werner–Brill argument essentially incomplete? We have actually already analyzed diffraction through a thin film in Sec. II. There we showed that there is no effect at all due to the bending of the beam, but rather, the phase shift due to the potential produces a fringe shift, and at the same time a shift in the envelope of the beam. When one considers that the ray is deflected by the perturbing force, as in Fig. 31, one is actually saying that the classical trajectory of the particle has been shifted. But the classical trajectory is just the center of the quantum-mechanical wave packet, or the envelope of the wave. So an argument based on the drawing of semiclassical rays can be interpreted as referring to the envelope of the wave packet.

As for the shift in phase of the wave fronts, they are given by the factor in Eq. (2.17). Therefore, one proper restatement of the calculation of Werner and Brill is that the envelope of the wave shifts by the same amount as the phase, which merely confirms the result of our calculation in Sec. II. So it is really not so amazing that the two effects are equal in their calculation, as in fact they must be equal. But from this point of view it would then be improper to think of their calculations as referring to two separate phase factors, or to think that the two effects can cancel out in any sense, as they are two different types of quantities.

Of course, if one carried through a perfectly consistent treatment by tracing rays, then one could interpret the results purely in terms of phases, and one should agree with our results. In terms of the Werner–Brill analysis, an extra effect enters, which was left out in their original paper. This is that the separated beams, when recombined, no longer meet at the same point. The sliding of one beam along the final screen, relative to the other, entails an extra phase factor which exactly cancels the effect due to the bending.

One can see this in detail by referring back to Fig. 2. If the original ray AB of the initially free particle strikes the screen at B, one can measure the phase at B by the optical path

$$\hbar\phi_0 = \int_A^B \mathbf{p}\cdot d\mathbf{r} = \mathbf{p}_{AB}\cdot\mathbf{r}_{AB} = p_0 r_0 . \tag{5.12}$$

where $\mathbf{p}_{AB}$ and $\mathbf{r}_{AB}$ are the momentum and displacement along this straight ray, of magnitude p_0, and r_0. The phase of the unperturbed wave at a nearby point B' will be given by the straight-line optical path

$$\begin{aligned}\hbar\phi_1 &= \int_A^{B'} \mathbf{p}\cdot d\mathbf{r} = \mathbf{p}_{AB'}\cdot\mathbf{r}_{AB'} = p_0\left|\mathbf{r}_{AB}+\Delta\mathbf{r}\right| \\ &\approx p_0(r_0^2 + 2\,\mathbf{r}_{AB}\cdot\Delta\mathbf{r})^{1/2} \approx p_0 r_0\left(1+\frac{\mathbf{r}_{AB}\cdot\Delta\mathbf{r}}{r_0^2}\right) \\ &\approx p_0 r_0 + \mathbf{p}_{AB}\cdot\Delta\mathbf{r} ,\end{aligned} \tag{5.13}$$

since $|p_{AB'}| = p_0$, $\mathbf{p}_{AB} = p_0\mathbf{r}_{AB}/r_0$, and $\Delta\mathbf{r} = \mathbf{r}_{AB'} - \mathbf{r}_{AB} = \mathbf{r}_{BB'}$. The second term in Eq. (5.13) is just the effect of the displacement along the screen.

If the ray AB is now deflected by a perturbation to the curved trajectory AB' then the optical path along the curved trajectory AB' will be given by

$$\begin{aligned}\hbar\phi_1' &= \int_A^{B'} (\mathbf{p}_{AB}+\delta\mathbf{p})\cdot d(\mathbf{r}+\delta\mathbf{r}) \\ &= p_0 r_0 + \int \delta\mathbf{p}\cdot d\mathbf{r}_{AB} + \mathbf{p}_{AB}\cdot\int d(\delta\mathbf{r}) \\ &= p_0 r_0 + \hbar\delta\phi + \mathbf{p}_{AB}\cdot\Delta\mathbf{r} = \hbar\phi_1 + \hbar\delta\phi .\end{aligned} \tag{5.14}$$

In this calculation the extra path length contribution due to the bending of the ray $\int \mathbf{p}\cdot d(\delta\mathbf{r})$ is exactly the same as the effect due to the displacement of the beam from B to B' along the screen. So while the phase at B' is not equal to the phase at B, neither were they equal in the original unperturbed beams. The only residual effect at B' that is due to the perturbation is $\phi_1' - \phi_1 = \delta\phi$, which is precisely the effect we have always included, $\int \delta\mathbf{p}\cdot d\mathbf{r} = -\int U dt \sim \int \mathbf{A}\cdot d\mathbf{l}$, in the potential or magnetic case. In other words, the only effect of the perturbation on the phase at a fixed point (in this case B') is $\delta\phi$. The bending and sliding effects cancel, leaving a result that exactly agrees with ours.

The original Werner–Brill calculation gave $\phi_1' - \phi_0$, and left out the sliding of the beam along the screen. Because of the fact that $\hbar\delta\phi = -\mathbf{p}_{AB}\cdot\Delta\mathbf{r}$ in their case, then $\phi_1' = \phi_0$, and one is led to the erroneous conclusion that there is no phase shift for the Marton or COW experiments. [M. Horne and C. Shull have independently arrived at the conclusion that the Werner–Brill analysis must be supplemented (unpublished).]

To recapitulate, in the Marton experiment, as in the COW experiment, as in all other Aharonov–Bohm-type experiments, the fringes do indeed shift, and the envelope of the wave shifts by the same amount, if the beam passes through the external field. However this raises one final question, namely, how was it possible for Marton to see any fringes at all, if these fringes were oscillating back and forth with an amplitude of about 100 fringes, about 60 times/sec? The answer is that in such a case the blurring effect is far from complete, because a sinusoidally oscillating beam spends most of its time at the extreme end points of its oscillation, and so the major effect is a dimming of the pattern, rather than a total obliteration of it.

To see this analytically, imagine a fringe pattern on

a screen, whose intensity is given by

$$I(x) = I_0 \cos^2 \pi x/L\,, \tag{5.15}$$

so that the fringes are separated by a distance L. If now the pattern is oscillating back and forth, according to the formula

$$I(x,t) = I_0 \cos^2[(\pi/L)(x - A\cos\omega t)]\,, \tag{5.16}$$

where

$$A/L = N \gg 1\,, \tag{5.17}$$

and N is the number of fringes swept out in the distance A, the pattern might be expected to wash out for $N \gg 1$. The average intensity at a point x (with $T = 2\pi/\omega$), will be given by

$$\bar{I}(x) = \frac{1}{T}\int_0^T I(x,t)\,dt = \frac{\omega I_0}{4\pi}\int_0^T dt\left[1 + \cos\left(\frac{2\pi}{L}(x - A\cos\omega t)\right)\right]$$
$$= \frac{I_0}{2} + \frac{\omega I_0}{4\pi}\int_0^T dt\left[\cos\left(\frac{2\pi x}{L}\right)\cos\left(\frac{2\pi A}{L}\cos\omega t\right) + \sin\left(\frac{2\pi x}{L}\right)\sin\left(\frac{2\pi A}{L}\cos\omega t\right)\right]. \tag{5.18}$$

The second integral vanishes by symmetry and the first is a standard integral representation of the Bessel function [Abromowitz and Stegun, 1964, formula (9.1.18)], giving

$$\bar{I} = \tfrac{1}{2}I_0 + (\omega I_0/4\pi)\,T\cos(2\pi x/L)J_0(2\pi A/L)$$
$$= (\tfrac{1}{2}I_0)[1 + J_0(2\pi N)\cos(2\pi x/L)]\,. \tag{5.19}$$

Then, since $N \gg 1$,

$$\bar{I} \approx (\tfrac{1}{2}I_0)[1 + (\pi^{-1}N^{-1/2})\cos(2\pi N - \tfrac{1}{4}\pi) \times \cos(2\pi x/L)]\,. \tag{5.20}$$

Thus the percentage variation in $\bar{I}$, from point to point, is

$$\frac{\delta\bar{I}}{\bar{I}} = \frac{\bar{I}_{\max} - \bar{I}_{\min}}{(\frac{1}{2}I_0)} \approx \frac{2}{\pi N^{1/2}}\left|\cos(2\pi N - \tfrac{1}{4}\pi)\right| \leq \frac{2}{\pi N^{1/2}}\,. \tag{5.21}$$

In Eq. (5.18), $\delta\bar{I}/\bar{I}$ can be anywhere between 0 and $2/\pi N^{1/2}$, depending on the exact value of N. The quantity N is proportional to A, which is proportional to the magnitude of the stray magnetic field.

So we see that in the Marton case, where $N \sim 100$, we would expect

$$\delta\bar{I}/\bar{I} \sim 10\%. \tag{5.22}$$

Even if N were 1000, we would still have $\delta\bar{I}/\bar{I} \sim 3\%$. If N varied during an exposure by about one fringe, it would wash out the effect, so that in order to see fringes we would need to have the stray field persistent and stable to the order

$$\frac{\Delta N}{N} = \frac{\Delta B}{B} < \frac{1}{N} \quad \text{(for a 6-min exposure)} \tag{5.23}$$

So we see that, even though the stray fields in the Marton experiment were great enough to cause an oscillation of 100 fringes, one could still expect an effect of up to 10%. We believe that these stray fields caused the great difficulties Marton had in obtaining fringes at all, and also explain why he was never able to obtain any of high visibility. On the other hand we can also understand why he *was* able to obtain weak fringes, as well as why they never persisted for very long. (Furthermore, both of Marton's published fringe patterns show multiple sets of fringes, consistent with the possibility that he was observing both extremes of the oscillation, or that the magnitude of the stray magnetic field varied during the exposure.) Thus we believe that all the facts are consistent with our explanation of the Marton experiment, and that most but not all of the effect was washed out by stray fields. This explanation is also completely consistent with the Chambers and Bayh experiments, and allows one to understand why the fringes are present in the COW experiment.

[We also received a strong but indirect corroboration of this explanation during a recent conversation with Professor G. Möllenstedt. He told us that he agrees that the reason his biprism experiments gave much cleaner results than the Marton one was that the enclosed area of his separated electronic beams was only about 10% of Marton's. This had the result of reducing the stray magnetic flux by a factor of 10. But he also noted that he still had great trouble performing his experiments in a stray field of 10^{-3} G, and had to remove them to a structure in which $B \sim 10^{-5}$ G, where he obtained his beautiful fringe patterns.

According to our analysis, the reduced flux would have given him about $N \sim 10$ fringes at $B \sim 10^{-3}$ G, from Eqs. (5.8) and (5.10), and then only $N \sim 0.1$ fringes at $B \sim 10^{-5}$ G. Thus the stray fields should have strongly affected his experiment in the former case, but not appreciably in the latter case—in perfect agreement with his actual observations.]

VI. SUMMARY

We have presented a discussion of the scattering of a neutron beam off a perfect crystal, emphasizing the effect of a small perturbing force, such as that due to gravity, on the outcome. We have shown that the only effect on the phase of the beam striking a given point on a screen beyond the scattering crystal, comes from a change in wavelength produced by the perturbing force. This will happen if there is a component of the force (or vector potential, in the magnetic case) parallel to the beam. There is no effect on the phase due purely to the bending of the wave front.

If, now, a beam is split into two coherent, spatially separated beams which are subsequently recombined, there will be a shift in the phase of the interference pattern at a given point due to the phase shifts described above. If the perturbing field is a static magnetic field, the total phase shift will be $\exp[(ie/\hbar c)\oint \mathbf{A}\cdot\mathbf{dl}]$, the line integral being taken around the closed path comprising

the two beams. If the effect is due to a static electric field of potential V, the phase shift will be $\exp[(-ie/\hbar)\int \Delta V\, dt]$, where the term ΔV denotes the difference between the potentials at corresponding points along the two beams. Similarly, if the effect is caused by a static, nonelectromagnetic field, with potential energy U, the phase shift will be $\exp[(-i/\hbar)\int \Delta U\, dt]$.

Beyond this, there is also a shift of the classical envelopes of the two beams, which keeps pace with this changing phase, so that overall, the entire interference pattern on the screen will be shifted, without changing its relative shape or the fringe distribution within the envelope.

The only exception to this rule occurs during the pure Aharonov–Bohm case, where the phase shift is present, but the split beams never pass through an external field, so there is no force exerted on the beams, and consequently no shift in the envelope of the beams. In this case the fringes shift position within the stationary beam envelope.

These statements are true regardless of whether the beam has been split by scattering off an inhomogeneous field, a two-dimensional diffraction grating, or a three-dimensional crystal, and we have corrected the original interpretation of the Marton experiment by Werner and Brill, who had concluded that these cases would not be similar. The results of the COW experiment are consistent with our conclusions, as well as those of all the experiments that have been used to confirm the Aharanov-Bohm effect.

We have discussed the coherence effects present in a thick crystal, especially the Borrmann effect, and presented a method for calculating the effect of displacing the crystal slabs, without recourse to the details of the dynamical theory of x rays, and have considered a number of experiments that illustrate the principles involved. And we have pointed out the differences between the transmission of neutron beams and that of x rays, due to their different absorption properties.

We have also analyzed the phase shift in the COW experiment, not only from the point of view given above, but also by transforming into the free-fall coordinate system, moving with the acceleration of gravity. In this system the beam is not falling, but rather the crystal is accelerating upward. In the Appendix we shall present a more general treatment of accelerated motion, as a guide to the analysis of future experiments using the earth's gravitational field.

ACKNOWLEDGMENTS

We should like to thank Professor Clifford Shull for allowing us to use some unpublished experimental results, and Professor Samuel Werner for providing some unpublished theoretical calculations. We should also like to thank Professor S. Werner, Professor R. Colella, Professor C. Shull, Professor A. Zeilinger, Professor M. Horne, Professor G. Squires, and Dr. B. Neyer for valuable discussions of various points of the subject. We are especially indebted to Professor F. Werner and Professor D. Brill for several long and fruitful discussions on the Aharonov–Bohm effect.

APPENDIX: UNIFORMLY ACCELERATED REFERENCE FRAMES

A. Nonrelativistic case

We have discussed the COW experiment from the point of view of an accelerated reference frame. We should like to justify some of the implicit assumptions in that discussion. But also, such an analysis provides a valuable check on the results obtained from an analysis in the laboratory system. Although the only coherence experiment which has been done to date that uses the earth's gravitational field used very low-energy neutrons, we shall also extend our discussion to include the relativistic case, partly in anticipation of possible future experiments, but partly also for its own intrinsic interest.

According to the principle of equivalence, a static uniform gravitational field in the laboratory should be equivalent to the situation experienced by a uniformly accelerating observer without a gravitational field. In the nonrelativistic case, we need not restrict ourselves to uniform acceleration, but we can consider any rigid acceleration of the entire reference frame (Rosen, 1972; Eliezer and Leach, 1977; Greenberger, to be published). We shall not consider rotations, however, although they can be included in the framework of such a discussion (Greenberger, 1968).

Thus we imagine the entire reference frame to be rigidly translated according to the formula

$$\mathbf{r}' = \mathbf{r} + \boldsymbol{\xi}(t), \quad t' = t. \tag{A1}$$

In this formula $(\mathbf{r}, t)$ represents the coordinates in the laboratory, which is considered to be an inertial system, while $(\mathbf{r}', t')$ are the coordinates in the accelerated reference system. The point $\mathbf{r}' = 0$ corresponds to the laboratory point $\mathbf{r} = -\boldsymbol{\xi}(t)$, so that the accelerated system is moving in the $(-\boldsymbol{\xi})$ direction. Thus the accelerated observer should feel an inertial force in the $+\boldsymbol{\xi}$ direction, producing an acceleration $+\ddot{\boldsymbol{\xi}}$. To an observer at rest in the accelerated reference frame, there should be a potential which corresponds to this force. Of course in the nonrelativistic limit there are no time dilatation effects.

1. The classical case

The Lagrangian in the laboratory is

$$L = \tfrac{1}{2} m v^2 - V(\mathbf{r} - \mathbf{r}_0). \tag{A2}$$

If there is an origin for the force, it is taken to be $\mathbf{r}_0$. Otherwise, any arbitrary point can be chosen as $\mathbf{r}_0$. The important consideration is that, since the entire system is being accelerated, the relative distance between two points will be unaffected by the transformation, which will therefore leave the potential unaffected, i.e.,

$$\mathbf{r}' - \mathbf{r}_0' = \mathbf{r} - \mathbf{r}_0, \quad V' = V. \tag{A3}$$

The potential V can be chosen to be any force acting in the laboratory (including a gravitational field).

Under the transformation (A1),

$$\mathbf{v} \to \mathbf{v}' = \mathbf{v} + \dot{\boldsymbol{\xi}}, \tag{A4}$$

and so the Lagrangian becomes

$$L' = \tfrac{1}{2} m(\mathbf{v}' - \dot{\boldsymbol{\xi}})^2 - V. \tag{A5}$$

The canonical momentum p' becomes

$$\mathbf{p}' = \frac{\partial L'}{\partial \mathbf{v}'} = m(\mathbf{v}' - \dot{\boldsymbol{\xi}}) = m\mathbf{v}, \tag{A6}$$

with the equation of motion

$$\dot{\mathbf{p}}' = m(\dot{\mathbf{v}}' - \ddot{\boldsymbol{\xi}}) = -\nabla V. \tag{A7}$$

The new Hamiltonian is

$$H' = \mathbf{p}' \cdot \mathbf{v}' - L' = p'^2/2m + V + \dot{\boldsymbol{\xi}} \cdot \mathbf{p}'. \tag{A8}$$

The above Hamiltonian yields the correct equation of motion but it contains a momentum-dependent potential. It is not the static potential we are seeking. Also, the canonical momentum is equal to the old momentum. To put the Hamiltonian into a more physically transparent form we make a canonical transformation (type 3 of Goldstein, 1950) to new variables $\mathbf{R}$, $\mathbf{P}$,

$$\begin{aligned} &\mathcal{H} = H' + \frac{\partial F}{\partial t}, \quad F = F(\mathbf{p}', \mathbf{R}), \\ &\mathbf{r}' = -\nabla_{p'} F, \quad \mathbf{P} = -\nabla_R F. \end{aligned} \tag{A9}$$

If we choose the generating function

$$F = -\mathbf{R} \cdot \mathbf{p}' - m\dot{\boldsymbol{\xi}} \cdot \mathbf{R} + f(t), \tag{A10}$$

then

$$\mathbf{r}' = \mathbf{R}, \quad \mathbf{P} = \mathbf{p}' + m\dot{\boldsymbol{\xi}} \tag{A11}$$

and

$$\begin{aligned} \mathcal{H} &= (\mathbf{P} - m\dot{\boldsymbol{\xi}})^2/2m + V + \dot{\boldsymbol{\xi}} \cdot (\mathbf{P} - m\dot{\boldsymbol{\xi}}) - m\ddot{\boldsymbol{\xi}} \cdot R + \dot{f} \\ &= P^2/2m + V - m\ddot{\boldsymbol{\xi}} \cdot \mathbf{R}, \end{aligned} \tag{A12}$$

provided we choose

$$\dot{f} = \tfrac{1}{2} m\dot{\xi}^2. \tag{A13}$$

Hamiltonian (A12) obviously gives the correct equivalence principle interpretation to the transformation, since the extra potential is of the expected static form, $-m\mathbf{a} \cdot \mathbf{R}$, where a is the inertial acceleration. It also gives a clear meaning to the coordinates,

$$\mathbf{R} = \mathbf{r} + \boldsymbol{\xi}, \quad \mathbf{P} = m(\mathbf{v} + \dot{\boldsymbol{\xi}}) = m\dot{\mathbf{R}}. \tag{A14}$$

The generating function F is

$$F = -\mathbf{R} \cdot \mathbf{p}' - m\left(\boldsymbol{\xi} \cdot \mathbf{R} - \frac{1}{2}\int \dot{\xi}^2 dt\right), \tag{A15}$$

where the first term is the identity transformation, while the second term generates the required changes.

2. The quantum case

If $\psi(\mathbf{r}, t)$ is the wave function in the unaccelerated system, obeying the Hamiltonian

$$-\left(\frac{\hbar^2}{2m}\right)\nabla^2\psi + V\psi = -\left(\frac{\hbar}{i}\right)\frac{\partial \psi}{\partial t}, \tag{A16}$$

then the transformation (A1) yields

$$\nabla = \nabla', \quad \frac{\partial}{\partial t} = \frac{\partial}{\partial t'} + \dot{\boldsymbol{\xi}} \cdot \nabla'. \tag{A17}$$

Making these substitutions, and setting $t' = t$, gives

$$-(\hbar^2/2m)(\nabla')^2\psi + V\psi + (\hbar/i)\dot{\boldsymbol{\xi}} \cdot \nabla'\psi = -(\hbar/i)\dot{\psi}. \tag{A18}$$

This equation suffers from the same defect as its classical counterpart, Eq. (A8).

However, if we make a unitary transformation derived from the classical generating function, we can write

$$\psi(\mathbf{r}, t) = u(\mathbf{r}', t)\exp\left[\frac{-im}{\hbar}\left(\dot{\boldsymbol{\xi}} \cdot \mathbf{r}' - \frac{1}{2}\int \dot{\xi}^2 dt\right)\right], \tag{A19}$$

and then the function u will obey the equation

$$-(\hbar^2/2m)(\nabla')^2 u + Vu - m\ddot{\boldsymbol{\xi}} \cdot \mathbf{r}' u = -(\hbar/i)\dot{u}, \tag{A20}$$

and this is the form of the equivalence principle in quantum theory. In the special case of uniform acceleration along the z axis,

$$\xi = \tfrac{1}{2}at^2, \quad \dot{\xi} = at, \quad \ddot{\xi} = a, \tag{A21}$$

and u satisfies the equation

$$-\left(\frac{\hbar^2}{2m}\right)(\nabla')^2 u + Vu - maz' u = -\left(\frac{\hbar}{i}\right)\frac{\partial u}{\partial t}. \tag{A22}$$

The transformation between wave functions, Eq. (A19), becomes

$$\begin{aligned} \psi(z, t) &= u(z', t)\exp[(i/\hbar)(-matz' + \tfrac{1}{6}ma^2t^3)] \\ &= u(z + \tfrac{1}{2}at^2, t)\exp[(i/\hbar)(-matz - \tfrac{1}{3}ma^2t^3)]. \end{aligned} \tag{A23}$$

If the potential V is $V = maz$, then u will represent a free particle. If $V = 0$, then u will represent a gravitating particle.

3. Connection between the wave functions

If $V = 0$ in Eq. (A20), and we consider only one dimension z, then the stationary solutions in the accelerated frame

$$u(z', t) = u_E(z')\, e^{-iEt/\hbar}, \tag{A24}$$

will be the Airy function (Landau and Lifschitz, 1958, Sec. 22, App. 6).

Introducing the dimensionless variable

$$\rho = (z' + E/ma)/l, \quad l^3 = \hbar^2/2ma, \tag{A25}$$

we have the solution

$$u_E(z') = A\phi(-\rho), \tag{A26}$$

where ϕ is the Airy function

$$\phi(\rho) = \pi^{-1/2}\int_0^\infty \cos(\tfrac{1}{3}\eta^3 + \eta\rho)\, d\eta. \tag{A27}$$

If we now substitute $z + \frac{1}{2}at^2$ for z', this becomes

$$\begin{aligned} \psi_E(z, t) = A\pi^{-1/2}\int \frac{d\eta}{\hbar}\cos\left(\tfrac{1}{3}\eta^3 - \frac{\eta(z + \frac{1}{2}at^2 + E/ma)}{l}\right) \\ \times \exp\left(\frac{-i}{\hbar}(Et + matz + \tfrac{1}{3}ma^2t^3\right). \end{aligned} \tag{A28}$$

Asymptotically, in the region $z' \gg 0$, the solution becomes

$$\phi \to \rho^{-1/4}\sin(\tfrac{2}{3}\rho^{3/2} + \tfrac{1}{4}\pi), \tag{A29}$$

so that we have

$$\psi_E(z, t) = (\psi_E^{(+)} - \psi_E^{(-)}), \tag{A30}$$

where

$$\psi_E^{(\pm)}(z,t) = A' \exp\left\{(\pm i)\left[\frac{2}{3}\left(\frac{z+\frac{1}{2}at^2+E/ma}{l}\right)^{3/2}+\tfrac{1}{4}\pi\right]\right.$$
$$\left. -\frac{i(Et+matz+\frac{1}{3}ma^2t^3)}{\hbar}\right\} \equiv A' e^{i\alpha}. \quad \text{(A31)}$$

In this equation, α is the phase of the exponential, and the slowly varying denominator has been incorporated into A'.

This is the transformation into the inertial system of the asymptotic stationary wave of the accelerated reference system. It is clearly not a plane wave, and so the question is, how is it related to the plane waves of the unaccelerated frame? A stationary wave in the accelerated frame will not be stationary in the inertial frame, since the transformation between them is explicitly time dependent.

One must look instead for a wave packet of accelerated solutions, to form the function $\psi(z,t)$. Take

$$\psi^{(+)}(z,t) = \int dE\, a(E)\, \psi_E^{(+)}(z,t) \quad \text{(A32)}$$

as the solution. We can consider the amplitude of a as slowly varying and need go only as far as the linear term in the phase,

$$a(E) \sim a e^{-ibE}. \quad \text{(A33)}$$

Then the phase in the integral of Eq. (A32) is

$$\alpha_1 = \alpha - ibE, \quad \text{(A34)}$$

where α is given by Eq. (A31). We evaluate the integral by the method of steepest descent. The phase will be stationary at some energy E_0 given by

$$\frac{\partial \alpha_1}{\partial E} = 0, \quad \text{at } E_0, \quad \text{(A35)}$$

and in the neighborhood of this point,

$$\alpha_1 \to \alpha_1(E_0) + i\beta(E-E_0)^2, \quad \text{(A36)}$$

where β will be real and positive, for the correctly chosen complex path, and so

$$\psi^{(+)} \to e^{i\alpha_1(E_0)} \int dE\, e^{-\beta(E-E_0)^2}. \quad \text{(A37)}$$

The integral will be a slowly varying amplitude factor, and therefore we are interested only in the phase $\alpha_1(E_0)$.

If we take the derivative in Eq. (A35), then setting it equal to zero gives a unique value for E_0,

$$E_0 = ma\{l\,[mal(b+t/\hbar)]^2 - (z+\tfrac{1}{2}at^2)\}. \quad \text{(A38)}$$

By placing this value of E_0 into α_1, and by using the definition of l, Eq. (A25), we reduce this phase to

$$\alpha_1(E_0) = \text{const} + mabz - \tfrac{1}{2}ma^2b^2\hbar t. \quad \text{(A39)}$$

If we call

$$mab \equiv k, \quad \text{(A40)}$$

then

$$\tfrac{1}{2}ma^2b^2\hbar = \hbar k^2/2m, \quad \text{(A41)}$$

and the phase becomes

$$\alpha_1(E_0) = \text{const} + kz - \hbar k^2 t/2m, \quad \text{(A42)}$$

which of course is the plane wave we are seeking. The role played by the constant b is to shift the time origin from t to $t+t_0 = t+\hbar b$. Then $v = \hbar k/m = at_0$, and b relates only to when the object was dropped and defines its velocity. In this solution, we could obviously have chosen $\psi(z,t)$ as the Airy function and derived the function u as the plane wave, which is actually the case in Sec. IV.

B. Relativistic case

In the case of relativity, we shall be restricted to the case of uniform acceleration, but it turns out that one can define the concept of a uniformly accelerating system in both special and general relativity. In special relativity[11] we look for the motion of a particle which has a constant acceleration in its own rest system. This can be generalized to the case of a static metric in general relativity, in which a particle has a uniform acceleration anywhere in space. This metric represents an accelerating coordinate system and is rigid in the sense that at constant time in this system every point in the original inertial system has the same velocity. Furthermore, the origin of this system undergoes uniform acceleration in the sense of special relativity. Once the concept of uniform acceleration is defined, one can set up the Klein–Gordon equation and Dirac equation in such a reference frame.

1. Uniform acceleration in special relativity

First, we establish our notation (with $c=1$): $x^0 = t$, $\mathbf{r} = (x^1, x^2, x^3) = (x, y, z)$; metric $\eta^{00} = 1$, $\eta^{ii} = -1$; Lorentz transformation $S(\theta)$ or $S(v)$, $z' = z\cosh\theta - t\sinh\theta$, $t' = t\cosh\theta - z\sinh\theta$, where $\gamma = (1-v^2)^{-1/2} = \cosh\theta$, $\sinh\theta = v\gamma$, $\tanh\theta = v$; $x^\mu = (x^0, x^1, x^2, x^3)$, or (x^0, x^3); $u^\mu = dx^\mu/d\tau = (\gamma, \mathbf{v}\gamma)$, $\mathbf{v} = d\mathbf{x}/dt$; $\alpha^\mu = du^\mu/d\tau = (\gamma^4 \mathbf{v}\cdot\mathbf{a}, \gamma^2 a^x, \gamma^2 a^y, \gamma^4 a^z)$, $\mathbf{a} = d\mathbf{v}/dt$. Latin letters run from 1 to 3, Greek from 0 to 3. Motion will generally be along the z axis, and we shall occasionally suppress x and y. The Lorentz transformation $S(\theta)$ will generally be to a system moving along the $+z$ axis with velocity v, and we shall specify when it is otherwise.

In order to define uniform acceleration, we seek the motion of a particle, which has a constant acceleration in the inertial system which is momentarily at rest with respect to it. If we transform the acceleration α^μ into a system moving instantaneously at the same velocity v as the accelerating body (assuming v along the z axis), we find

$$(\alpha^z)' = \gamma(\alpha^z - v\alpha^0) = \gamma^3 a^z, \quad (\alpha^x)' = \gamma^2 a^x, \quad (\alpha^y)' = \gamma^2 a^y,$$
$$(\alpha^0)' = \gamma(\alpha^0 - v\alpha^z) = 0; \quad \text{(A43)}$$
$$(\alpha^\mu)' = (0, \gamma^2 a^x, \gamma^2 a^y, \gamma^3 a^z).$$

Thus for motion along the z axis, with $a^x = a^y = 0$, such that the acceleration remains constant, we have

[11] Rohrlich, 1965, Chaps. 5 and 8. His general relativistic metric is not the same as ours. The problem is also discussed in Hamilton, 1978. A more general treatment of the problem of non-inertial motion also appears in Schmutzer and Plebanski, 1977.

$$\gamma^3 a^z = \text{const} \equiv \alpha \,. \tag{A44}$$

This equation is equivalent to

$$dv(1-v^2)^{-3/2} = \alpha dt \,, \tag{A45}$$

and integrates to

$$v = \alpha t(1+\alpha^2 t^2)^{-1/2} = \frac{dz}{dt} \,, \tag{A46}$$

choosing $v=0$ at $t=0$. Equation (A46) integrates to

$$z = [(1+\alpha^2 t^2)^{1/2} - 1]/\alpha \,, \tag{A47}$$

where we choose $z=0$ at $t=0$. This can be written

$$(\alpha z + 1)^2 = 1 + \alpha^2 t^2 \,, \tag{A48}$$

and represents uniform acceleration. It is sometimes called hyperbolic motion. For $\alpha z \ll 1$, Eq. (A48) reduces to

$$z \sim \tfrac{1}{2}\alpha t^2 \,. \tag{A49}$$

Equations (A47) and (A48) are the equations $z=f(t)$ for the coordinates of a particle in the laboratory (inertial) frame, the particle accelerating in such a way that an inertial observer moving with the same velocity as the particle will measure acceleration α. Some other useful formulas relating to this motion are

$$\gamma = (1+\alpha^2 t^2)^{1/2}, \quad d\tau = (1-v^2)^{1/2} dt, \quad \alpha t = \sinh \alpha\tau,$$
$$v = \tanh \alpha\tau, \quad \gamma = \cosh \alpha\tau = \alpha z + 1 \,. \tag{A50}$$

2. Uniform acceleration in general relativity

We should like to find a metric representing a system where particles have a uniform acceleration along the z axis. We are seeking a static metric, $g_{\mu\nu} = g_{\mu\nu}(z)$, with no t dependence, so that it will appear that a static gravitational field is present. Also, we want there to be no curvature, thus $R_{\mu\nu}=0$, so that there is no matter present, but the field is a pure acceleration field. We assume a metric of the form

$$ds^2 = f(z)dt^2 - g(z)dz^2 - dx^2 - dy^2 \,. \tag{A51}$$

(In what follows, $\dot{} \equiv d/ds \equiv d/d\tau$ and $' \equiv \partial/\partial z$). The geodesic equations are

$$\begin{aligned}
&(0)\ \ \ddot{t} + f'\dot{z}\dot{t}/f = 0, \quad (f\dot{t}) = \text{const} \equiv l \,; \\
&(3)\ \ \ddot{z} + f'\dot{t}^2/2g + g'\dot{z}^2/2g = 0 \,; \\
&(1)\ \ \ddot{x} = 0 \,; \\
&(2)\ \ \ddot{y} = 0 \,.
\end{aligned} \tag{A52}$$

A first integral of the motion is

$$l^2/f - g\dot{z}^2 - \dot{x}^2 - \dot{y}^2 = 1 \,. \tag{A53}$$

In these coordinates, constant acceleration means

$$\ddot{z} = \alpha = -f' l^2/2gf^2 - g'\dot{z}^2/2g \,. \tag{A54}$$

If we assume motion along only the z axis, Eq. (A53) becomes

$$g\dot{z}^2 = -(1 - l^2/f) \,, \tag{A55}$$

so that

$$\alpha = -l^2(f'/f + g'/g)/2gf + g'/2g^2 \,. \tag{A56}$$

We can choose our solution to be independent of the time scale, by setting

$$f'/f + g'/g = 0 \,, \tag{A57}$$

the solution to which is

$$\ln fg = \text{const}, \quad g = B/f \,. \tag{A58}$$

Then, for constant acceleration,

$$\alpha = g'/2g^2 \,, \tag{A59}$$

the solution to which is

$$g = (1 - 2\alpha z)^{-1} \,, \tag{A60}$$

where we have chosen $g(0)=1$, which sets the z scale for small z.

Independently of this we can ask for solutions of the metric, Eq. (A51), which represent zero curvature. The geodesic equations can be written in the form

$$\frac{d^2x^\lambda}{ds^2} + \left\{ \begin{matrix} \lambda \\ \mu\ \nu \end{matrix} \right\} \frac{dx^\mu}{ds}\frac{dx^\nu}{ds} = 0 \,, \tag{A61}$$

(the $\left\{ \begin{smallmatrix} \lambda \\ \mu\nu \end{smallmatrix} \right\}$ are the Christoffel symbols, and our notation is chosen to conform with that of Adler *et al.*, 1975; note that $A^\mu_{|\nu} \equiv \partial A^\mu/\partial x^\nu$, the partial derivative, while $A^\mu_{\|\nu} \equiv DA^\mu/DA^\nu$, the covariant derivative) which enables us to read off the Christoffel symbols from Eqs. (A52),

$$\left\{ \begin{matrix} 0 \\ 0\ 3 \end{matrix} \right\} = \frac{f'}{2f}, \quad \left\{ \begin{matrix} 3 \\ 0\ 0 \end{matrix} \right\} = \frac{f'}{2g}, \quad \left\{ \begin{matrix} 3 \\ 3\ 3 \end{matrix} \right\} = \frac{g'}{2g} \,, \tag{A62}$$

the others being zero.

The curvature equation becomes

$$R_{\beta\delta} = \left\{ \begin{matrix} \alpha \\ \beta\ \alpha \end{matrix} \right\}_{|\delta} - \left\{ \begin{matrix} \alpha \\ \beta\ \delta \end{matrix} \right\}_{|\alpha} + \left\{ \begin{matrix} \alpha \\ \tau\ \delta \end{matrix} \right\} \left\{ \begin{matrix} \tau \\ \beta\ \alpha \end{matrix} \right\} - \left\{ \begin{matrix} \alpha \\ \tau\ \alpha \end{matrix} \right\} \left\{ \begin{matrix} \tau \\ \beta\ \delta \end{matrix} \right\} = 0 \,. \tag{A63}$$

This equation has only one independent component in our metric,

$$\begin{aligned}
R_{00} &= -f''/2g + (f'/4g)(f'/f + g'/g) = 0 \,, \\
R_{33} &= -(g/f)R_{00} = 0 \,,
\end{aligned} \tag{A64}$$

the other components being identically zero. The solution to the equation $R_{00}=0$ is

$$g = A(f')^2/f \,. \tag{A65}$$

Thus for any value of f, this choice of g will give zero curvature. However the only choice consistent with constant acceleration is

$$g = B/f = (1 - 2\alpha z)^{-1} \,, \tag{A66}$$

which implies

$$f = (1 - 2\alpha z)/B, \quad f' = -2\alpha/B = \text{const} \,, \tag{A67}$$

and which is clearly consistent with Eq. (A65). We set $B=1$, in order to set the time scale $\dot{t}=1$ near the origin. Then our metric becomes

$$ds^2 = (1 - 2\alpha z)dt^2 - dz^2/(1 - 2\alpha z) - dx^2 - dy^2 \,. \tag{A68}$$

For regions of weak field, we expect $g_{00} \sim 1 + 2\phi/c^2$, where ϕ is the gravitational potential; in our case, this is the region around the origin. For $\alpha z \ll 1$ (dimensionally, this means $\alpha z/c^2 \ll 1$) we have

$$\phi \sim -\alpha z \,, \tag{A69}$$

which agrees with the equivalence principle, since any particle will feel a force accelerating it upward, and this is equivalent to this gravitational potential. We note that our solution corresponds to the entire coordinate system we are in being accelerated downward, so that any particle released from rest will feel a constant acceleration upward. Our metric, Eq. (A68), is the *static* solution representing constant acceleration.

3. Connection between the special and general relativistic solutions

In our solution to the general relativistic problem we have found a coordinate system in which the equation of motion for any particle is $\ddot{z}=\alpha$, $\ddot{x}=\ddot{y}=0$. Since $R_{\mu\nu}=0$, there is no real gravitational field present. Therefore the coordinate system itself is uniformly accelerating, in the sense that at a given time t in this system, which is static, every point has the same acceleration relative to an inertial system at that point. What we should like to do is to find this inertial system $(x^\mu)'$ relative to which our system x^μ is uniformly accelerating.

The problem then is this: to find a transformation from the metric of Eq. (A68) to a coordinate system with the metric

$$ds^2=(dt')^2-(dx')^2-(dy')^2-(dz')^2 . \tag{A70}$$

Such a metric must exist, since $R_{\mu\nu}=0$. We write

$$dz'=a\,dz-b\,dt,\quad dt'=c\,dt-d\,dz,\quad x'=x,\quad y'=y, \tag{A71}$$

where a, b, c, d are functions of x^μ. Since our x^μ coordinate system is itself accelerating in the $-z'$ direction, the transformation of Eq. (A71) will be along the $+z$ direction, and therefore the coefficients a, b, c, d will all be positive. If we substitute Eqs. (A71) into Eq. (A70), and compare the result with Eq. (A68), this will give us three conditions on the four functions a, b, c, d from matching the coefficients of the dt^2, dz^2, and $dz\,dt$ terms. These conditions can all be satisfied by writing

$$\begin{aligned} dz' &= \frac{\cosh w}{(1-2\alpha z)^{1/2}}\,dz-(\sinh w)(1-2\alpha z)^{1/2}\,dt , \\ dt' &= (\cosh w)(1-2\alpha z)^{1/2}\,dt-\frac{\sinh w}{(1-2\alpha z)^{1/2}}\,dz , \end{aligned} \tag{A72}$$

where $w=f(x^\mu)$. This is as far as one can go algebraically.

We can obtain two further restrictions on the derivatives of w by requiring that Eqs. (A72) should be integrable. Then we could write $(t', z')=f(t, z)$. These restrictions come from equating the crossed partial derivatives in Eqs. (A72). However, if we assume that $w=w(t)$ only, then both equations will be solved by $w=\alpha t$. (Actually, this is the only integrable solution.) Thus Eqs. (A72) become

$$\begin{aligned} dz' &= \frac{\cosh\alpha t}{(1-2\alpha z)^{1/2}}\,dz-(1-2\alpha z)^{1/2}\sinh\alpha t\,dt , \\ dt' &= (1-2\alpha z)^{1/2}\cosh\alpha t\,dt-\frac{\sinh\alpha t}{(1-2\alpha z)^{1/2}}\,dz . \end{aligned} \tag{A73}$$

These equations integrate to

$$\begin{aligned} z' &= [1-(1-2\alpha z)^{1/2}\cosh\alpha t]/\alpha , \\ t' &= [(1-2\alpha z)^{1/2}\sinh\alpha t]/\alpha . \end{aligned} \tag{A74}$$

This is the transformation for which we have been looking. The integration constants have been chosen so that $t=0$ implies $t'=0$, independently of z, and also so that at $t=0$, $z\sim z'$, for $\alpha z\ll 1$. So the two coordinate systems approximately coincide for $t=0$ and small z.

We can invert the transformation (A74). This gives the equations

$$\begin{aligned} 2\alpha z &= [1+\alpha^2(t')^2]-(1-\alpha z')^2 \\ \tanh\alpha t &= \alpha t'/(1-\alpha z') . \end{aligned} \tag{A75}$$

Note that this implies that the origin of the accelerated system $z=0$ obeys the equation

$$1+\alpha^2(t')^2=(1-\alpha z')^2 . \tag{A76}$$

Comparison with Eq. (A48) shows that the origin is uniformly accelerating along the $-z'$ axis with acceleration α. The special relativistic transformation allows us to analyze the problem from the inertial system z'. But we now have a transformation that enables us to discuss the problem from any point in either coordinate system. For convenience, we also write the differential form of Eqs. (A75),

$$\begin{aligned} dz &= (1-\alpha z')dz'+\alpha t'dt' , \\ dt &= \frac{(1-\alpha z')dt'+\alpha t'dz'}{(1-\alpha z')^2-\alpha^2(t')^2} . \end{aligned} \tag{A77}$$

Subsequently, we shall call the accelerating system O, with coordinates x^μ, and the inertial system O', with coordinates $(x^\mu)'$. Note that a point at rest in the O system, for which $dz=0$, obeys

$$v'=dz'/dt'=-\alpha t'/(1-\alpha z')=-\tanh\alpha t . \tag{A78}$$

This answer is independent of z, so that all points in O at fixed t are moving with the same speed with respect to O'. Thus in this sense the accelerating system is *rigid*, in that simultaneously in O, all points of O have this speed. This is not true if one looks at a fixed time t' in O'. If one compares Eq. (A78) with the equation for v in Eqs. (A50), one sees that t measures the proper time for a particle at the origin of O, and it is with respect to this time that the system is rigid.

4. The Klein-Gordon equation

Once we have our transformation completely determined, it is a simple matter to write the transformed Klein–Gordon equation. In the inertial system O' (setting $\hbar=1$)

$$\left(\frac{\partial^2}{\partial(t')^2}-\frac{\partial^2}{\partial(z')^2}-\frac{\partial^2}{\partial(x')^2}-\frac{\partial^2}{\partial(y')^2}\right)\phi+m^2\phi=0 . \tag{A79}$$

The operator appearing in this equation is the operator $\partial^\mu\partial_\mu\phi$. However, if one wants an equation which is valid in a noninertial system, one must replace the derivatives by covariant derivatives, $\partial_\mu\to D_\mu$. For a scalar,

$$D_\mu\phi=\partial_\mu\phi . \tag{A80}$$

For a vector,

$$\begin{aligned} D^\mu(\partial_\mu\phi) &= g^{\mu\nu}D_\nu(\partial_\mu\phi)=g^{\mu\nu}\left(\partial_\nu\partial_\mu\phi-\begin{Bmatrix}\lambda\\ \nu\ \mu\end{Bmatrix}\partial_\lambda\phi\right) \\ &= \partial^\mu\partial_\mu\phi-\left(g^{00}\begin{Bmatrix}3\\ 0\ 0\end{Bmatrix}+g^{33}\begin{Bmatrix}3\\ 3\ 3\end{Bmatrix}\right)\partial_3\phi . \end{aligned} \tag{A81}$$

In our metric, the nonzero Christoffel symbols, Eq. (A62), become

$$\begin{Bmatrix} 0 \\ 0\ 3 \end{Bmatrix} = -\alpha(1-2\alpha z)^{-1} = -\begin{Bmatrix} 3 \\ 3\ 3 \end{Bmatrix}, \quad \begin{Bmatrix} 3 \\ 0\ 0 \end{Bmatrix} = -\alpha(1-2\alpha z), \tag{A82}$$

so that

$$D^\mu D_\mu \phi + m^2\phi = \partial^\mu \partial_\mu \phi + 2\alpha \frac{\partial \phi}{\partial z} + m^2\phi = 0. \tag{A83}$$

This is the Klein–Gordon equation. We could have used our transformations (A73) and (A77) directly to calculate this result without using the Christoffel symbols. Specifically,

$$\begin{aligned} \frac{\partial}{\partial z'} &= (1-2\alpha z)^{1/2}\cosh\alpha t\, \frac{\partial}{\partial z} + \frac{\sinh\alpha t}{(1-2\alpha z)^{1/2}} \frac{\partial}{\partial t}, \\ \frac{\partial}{\partial t'} &= \frac{\cosh\alpha t}{(1-2\alpha z)^{1/2}} \frac{\partial}{\partial t} + (1-2\alpha z)^{1/2}\sinh\alpha t \frac{\partial}{\partial z}, \end{aligned} \tag{A84}$$

and substituting this directly into Eq. (A79) gives

$$\begin{aligned} \left(\frac{\partial^2}{\partial(t')^2} - \frac{\partial^2}{\partial(z')^2}\right)\phi &= (1-2\alpha z)^{-1}\frac{\partial^2\phi}{\partial t^2} - (1-2\alpha z)\frac{\partial^2\phi}{\partial z^2} + 2\alpha\frac{\partial\phi}{\partial z} \\ &= [g^{00}(\partial_0)^2 + g^{33}(\partial_3)^2 + 2\alpha\partial_3]\phi \\ &= (\partial^0\partial_0 + \partial^3\partial_3 + 2\alpha\partial_3)\phi. \end{aligned} \tag{A85}$$

To examine the nonrelativistic limit of this equation, we write

$$\begin{aligned} \phi &= ue^{-imt}, \\ \frac{\partial^2\phi}{\partial t^2} &= \left(-m^2u - 2im\frac{\partial u}{\partial t} + \frac{\partial^2 u}{\partial t^2}\right)e^{-imt}. \end{aligned} \tag{A86}$$

The second term in this expression is down by v^2/c^2, and the last term is down by v^4/c^4; thus we drop it. We also note that αz is of the order v^2/c^2. So, to order v^2/c^2, Eq. (A83) becomes

$$-(2m)^{-1}\frac{\partial^2 u}{\partial z^2} - m\alpha z u - i\frac{\partial u}{\partial t} \approx -\left(\frac{\alpha}{m}\right)\frac{\partial u}{\partial z} \approx 0. \tag{A87}$$

Equation (A87) is just the nonrelativistic Schrödinger equation. The right-hand side vanishes because, putting in dimensional constants, $(\hbar^2\alpha/mc^2)\,\partial u/\partial z \sim \hbar^2\alpha k u/mc^2$, and after the particle has moved slightly we will have $k > \Delta k$, $\bar{z} > \Delta z$, and $\bar{z}k > \Delta k \Delta z > 1$, so

$$\frac{\hbar^2\alpha k u}{mc^2} < \frac{\hbar^2\alpha\bar{z}k^2u}{mc^2} = \frac{m\alpha\bar{z}}{mc^2}\frac{p^2}{m}u \sim O\left(\frac{v^4}{c^4}\right). \tag{A88}$$

5. The Dirac equation

For a free particle in an inertial frame x', the Dirac equation is

$$-i\gamma^\mu \frac{\partial}{\partial x^{\mu'}}\psi + m\psi = 0. \tag{A89}$$

We shall use the notation of Schweber, 1961, where

$$\gamma^0 = \beta = \begin{pmatrix} 1 & 0 \\ 0 & -1 \end{pmatrix}, \quad \alpha^k = \begin{pmatrix} 0 & \sigma^k \\ \sigma^k & 0 \end{pmatrix}, \quad \gamma^k = \beta\alpha^k = \begin{pmatrix} 0 & \sigma^k \\ -\sigma^k & 0 \end{pmatrix},$$

$$\gamma^5 = \gamma^0\gamma^1\gamma^2\gamma^3 = \begin{pmatrix} 0 & i \\ -i & 0 \end{pmatrix}, \quad \{\gamma^\mu, \gamma^\nu\}_+ = g^{\mu\nu},$$

$$\gamma^0\gamma^3 = \alpha^3 = -\gamma^3\gamma^0, \quad \gamma^0\alpha^3 = \gamma^3 = -\alpha^3\gamma^0, \quad \gamma^3\alpha^3 = \gamma^0 = -\alpha^3\gamma^3,$$

$$(\alpha^3)^2 = (\gamma^0)^2 = 1, \quad (\gamma^3)^2 = -1.$$

(These γ are 4×4 matrices). To write the equation in the x frame, we use Eq. (A84) for $\partial/\partial z'$, $\partial/\partial t'$. If we call the vector $\partial/\partial x^{\mu'}$, expressed in terms of x^μ, via Eq. (A84), the vector operator d_μ,

$$\frac{\partial}{\partial x^{\mu'}} \equiv d_\mu(x), \tag{A90}$$

then the Dirac equation becomes

$$-i\gamma^\mu d_\mu\psi + m\psi = 0. \tag{A91}$$

The second-order equation is, writing $\psi = (-i\gamma\cdot d - m)\chi$,

$$(-i\gamma\cdot d + m)(-i\gamma\cdot d - m)\chi = -[(\gamma\cdot d)(\gamma\cdot d) + m^2]\chi = 0. \tag{A92}$$

Since

$$\begin{aligned} (\gamma^0 d_0 + \gamma^3 d_3)^2 &= (1-2\alpha z)^{-1}\frac{\partial^2}{\partial t^2} + (1-2\alpha z)\frac{\partial^2}{\partial z^2} + 2\alpha\frac{\partial}{\partial z} \\ &= D_0D^0 + D_3D^3, \end{aligned} \tag{A93}$$

this exactly gives Eq. (A83) of the Klein–Gordon case. Nonetheless, this is not the appropriate Dirac equation, because our γ matrices are lined up along the old $x^{\mu'}$ axes. One wants the matrices to have their conventional numerical form along the new axes x^μ, in the O system.

Thus we must make a unitary transformation to rearrange the γ's. We do this by boosting them into the inertial system instantaneously moving at the same velocity as the accelerating system x^μ. In general, for a boost along the z axis to velocity v, where $v = \tanh w$,

$$S(v) = \exp(\tfrac{1}{2}w\gamma^0\gamma^3) = \exp(\tfrac{1}{2}w\alpha^3) = \cosh(\tfrac{1}{2}w) + \alpha^3\sinh(\tfrac{1}{2}w). \tag{A94}$$

As with any vector components, we shall have

$$\begin{aligned} S\gamma^0S^{-1} &= \gamma^0\cosh w - \gamma^3\sinh w, \\ S\gamma^3S^{-1} &= \gamma^3\cosh w - \gamma^0\sinh w. \end{aligned} \tag{A95}$$

In our case, at time t in the O system, the entire system has velocity $v = -\tanh\alpha t$, simultaneously, so we choose [using $(-\tanh\alpha t) = \tanh(-\alpha t)$]

$$\begin{aligned} w &= -\alpha t, \\ S(v) &= \cosh(\tfrac{1}{2}\alpha t) - \alpha^3\sinh(\tfrac{1}{2}\alpha t). \end{aligned} \tag{A96}$$

In the new system O, the γ's, which we shall call $\bar{\gamma}$, will have the same numerical representation as they had in the old system, with reference to the old axes. Specifically,

$$\begin{aligned} S\gamma^0S^{-1} &= \gamma^0\cosh\alpha t + \gamma^3\sinh\alpha t \equiv \bar{\gamma}^0, \\ S\gamma^3S^{-1} &= \gamma^3\cosh\alpha t + \gamma^0\sinh\alpha t \equiv \bar{\gamma}^3, \\ \gamma^2 &= \bar{\gamma}^2, \quad \gamma^3 = \bar{\gamma}^3. \end{aligned} \tag{A97}$$

One should note, however, that even though the $\bar{\gamma}$ are numerical matrices, whose elements at time t in the O system are $0, \pm1, \pm i$, nonetheless, at every different instant they are lined up in a different coordinate system. So even though they are numerical, $(\partial\bar{\gamma}^\mu/\partial t) \neq 0$. In fact, from Eq. (A97) we can see that

$$\frac{d\bar{\gamma}^0}{dt} = \alpha\bar{\gamma}^3, \quad \frac{d\bar{\gamma}^3}{dt} = \alpha\bar{\gamma}^0. \tag{A98}$$

In order to write the static form of the Dirac equation, we invert Eq. (A97) to find γ as $f(\bar{\gamma})$, which we can do by merely changing t to $(-t)$ in Eq. (A97),

$$\gamma^0 = \bar{\gamma}^0 \cosh\alpha t - \bar{\gamma}^3 \sinh\alpha t\,, \qquad \gamma^3 = \bar{\gamma}^3 \cosh\alpha t - \bar{\gamma}^0 \sinh\alpha t\,. \tag{A99}$$

Then we calculate $\gamma^\mu d_\mu$, expressing γ^μ as a function of $\bar{\gamma}^\mu$, which gives

$$\gamma^0 d_0 + \gamma^3 d_3 = \bar{\gamma}^0 (1-2\alpha z)^{-1/2} \frac{\partial}{\partial t} + \bar{\gamma}^3 (1-2\alpha z)^{1/2} \frac{\partial}{\partial z}\,. \tag{A100}$$

Thus the static Dirac equation is

$$-i\left(\bar{\gamma}^0 (1-2\alpha z)^{-1/2} \frac{\partial}{\partial t} + \bar{\gamma}^3 (1-2\alpha z)^{1/2} \frac{\partial}{\partial z} + \bar{\gamma}^1 \frac{\partial}{\partial x} + \bar{\gamma}^2 \frac{\partial}{\partial y}\right)\psi + m\psi = 0\,, \tag{A101}$$

where ψ is the wave function in the system O, expressed in terms of the axes of the system O.

We might note that an alternative derivation of this equation can be made by introducing a vierbein, which is a set of four independent vectors in the tangent space O'' to the space O. In our case it is easy to find the tangent space, which is an inertial system moving at exactly the velocity of the point x^μ in O. Since at time t the entire system O is moving at speed $v = \tanh(-\alpha t)$ with respect to O', all we must do is transform from O' to the inertial system O'' moving at this speed, via the Lorentz transformation $S(v)$,

$$dz'' = dz' \cosh\alpha t + dt' \sinh\alpha t = (1-2\alpha z)^{-1/2} dz\,, \qquad dt'' = dt' \cosh\alpha t + dz' \sinh\alpha t = (1-2\alpha z)^{1/2} dt\,, \tag{A102}$$

using Eqs. (A73). This transformation completely defines the vierbein, and the Dirac equation can be written directly in terms of it via the recipe in Sec. 12.5 of Weinberg, 1972. The result is Eq. (A101). (Anandan, 1977, discusses the higher-order effect of performing the COW experiment in a field with real curvature.)

In the Dirac equation, since only one space dimension is important, we can factor out the t, x, and y dependence. Introducing the vector

$$k^\mu = (E, \mathbf{k})\,, \tag{A103}$$

we can write

$$\psi = \chi \exp(-iEt + ik^1 x + ik^2 y)\,, \tag{A104}$$

which yields the stationary form of the Dirac equation (we omit the bars from $\bar{\gamma}$ hereafter):

$$\left(-\gamma^0 E(1-2\alpha z)^{-1/2} - i\gamma^3 (1-2\alpha z) \frac{\partial}{\partial z} + \gamma^1 k^1 + \gamma^2 k^2 + m\right)\chi = 0\,. \tag{A105}$$

One can change variables from z to ρ, where

$$(1-2\alpha z)^{1/2} = 1 - \alpha\rho\,. \tag{A106}$$

For $\alpha z \ll 1$, the nonrelativistic region, $\rho \sim z$, and

$$(1-2\alpha z)^{1/2} \frac{\partial}{\partial z} = \frac{\partial}{\partial \rho}\,. \tag{A107}$$

Thus the stationary Dirac equation becomes

$$(-\gamma^0 E(1-\alpha\rho)^{-1} - i\gamma^1 \partial/\partial\rho + \gamma^2 k^2 + \gamma^3 k^3 + m)\chi = 0\,. \tag{A108}$$

We can write the two-component form of this equation by setting

$$\chi = \begin{pmatrix} u \\ v \end{pmatrix} \tag{A109}$$

and using our explicit form for the Dirac matrices. Then

$$-i\sigma^3 v' + \boldsymbol{\sigma}\cdot\mathbf{n} v = [E(1-\alpha\rho)^{-1} - m]u\,, \qquad i\sigma^3 u' - \boldsymbol{\sigma}\cdot\mathbf{n} u = -[E(1-\alpha\rho)^{-1} + m]v\,, \tag{A110}$$

where $' \equiv \partial/\partial\rho$, and $\mathbf{n} = k^1 \mathbf{u}_x + k^2 \mathbf{u}_y$. From this we see that for nonrelativistic positive-energy solutions, $v \sim (k/m)u \ll u$.

We can also express Eqs. (A110) as a second-order equation for the large component u alone,

$$-\left(\frac{(1-\alpha\rho)u'}{E + m(1-\alpha\rho)}\right)' + \left(\frac{(\boldsymbol{\sigma}\times\mathbf{n})^3 E\alpha}{[E + m(1-\alpha\rho)]^2} + \frac{n^2(1-\alpha\rho)}{E + m(1-\alpha\rho)}\right)u = \left(\frac{E - m(1-\alpha\rho)}{1-\alpha\rho}\right)u\,. \tag{A111}$$

[Here $(\boldsymbol{\sigma}\times\mathbf{n})^3 = (\sigma^1 k^2 - \sigma^2 k^1)$ and $n^2 = \mathbf{n}\cdot\mathbf{n}$.] The nonrelativistic limit of Eq. (A111) is

$$-(\hbar^2/2m)u'' + [(\hbar\mathbf{n})^2/2m]u = (\varepsilon + m\alpha\rho)u\,, \tag{A112}$$

where $E = m + \varepsilon$. The second term is just the transverse kinetic energy, so that if we write

$$\varepsilon_z = \varepsilon - (\hbar\mathbf{n})^2/2m\,, \tag{A113}$$

the equation becomes

$$-(\hbar^2/2m)u'' - m\alpha\rho u = \varepsilon_z u\,, \tag{A114}$$

the nonrelativistic Schrödinger equation.

REFERENCES

Abramowitz, M., and I. Stegun, 1964, *Handbook of Mathematical Functions* [Natl. Bur. Stand. (U.S.), Washington, D. C.].

Adler, R. J., M. J. Bazin, and M. Schiffer, 1975, *Introduction to General Relativity* (McGraw-Hill, New York).

Aharonov, Y., and D. Bohm, 1959, Phys. Rev. **115**, 485.

Aharonov, Y., and D. Bohm, 1961, Phys. Rev. **123**, 1511.

Aharonov, Y., and D. Bohm, 1962, Phys. Rev. **125**, 2192.

Aharonov, Y., and D. Bohm, 1963, Phys. Rev. **130**, 1625.

Anandan, J., 1977, Phys. Rev. D **15**, 1448.

Ashkin, M., and M. Kuriyama, 1966, J. Phys. Soc. Jpn. **21**, 1549.

Azaroff, L. V., R. Kaplow, N. Kato, R. J. Weiss, A. J. C. Wilson, and R. A. Young, 1974, *X-Ray Diffraction* (McGraw-Hill, New York).

Batterman, B. W., and H. Cole, 1964, Rev. Mod. Phys. **36**, 681.

Bayh, W., 1962, Z. Phys. **169**, 492.

Baym, G., 1969, *Lectures on Quantum Mechanics* (Benjamin, New York), Chap. 9.

Belinfante, F. J., 1962, Phys. Rev. **128**, 2832.

Blatt, J. M., and V. Weisskopf, 1952, *Theoretical Nuclear Physics* (Wiley, New York).

Boersch, H., H. Hamisch, D. Wohlleben, and K. Grohmann, 1960, Z. Phys. **159**, 397.

Bonse, U., and W. Graeff, 1977, "X-Ray and Neutron Interferometry," chapter in *X-Ray Optics*, edited by H.-J.

Queisser, Vol. 22 of Topics in Applied Physics (Springer, Berlin), p. 93.
Bonse, U., and M. Hart, 1965a, Appl. Phys. Lett. **6**, 155.
Bonse, U., and M. Hart, 1965b, Z. Phys. **188**, 154.
Bonse, U., and M. Hart, 1966a, Z. Phys. **190**, 455.
Bonse, U., and M. Hart, 1966b, Z. Phys. **194**, 1.
Bonse, U., and H. Rauch, 1978, *Proceedings of the First International Workshop on Neutron Interferometry*, Inst. Laue-Langevin, Grendale, June 1978 (Oxford U.P., New York).
Borrmann, G., 1941, Phys. Z. **42**, 157.
Borrmann, G., 1950, Z. Phys. **127**, 297.
Boyer, T., 1973, Phys. Rev. D **8**, 1679.
Brill, D. R., D. M. Greenberger, B. Naier, A. W. Overhauser, and F. G. Werner, (to be published).
Campbell, H. N., 1951a, J. Appl. Phys. **22**, 1139.
Campbell, H. N., 1951b, Acta Crystallogr. **4**, 180.
Chambers, R. G., 1960, Phys. Rev. Lett. **5**, 3.
Colella, R., A. W. Overhauser, and S. A. Werner, 1975, Phys. Rev. Lett. **34**, 1472.
DeWitt, B. S., 1962, Phys. Rev. **125**, 2189.
Ehrenberg, W., and R. E. Siday, 1949, Proc. R. Soc. Lond. B **62**, 8.
Ehrlichson, H., 1970, Am. J. Phys. **38**, 162.
Eliezer, C. J., and P. G. Leach, 1977, Am. J. Phys. **45**, 1218.
Fowler, H. A., L. Marton, J. A. Simpson, and J. A. Suddeth, 1961, J. Appl. Phys. **32**, 1153.
Furry, W. H., and N. F. Ramsey, 1960, Phys. Rev. **118**, 623.
Goldberger, M., and F. Seitz, 1947, Phys. Rev. **71**, 294.
Goldstein, H., 1950, *Classical Mechanics* (Addison-Wesley, Reading, Mass.).
Greenberger, D. M., 1968, Ann. Phys. (N.Y.) **47**, 116.
Greenberger, D. M., Am. J. Phys. **47**, 35.
Hamilton, J. D., 1978, Am. J. Phys. **46**, 83.
Horne, M., C. Shull, G. Squires, and A. Zeilinger, (to be published).
Indenbom, V. L., and F. N. Chukhovskii, 1972, Sov. Phys. Uspekhi **15**, 298.
Indenbom, V. L., E. V. Suvorov, and I. Sh. Slobodetskii, Sov. Phys.-JETP **44**, 187.
James, R. W., 1963, *The Dynamical Theory of X-Ray Scattering*, in *Solid State Physics*, edited by F. Seitz and D. Turnbull (Academic, New York), Vol. **15**, p. 53.
Landau, L. D., and E. M. Lifschitz, 1958, *Quantum Mechanics* (Addison-Wesley, Reading, Mass.).
von Laue, M., 1949, Acta Crystallogr. **2**, 106.
Liebowitz, B., 1965, Nuovo Cimento **38**, 932.
Marton, L., 1952, Phys. Rev. **85**, 1057.
Marton, L., J. A. Simpson, and J. A. Suddeth, 1953, Phys. Rev. **90**, 490.
Marton, L., J. A. Simpson, and J. A. Suddeth, 1954, J. Sci. Instrum. **25**, 1099.
Mendlowitz, H., 1960, post-deadline paper, January Am. Phys. Soc. meeting, New York (unpublished).
Möllenstedt, G., and W. Bayh, 1962a, Naturwissenschaften **49**, 81.
Möllenstedt, G., and W. Bayh, 1962b, Phys. Bl **18**, 299.
Oberteuffer, J. A., and C. G. Shull, 1972, Phys. Rev. Lett. **29**, 871.
Overhauser, A. W., and R. Colella, 1974, Phys. Rev. Lett. **33**, 1237.
Peierls, R. E., 1955, *Quantum Theory of Solids* (Oxford U.P., London).
Rauch, H., and D. Petrascheck, 1979, *Neutron Diffraction*, in series *Topics in Current Physics* (Springer, Berlin), Chap. 9.
Rauch, H., and M. Suda, 1974, Phys. Status Solidi A **25**, 495.
Rauch, H., W. Treiman, and U. Bonse, 1974, Phys. Lett. A **47**, 369.
Rauch, H., A. Zeilinger, G. Badurek, A. Wilfing, W. Bauspiess, and U. Bonse, 1975, Phys. Lett. A **54**, 425.
Rohrlich, F., 1965, *Classical Charged Particles* (Addison-Wesley, Reading, Mass.).
Rosen, G., 1972, Am. J. Phys. **40**, 683.
Schweber, S. S., 1961, *An Introduction to Relativistic Quantum Field Theory* (Row, Peterson, Evanston, Illinois).
Schmutzer, E., and J. Plebanski, 1977, Fortschr. Phys. **25**, 37.
Simpson, J. A., 1954, J. Sci. Instrum. **25**, 1105.
Shull, C. G., 1968, Phys. Rev. Lett. **21**, 1585.
Shull, C. G., and W. M. Shaw, 1973, Z. Naturforsch. A **28**, 657.
Slater, J. C., 1958, Rev. Mod. Phys. **30**, 197.
Squires, G., 1978, Summary talk, in *Proceedings of the First International Workshop on Neutron Interferometry*, see reference to Bonse, U., and H. Rauch above.
Tassie, L. J., and M. Peshkin, 1961, Ann. Phys. (N.Y.) **16**, 177.
Weinberg, S., 1972, *Gravitation and Cosmology* (Wiley, New York).
Werner, F. G., and D. R. Brill, 1960, Phys. Rev. Lett. **4**, 344.
Werner, S. A., R. Colella, A. W. Overhauser, and C. F. Eagen, 1975, Phys. Rev. Lett. **35**, 1053.
Werner, S. A., R. Colella, A. W. Overhauser, and C. F. Eagen, 1976, in *Proceedings of the Conference on Neutron Scattering*, Gatlinberg, Tennessee (held June 6–10, 1976).
Woodilla, J., and H. Schwarz, 1971, Am. J. Phys. **39**, 111.